

Derivation of Victorian Sea-Level Planning Allowances

Research conducted for
The Victorian Coastal Council

J. R. Hunter

Flexible Contracting Services,
GPO Box 2181, Hobart, Tasmania 7001

29 May 2013

The information contained in this document is solely for the use of the client identified in the report and for the purpose for which it has been prepared. No responsibility is accepted to any third party who may rely upon this document.

The user of this data accepts any and all risks of such use, whether direct or indirect, and in no event shall Flexible Contracting Services be liable for any damages and/or costs, including but not limited to incidental or consequential damages of any kind, including economic damage or loss or injury to person or property, regardless of whether Flexible Contracting Services shall be advised, have reason to know, or in fact shall know of the possibility.

This work is copyright. It may be reproduced in whole or in part for research, study or training purposes subject to the inclusion of an acknowledgment of the source, but not for commercial sale or use.

Contents

Executive Summary	1
1 Introduction	2
2 Climate Change and Sea-Level Rise	3
3 Summary of Australian Planning Allowances	4
4 The Background Behind the Sea-Level Planning Allowance	8
5 Sea-Level Planning Allowances for Victoria	11
5.1 Introduction	11
5.2 2010-2040	12
5.3 2010-2070	12
5.4 2010-2100	13
6 Recommendations for Future Work	13
7 Glossary of Terms	21
8 Acknowledgements	21
A Copy of Hunter(2012) and Electronic Supplementary Material	25
B Copy of Hunter et al. (2013)	47

List of Tables

1	Summary of present sea-level rise allowances for Australia.	7
2	Summary of locations, Gumbel scale parameter (from tide-gauge data), mean and standard deviation of sea-level projections, 5- 95-percentile range of sea-level projections, and sea-level planning allowances, for SRES scenario A1FI, years 2010-2040 and tide-gauge stations only.	15
3	Summary of locations, Gumbel scale parameter (from storm-tide model), mean and standard deviation of sea-level projections, 5- 95-percentile range of sea-level projections, and sea-level planning allowances, for SRES scenario A1FI, years 2010-2040, and all locations.	16
4	Summary of locations, Gumbel scale parameter (from tide-gauge data), mean and standard deviation of sea-level projections, 5- 95-percentile range of sea-level projections, and sea-level planning allowances, for SRES scenario A1FI, years 2010-2070 and tide-gauge stations only.	17
5	Summary of locations, Gumbel scale parameter (from storm-tide model), mean and standard deviation of sea-level projections, 5- 95-percentile range of sea-level projections, and sea-level planning allowances, for SRES scenario A1FI, years 2010-2070, and all locations.	18
6	Summary of locations, Gumbel scale parameter (from tide-gauge data), mean and standard deviation of sea-level projections, 5- 95-percentile range of sea-level projections, and sea-level planning allowances, for SRES scenario A1FI, years 2010-2100 and tide-gauge stations only.	19
7	Summary of locations, Gumbel scale parameter (from storm-tide model), mean and standard deviation of sea-level projections, 5- 95-percentile range of sea-level projections, and sea-level planning allowances, for SRES scenario A1FI, years 2010-2100, and all locations.	20

List of Figures

1	Global-average projections of sea-level rise relative to 1990, based on the IPCC AR4 (Meehl et al, 2007) and reproduced in Church et al (2011). The outer light lines and the shaded region show the 5- to 95-percentile range of projections with and without ‘scaled-up ice sheet discharge’ (SUISD), respectively. The continuous coloured lines from 1990 to 2100 indicate the central value of the projections, with SUISD. The open and shaded bars at the right show the 5- to 95-percentile range of projections for 2100 for the various SRES scenarios, with and without SUISD. The diamonds and horizontal lines in the bars are the central values with and without SUISD. The observational estimates of global-average sea level based on tide-gauge measurements and satellite altimeter data are shown in black and red, respectively. The tide-gauge data are set to zero at the start of the projections in 1990, and the altimeter data are set equal to the tide-gauge data at the start of the record in 1993.	5
2	The regional distribution of the projections of sea-level change from 1990 to 2090, for the A1B emission scenario. This was obtained by combining global average sea-level rise, a spatially-varying component due to changes in ocean density and dynamics, and regional components associated with the changing distribution of land ice. The black contour and the black bar on the key indicate the global-average change (0.38 m), dividing those regions with above- and below-average sea-level rise. After Church et al, 2011.	6
3	Locations of sites where sea-level planning allowance has been estimated. Red circles indicate locations where regional sea-level rise projections and the modelled storm-tide statistics (specifically, the Gumbel scale parameter) have been evaluated. Black rings indicates locations of tide gauges.	11
4	Sea-level projections (black bars; crosses indicating central value, inner range indicating \pm one standard deviation, and outer range indicating 5- to 95-percentile limits) and sea-level planning allowance (red curve), for SRES scenario A1FI and years 2010-2040, plotted against longitude for tide-gauge locations only. The allowances were derived using tide-gauge data.	15
5	Sea-level projections (black bars; crosses indicating central value, inner range indicating \pm one standard deviation, and outer range indicating 5- to 95-percentile limits) and sea-level planning allowance (red curve), for SRES scenario A1FI and years 2010-2040, plotted against longitude for all locations. The allowances were derived using the storm-tide model.	16
6	Sea-level projections (black bars; crosses indicating central value, inner range indicating \pm one standard deviation, and outer range indicating 5- to 95-percentile limits) and sea-level planning allowance (red curve), for SRES scenario A1FI and years 2010-2070, plotted against longitude for tide-gauge locations only. The allowances were derived using tide-gauge data.	17

7	Sea-level projections (black bars; crosses indicating central value, inner range indicating \pm one standard deviation, and outer range indicating 5- to 95-percentile limits) and sea-level planning allowance (red curve), for SRES scenario A1FI and years 2010-2070, plotted against longitude for all locations. The allowances were derived using the storm-tide model.	18
8	Sea-level projections (black bars; crosses indicating central value, inner range indicating \pm one standard deviation, and outer range indicating 5- to 95-percentile limits) and sea-level planning allowance (red curve), for SRES scenario A1FI and years 2010-2100, plotted against longitude for tide-gauge locations only. The allowances were derived using tide-gauge data.	19
9	Sea-level projections (black bars; crosses indicating central value, inner range indicating \pm one standard deviation, and outer range indicating 5- to 95-percentile limits) and sea-level planning allowance (red curve), for SRES scenario A1FI and years 2010-2100, plotted against longitude for all locations. The allowances were derived using the storm-tide model.	20

Executive Summary

Sea-level planning allowances for the Victorian coastline are here derived, based on the method of Hunter (2012). These allowances ensure that the average number of inundation events in a given period is preserved. In other words, any asset raised by this allowance would experience the same frequency of inundation events under sea-level rise as it would without the allowance and without sea-level rise.

These allowances are based on the latest projections of regional sea-level rise, and on the present statistics of storm tides (the combination of tides and storm surges). The latter have been derived from both tide-gauge observations (at Geelong, Point Lonsdale and Williamstown) and the results of a storm-tide model of the Australian region. In deriving the allowance, it has been assumed that the statistics of storm tides will not change significantly during the 21st century.

For the periods 2010-2040, 2010-2070 and 2010-2100, the suggested allowances are 0.1, 0.3 (0.4) and 0.7 (0.8) metres, respectively (where the figures in brackets indicate more protective options).

NOTE that, in order to enable skimming of this report for its most salient features, the most important text is highlighted in red.

1 Introduction

The work described in this document was commissioned by the Victorian Coastal Council in January 2013, in order to provide advice concerning appropriate vertical allowances¹ for sea-level rise for Victoria for this century. **The methodology is similar to that used for the recent derivation of the Tasmanian Sea Level Rise Planning Allowances (Tasmanian Climate Change Office, 2012).**

The earlier sea-level planning allowances for Victoria (and for other Australian states) were based on global projections of sea-level rise reported in the Assessment Reports of the Intergovernmental Panel on Climate Change (IPCC). The New South Wales allowance (which has now been abandoned) had a small component added to the global projection to allow for regional variation, based on the model results reported in the Fourth Assessment Report (AR4) of the IPCC (Meehl et al, 2007)². All the allowances other than the Tasmanian one (Tasmanian Climate Change Office, 2012) were based on somewhat subjective estimates of the upper limit of the range of the projections (e.g. the 95-percentile of the projection). **The technique used here avoids the problem posed by the question ‘how different would the future be if I chose the 50-percentile (the central value) rather than the 95-percentile maximum for the allowance?’.**

The derivation of the sea-level allowances reported here involves two innovations:

1. It uses recent estimates of future regional sea-level rise (Church et al, 2011), which are based on the regional projections reported by the IPCC AR4 (Meehl et al, 2007) and additional contributions to account for vertical land motion due to changes in the Earth’s loading and gravitational field, caused by past and ongoing changes in land ice. The projections therefore represent an approximation of *relative sea level* (i.e. sea level relative to the land), but do not include effects due to local land subsidence caused, for example, by groundwater withdrawal (*separate allowances should be applied to account for such effects*).
2. It uses an objective method (Hunter, 2012) of combining the (uncertain) projections of sea-level rise with the statistics of local tides and storm surges (collectively called *storm tides*). The statistics of storm tides are here derived both from tide-gauge observations and from the results of a storm-tide model of the Australian region). The technique ensures that the expected, or average, number of extreme (inundation) events in a given period is preserved. In other words, any asset raised by this allowance would experience the same frequency of inundation events under sea-level rise as it would without the allowance and without sea-level rise.

The allowances presented here are subject to a number of caveats:

- a. These allowances only relate to the effect of sea-level rise on *inundation* and *not* on the recession of soft (e.g. sandy) shorelines or on other impacts.
- b. While these allowances include the effects of vertical land motion due to changes in the Earth’s loading and gravitational field, caused by past and ongoing changes in

¹In this context, an ‘allowance’ is the vertical distance that a coastal entity needs to be raised in order to cope with the projected sea-level rise.

²See also www.cmar.csiro.au/sealevel/sl_proj_regional.html

land ice, they do not include effects due to local land subsidence produced, for example, by groundwater withdrawal; *separate allowances should be applied to account for these latter effects.*

- c. These allowances are based on the assumption that the statistics of the storm tides will not change in time. This is supported by the fact that present evidence (Bindoff et al, 2007, Lowe et al, 2012, Menéndez and Woodworth, 2010, Woodworth and Blackman, 2004) suggests that the rise in mean sea level is generally the dominant cause of any observed increase in the frequency of inundation events. In addition, using model projections of storm tides in southeast Australia to 2070, McInnes et al (2009) showed that the increase in the frequency of inundation events was dominated by sea-level rise.
- d. These allowances include no contribution due to possible changes in wave setup or runup.
- e. These allowances include no contribution due to the change in tides caused by sea-level rise, which are generally small and confined to quite specific locations in shelf seas.
- f. These allowances depend on an assumed probability distribution for the uncertainty of the sea-level rise projections. Here, a normal or Gaussian distribution has been used, which represents a pragmatic compromise between a tightly confined distribution, and one with a fat upper tail (i.e. one in which there is a low probability of having a very high sea-level rise relative to the best estimate of that rise). The allowances represent a practical solution to planning for sea-level rise while preserving an acceptable level of inundation likelihood, in cases where ‘getting the allowance wrong’ is manageable. However, in cases where the consequence of inundation would be ‘dire’ (in the sense that the consequence of inundation would be unbearable, no matter how low the likelihood, as in case of the Netherlands), a precautionary approach would be to *not* use the allowances presented here, but to base an allowance on the best estimate of the maximum possible rise.

The technique and its caveats are more fully described by Hunter et al (2013).

2 Climate Change and Sea-Level Rise

We are now living in a world in which the climate is being substantially modified by human activity (IPCC, 2007a). These changes are leading to a wide range of impacts, just one of which is a rise in sea level at a sustained rate which has not been experienced for at least 5,000 years (Church et al, 2008, Fig. 1 of that paper).

Beginning at the end of the 19th century, an increase in the concentration of greenhouse gases in the atmosphere, caused primarily by anthropogenic emissions, is contributing to a warming of the climate. The rise in global temperature during the latter half of the 20th century and beyond is dominated by the effect of these anthropogenic greenhouse gases, over other influences, such as solar activity. From 1850-1899 to 2001-2005, global-average surface temperature increased by about 0.76°C (IPCC, 2007b), leading to warming of the oceans and melting of ice on land (Lemke et al, 2007; Bindoff et al, 2007). Church and White (2011) used a combination of tide-gauge records and satellite-altimeter data to

reconstruct sea level from 1880 to 2009, showing a global-average rise of about 0.17 metres and a statistically significant acceleration of about $0.009 \text{ mm year}^{-2}$ since 1900. They also indicated that, from 1993 to 2009, global average sea level rose at a rate of about 3 mm year^{-1} , which is near the upper end of the sea level projections of the IPCC's TAR (Third Assessment Report) and AR4. However, other reconstructions, using only tide-gauge data (Holgate and Woodworth, 2004; Jevrejeva et al, 2006; Woodworth et al, 2008), have indicated similar rates of rise earlier in the 20th century.

Computer modelling has been used to provide projections of the future climate over time scales of centuries. Two inherent uncertainties are involved. The first (the 'scenario uncertainty') arises from the fact that the future social, economic and technological development of the world, and the consequent greenhouse-gas emissions, are poorly known. A range of plausible futures, or scenarios³, have been used to describe the way in which emissions may change in the future. The second uncertainty (the 'model uncertainty') is related to shortcomings in the present knowledge of the science of climate change, partly due to the fact that we do not know exactly the present climate state (the 'initial conditions'), and partly due to the fact that no model gives a perfect representation of the real world. The IPCC AR4 provided projections of sea-level rise at 2095 relative to 1990 (strictly, the difference between the average sea level over 2090-2099 and over 1980-1999; Meehl et al, 2007). The 5-percentile minimum and 95-percentile maximum rises projected by the models for this period were 0.18 to 0.59 m, respectively, for a range of scenarios covering B1 (low emission) to A1FI (high emission), and including an uncertainty estimate based on the range of projections from the different models. The IPCC also recommended that an additional scenario-dependent contribution (called the 'scaled-up ice sheet discharge') of up to about 0.2 m should be added to the upper limits of the projections to account for processes involving land ice in Greenland and Antarctica that are not fully included in the models; it should be noted that the AR4 added the caveat that 'larger values cannot be excluded' (IPCC, 2007b). The resultant upper (95-percentile) limit of the A1FI projection at 2095 (0.76 metres) is in good agreement with the similar projection from the TAR (Church et al, 2001). The AR4 lower (5-percentile) limit for B1 (0.18 metres) is roughly 0.1 m higher than the lower limit from the TAR. In summary, the AR4 range (5- to 95-percentile) of projected sea level at 2095 is 0.18 metres to 0.76 metres, relative to 1990.

Regional projections of sea-level rise were presented in the IPCC AR4. Since then, improved regional projections have been developed, including additional contributions to account for vertical land motion due to changes in the Earth's loading and gravitational field, caused by past and ongoing changes in land ice (e.g. Church et al, 2011 and Slangen et al, 2012); one derivation is described in detail in Appendix A of Hunter et al (2013)). The global-average of the projections of Church et al (2011) is shown in Figure 1, and the regional distribution from 1990 to 2090 for the A1B emission scenario is shown in Figure 2.

The purpose of this report is to provide *sea-level planning allowances* for Victoria. In this context, an 'allowance' is the vertical distance that a coastal entity needs to be raised in order to cope with the projected sea-level rise.

³The main emission scenarios used for the IPCC TAR and AR4 modelling are described in the Special Report on Emission Scenarios (SRES; Nakicenovic et al, 2000).

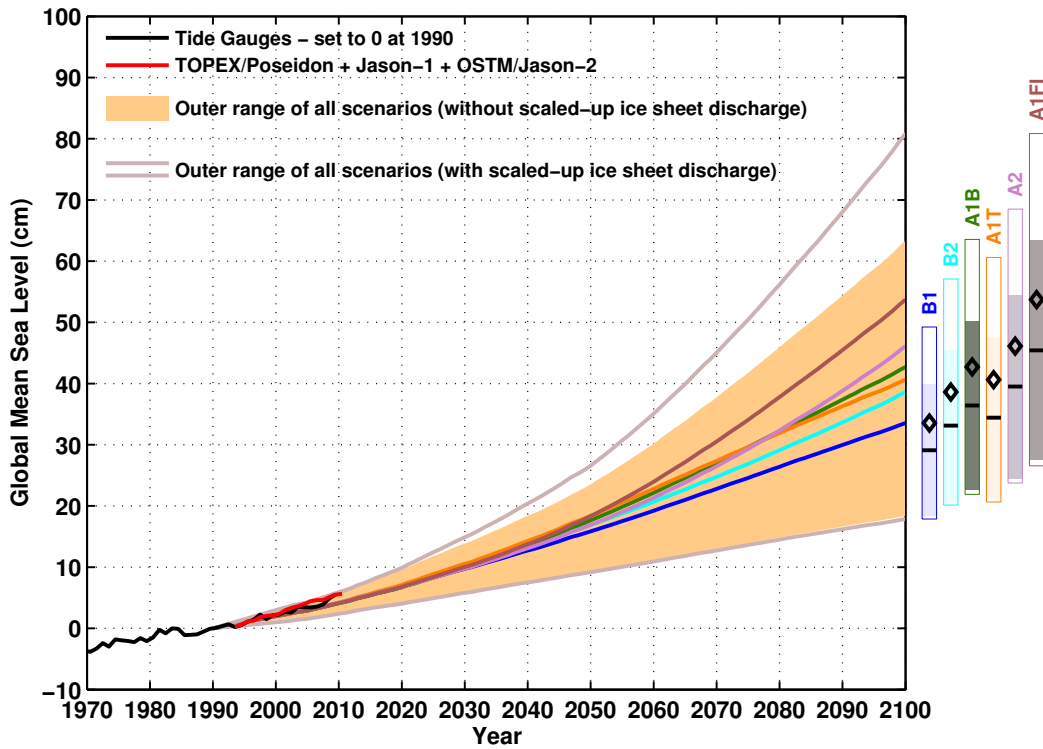


Figure 1: Global-average projections of sea-level rise relative to 1990, based on the IPCC AR4 (Meehl et al, 2007) and reproduced in Church et al (2011). The outer light lines and the shaded region show the 5- to 95-percentile range of projections with and without ‘scaled-up ice sheet discharge’ (SUI SD), respectively. The continuous coloured lines from 1990 to 2100 indicate the central value of the projections, with SUI SD. The open and shaded bars at the right show the 5- to 95-percentile range of projections for 2100 for the various SRES scenarios, with and without SUI SD. The diamonds and horizontal lines in the bars are the central values with and without SUI SD. The observational estimates of global-average sea level based on tide-gauge measurements and satellite altimeter data are shown in black and red, respectively. The tide-gauge data are set to zero at the start of the projections in 1990, and the altimeter data are set equal to the tide-gauge data at the start of the record in 1993.

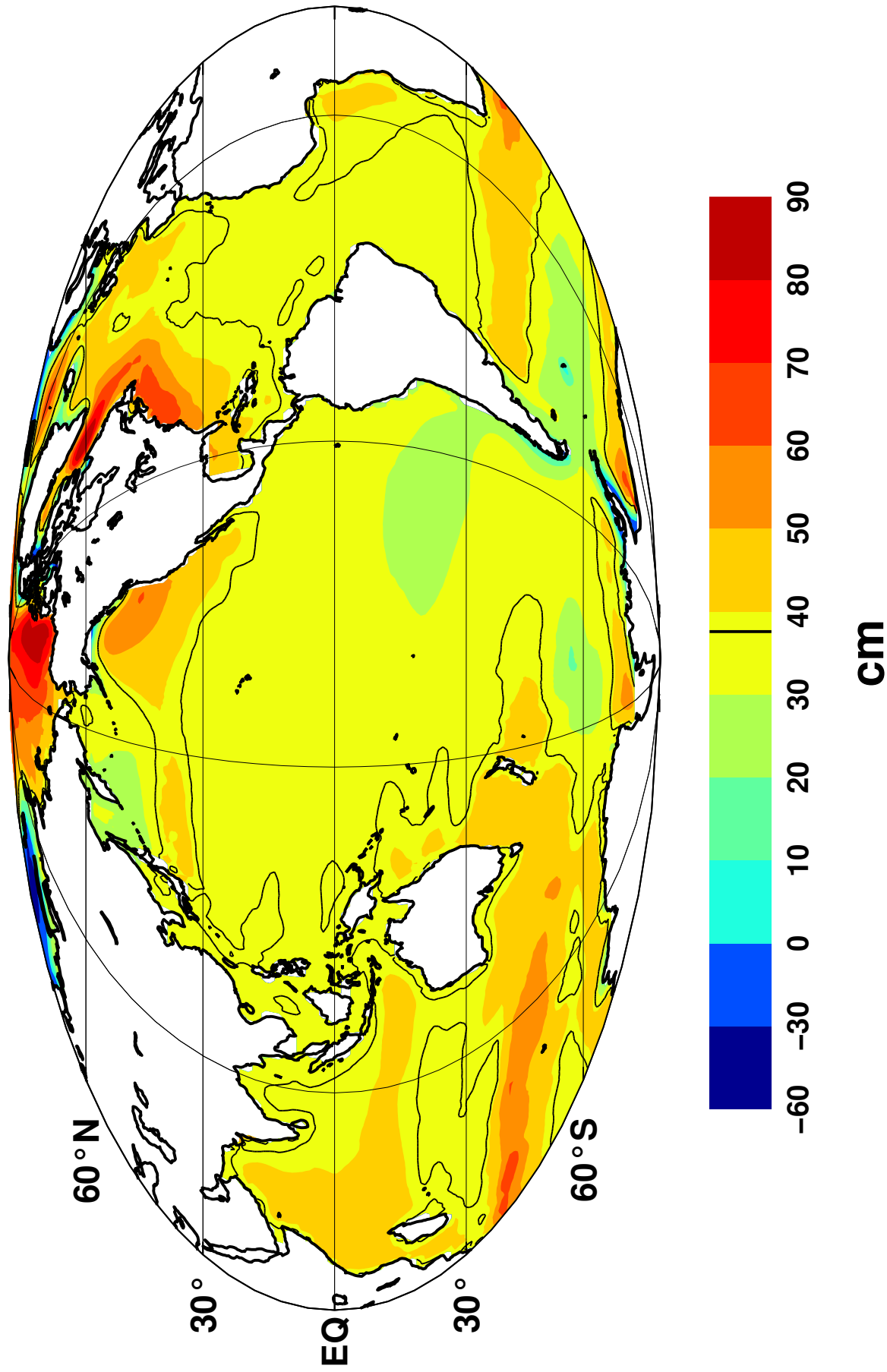


Figure 2: The regional distribution of the projections of sea-level change from 1990 to 2090, for the A1B emission scenario. This was obtained by combining global average sea-level rise, a spatially-varying component due to changes in ocean density and dynamics, and regional components associated with the changing distribution of land ice. The black contour and the black bar on the key indicate the global-average change (0.38 m), dividing those regions with above- and below-average sea-level rise. After Church et al, 2011.

3 Summary of Australian Planning Allowances

All Australian States have declared some form of sea-level planning allowance (see Table 1, although New South Wales recently abandoned theirs and replaced it with a general policy ‘giving councils the flexibility to consider coastal hazards in the context of their local circumstances’⁴. All the States except Tasmania have based their allowances on a perceived ‘upper limit’ (mainly, the 95-percentile maximum) of the available projections of sea-level rise (mostly from the IPCC). In 2012, Tasmania announced an allowance based on the method that is used in this report (Tasmanian Climate Change Office, 2012).

Table 1 shows that all Australian allowances for this century⁵ are in the range 0.8 to 1.0 metres. The current Victorian allowance is 0.2 metres for 1990-2040 (applicable to new urban infill developments) and 0.8 metres for 1990-2100 (applicable to greenfield developments).

State	Period	Allowance (m)	Notes
New South Wales	1990-2050	0.4 m	Now abandoned. Therefore, no present planning allowance.
	1990-2100	0.9 m	
NT	–		No planning allowance.
Queensland	1990-2100	0.8 m	For development not subject to a development commitment.
	1990-2050	0.3 m	For development already subject to a development commitment.
	1990-2060	0.4 m	” ”
	1990-2070	0.5 m	” ”
	1990-2080	0.6 m	” ”
	1990-2090	0.7 m	” ”
	1990-2100	0.8 m	” ”
South Australia	1990-2050	0.3 m	Infrastructure only needs be capable, by reasonably practical means, of being protected or raised to withstand this total sea level rise.
	1990-2100	1.0 m	
Tasmania	2010-2050	0.2 m	Based on the method of Hunter (2012), which is also used in this report.
	2010-2100	0.8 m	
Victoria	1990-2040	0.2 m	For new urban infill developments.
	1990-2100	0.8 m	For greenfield developments.
Western Australia	2010-2110	0.9 m	

Table 1: Summary of present sea-level rise allowances for Australia.

A disadvantage of basing an allowance on a perceived ‘upper limit’ of the sea-level rise projections is that it prompts the question: ‘how different would the future be if I chose the 50-percentile (the central value) rather than the 95-percentile maximum for my allowance?’. For example, it would appear at first sight that, basing an allowance on the 95-percentile maximum projections would be 19 times more likely to lead to over-adaptation than to under-adaptation; in other words, that it would be a significant over-reaction to the prospect of sea-level rise. Why should not an allowance be based on the best estimate (or central value) of the projections, rather than a higher value? The *precautionary principle*⁶

⁴See www.environment.nsw.gov.au/coasts/stage1coastreforms.htm

⁵Note that the exact period for ‘this century’ varies between States, with starting years of 1990 and 2010, and ending years of 2100 and 2110.

⁶e.g. www.environment.gov.au/epbc/about and www.environment.gov.au/about/esd/publications/igae

(Stein, 1999) is often given as a reason for basing decisions on ‘worst case’ scenarios, rather than the most likely ones. However, the precautionary principle has numerous definitions (Peel, 2005), some of which contain ‘vague statements . . . as well as ambiguities, inconsistencies and uncertainties’ (Stein, 1999). As a consequence, the principle is poorly understood by decision-makers and the courts (Stein, 1999), and gives little guidance as to which percentile level of a projection should be chosen as the basis for an allowance.

For the case of allowances for sea-level rise, the above problem may be avoided by employing a more objective technique (Hunter, 2012), which is described in Section 4. The resultant allowances *are independent of the required level of precaution*.

4 The Background Behind the Sea-Level Planning Allowance

Sea-level rise, like the change of many other climate variables, will be experienced mainly as an increase in the frequency or likelihood (probability) of extreme events, rather than simply as a steady increase in an otherwise constant state. One of the most obvious adaptations to sea-level rise is to raise an asset (or its protection) by an amount that is sufficient to achieve a required level of precaution. As noted in Section 3, the selection of such an allowance has generally been somewhat arbitrary, involving the identification of a perceived ‘upper limit’ of the sea-level rise projections. Hunter (2012) described a simple technique for estimating an allowance for sea-level rise using extreme-value theory. **This allowance ensures that the expected, or average, number of extreme (inundation) events in a given period is preserved. In other words, any asset raised by this allowance would experience the same frequency of inundation events under sea-level rise as it would without the allowance and without sea-level rise. It is important to note that this allowance only relates to the effect of sea-level rise on *inundation* and not on the recession of soft (e.g. sandy) shorelines or on other impacts.**

Under conditions of uncertain sea-level rise, the ‘expected number of inundation events in a given period’ is here defined in the following way. It is supposed that there are n possible futures, each with a probability, P_i , of being realised. For each of these futures, the expected number of inundation events in a given period is given by N_i . The effective, or overall, expected number of inundation events (considering all possible futures) is then considered to be $\sum_{i=1}^n P_i N_i$.

In the terminology of risk assessment (e.g. ISO, 2009), the expected number of inundation events in a given period is known as the *likelihood*. If a specific cost may be attributed to one inundation event, then this cost is termed the *consequence*, and the combined effect (generally the product) of the likelihood and the consequence is the *risk* (i.e. the total effective cost of damage from inundation over the given period). The allowance is therefore the height that an asset needs to be raised under sea-level rise in order to keep the inundation risk the same.

An important property of the allowance is that it is *independent of the required level of precaution*. In the case of coastal infrastructure, an appropriate height should first be selected, based on *present* conditions and an acceptable degree of precaution (e.g. an

average of one inundation event in 100 years). If this height is then raised by the allowance calculated for a specific period, the required level of precaution will be sustained until the end of this period.

The method assumes that there is no change in the variability of the extremes (specifically, the value of the *scale parameter of the Gumbel distribution*⁷ which describes this variability). In other words, the statistics of storm tides relative to mean sea level are assumed to be unchanged. It is also assumed that there is no change in wave climate (and therefore in wave setup and runup). The allowance derived from this method depends also on the probability distribution of the uncertainty in the rise in mean sea level at some future time. However, once this distribution and the Gumbel scale parameter has been chosen, the remaining derivation of the allowance is entirely objective.

Hunter (2012) combined the Gumbel scale parameters derived from 198 tide-gauge records in the *GESLA* (Global Extremes Sea-Level Analysis) database (see Menéndez and Woodworth, 2010) with projections of global-average sea-level rise, in order to derive estimates of the allowance around much of the world's coastlines. The spatial variation of this allowance therefore depended only on variations of the Gumbel scale parameter. Hunter et al (2013) derived improved estimates of the allowance using the same *GESLA* tide-gauge records, but with spatially-varying projections of sea level from the IPCC AR4 (Meehl et al, 2007) and enhancements to account for vertical land motion due to changes in the Earth's loading and gravitational field, caused by past and ongoing changes in land ice (Church et al, 2011).

The projections of the IPCC AR4 require some qualification. Even though the AR4 represents an extensive assessment of the state of climate science at the present time, some scientists have suggested that the sea-level projections (produced by process-based models) may be underestimates. Rahmstorf (2007), and later Horton et al (2008), Vermeer and Rahmstorf (2009), Grinsted et al (2010) and others, developed 'semi-empirical' models, whereby the relationship between temperature and sea level during the 20th century was used to project sea level into the 21st century based on the TAR and AR4 temperature projections (which are considered to be more reliable than the modelled sea-level projections). Rahmstorf's (2007) results suggested a rise of 0.5 to 1.4 metres at 2100 relative to 1990, but models of this simple type have attracted some controversy (e.g. Holgate et al, 2007; Schmith et al, 2007).

Nicholls et al (2011) summarised projections of sea-level rise published since the AR4. They suggested 'a pragmatic range of 0.5-2 m for twenty-first century sea-level rise, assuming a 4° C or more rise in temperature'. This temperature rise is achieved by the AR4 temperature projections for emission scenarios A1B, A2 and A1FI. They also concluded that 'the upper part of this range is considered unlikely to be realized' (the 2 m upper limit of this range being derived from Pfeffer et al (2008)). However, some of these estimates were based on maximum rates of rise (and not on the expected average rate over the 21st century) and some were based on semi-empirical models, the results of which (as noted above) are controversial.

Rahmstorf et al (2007) and Rahmstorf et al (2012) showed that, since 1990, global sea level have been tracking near the upper limit of the projections, again suggesting that the model projections may be underestimates. However, simple comparisons between the projected

⁷The statistics of extreme value distributions and the detailed derivation of the allowances will not be further explained here; they have been fully described by Hunter (2012).

and observed sea-level rise over the past two decades should be treated with some caution for two main reasons:

1. The comparison may be confounded by interannual and decadal variability. For example, Church and White (2011) showed that the satellite altimeter observations started (in 1993) during a period of relatively low sea level following (and possibly forced by) the Mt Pinatubo eruption in 1991; allowance for this relative low in observed sea level reduces the disagreement between observed and projected rates of rise for 1990-2010 from 60% to about 45% (the observations still being larger than the projections).
2. It is not at all clear how the current disagreement between observation and projections would translate into a comparable disagreement (either in rise or rate of rise) later in the century.

Bearing in mind the uncertainties in post-AR4 projections of sea-level rise, the allowances presented here use the spatially-varying projections developed by Hunter et al (2013). These are based on projections reported in the IPCC AR4 (Meehl et al, 2007) and enhancements to account for vertical land motion due to changes in the Earth's loading and gravitational field, caused by past and ongoing changes in land ice (Church et al, 2011). It is recommended that these projections are replaced by ones based on the IPCC AR5, when they become available in September 2013⁸. Church et al (2013) found good agreement between 20th century observations and hindcasts based on the models used for the AR5, providing additional support for these process-based models.

The allowances derived here are based on the following information:

1. the regional projections of sea-level rise for the A1FI emission scenario (which the world is broadly following at present; Le Quéré et al, 2009) used by Hunter et al (2013), extended to yield higher resolution along the Victorian coastline,
2. the statistics of storm tide extremes (i.e. the Gumbel scale parameter) from tide-gauge observations at Geelong, Point Lonsdale and Williamstown (from the GESLA database), and
3. the statistics of storm tide extremes (i.e. the Gumbel scale parameter) from the results of a storm-tide model of the Australian region (Haigh et al, 2012) (two versions of this model exist: one for simulating the effects of mid-latitude storms and the other for simulating the effects of tropical cyclones; due to Victoria's southerly location, only the results from the first version have been used here).

A normal or Gaussian distribution has been used to describe the uncertainty distribution of the sea-level rise projections. This represents a pragmatic compromise between a tightly confined distribution, and one with a fat upper tail (i.e. one in which there is a low probability of having a very high sea-level rise relative to the best estimate of that rise).

⁸See www.ipcc.ch/activities/key_dates_AR5_schedulepdf.pdf

Following Hunter (2012), the allowance A is given by:

$$A = \Delta z + \frac{\sigma^2}{2\lambda} \quad (1)$$

where Δz is the central value of the sea-level rise projection, σ is the standard deviation of the uncertainty of the sea-level rise projection, and λ is the Gumbel scale parameter (derived either from tide-gauge records or the storm-tide model). The standard deviation, σ , is derived from 5- and 95-percentile limits of the projections assuming that the uncertainty is normally distributed.

5 Sea-Level Planning Allowances for Victoria

5.1 Introduction

The locations used for the evaluation of the Victorian sea-level planning allowances are shown in Figure 3. Regionally-varying sea-level rise projections are available at all ten locations. The A1FI emission scenario (which the world is broadly following at present; Le Quéré et al, 2009) has been used throughout.

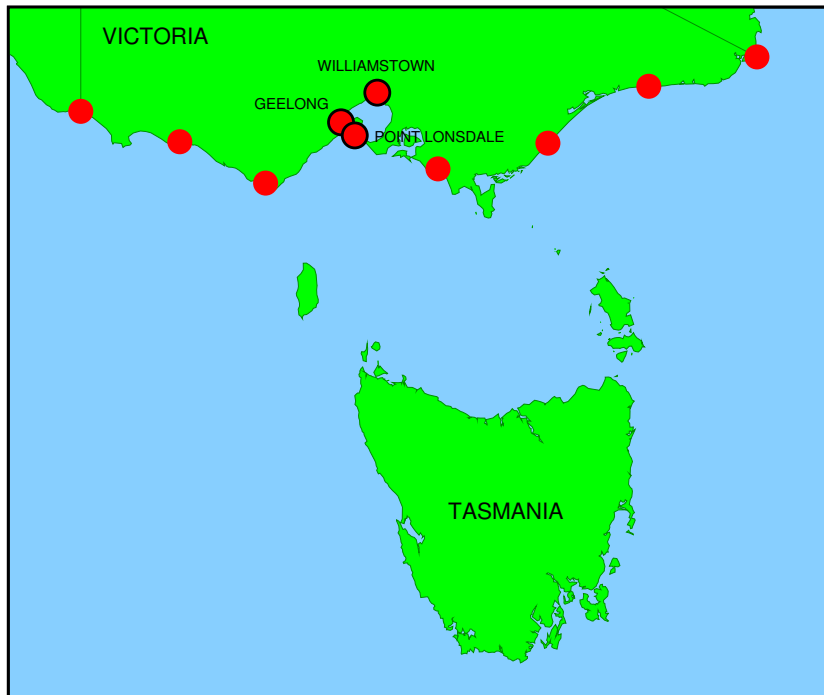


Figure 3: Locations of sites where sea-level planning allowance has been estimated. Red circles indicate locations where regional sea-level rise projections and the modelled storm-tide statistics (specifically, the Gumbel scale parameter) have been evaluated. Black rings indicates locations of tide gauges.

The statistics of present storm tides (specifically, the Gumbel scale parameter) have been estimated at all these sites using the storm-tide model of Haigh et al (2012), and from

tide-gauge data at Geelong, Point Lonsdale and Williamstown (shown by black rings in Figure 3). There are therefore two groups of allowances:

1. allowances for three locations, derived using the regionally-varying sea-level rise projections, combined with the Gumbel scale parameter from the tide gauges at Geelong, Point Lonsdale and Williamstown, and
2. allowances for ten locations, derived using the regionally-varying sea-level rise projections, combined with the Gumbel scale parameter from the storm-tide model of Haigh et al (2012).

It may be seen, from inspection of Tables 6 and 7, that the Gumbel scale parameters estimated from the tide gauges are about 0.015 metres greater than those estimated from the storm-tide model, and that the corresponding allowances estimated from the tide gauges are slightly *smaller* than those estimated from the storm-tide model (by about 0.03 metres for the period 2010-2100). *It is therefore recommended that sea-level planning allowances should be based on the allowances derived using the storm-tide model, because they are slightly larger (and therefore more conservative) and because they cover all ten locations along the coast.* However, the allowances derived using the tide-gauge data have been included here for completeness.

All allowances have been derived using Equation 1. The following Sections describe the results for planning periods of 2010-2040, 2010-2070 and 2010-2100.

Figures 5, 7 and 9, and Tables 3, 5 and 7 show an increasing trend in the allowance from west to east, particularly for the period 2010-2100. This suggests that it may be appropriate to prescribe different allowances in different regions, for any give period. However, this would represent a deviation from the current (or abandoned) policies in all Australian States; the suggestions given in Sections 5.2 to 5.4 are therefore based on the assumption that a single Victorian sea-level planning allowance will be prescribed for each period.

5.2 2010-2040

The results derived using the present storm-tide statistics from tide-gauges for the period 2010-2040 are shown in Figure 4 and Table 2.

The results derived using the present storm-tide statistics from the storm-tide model for the period 2010-2040 are shown in Figure 5 and Table 3. As noted in Section 5.1, the following discussion is confined to these results, rather than to those that were derived using the tide-gauge data.

Figure 5 and Table 3 suggest a suitable allowance of 0.1 metres, on the assumption that the allowances will be rounded to the nearest 0.1 metres.

5.3 2010-2070

The results derived using the present storm-tide statistics from tide-gauges for the period 2010-2070 are shown in Figure 6 and Table 4.

The results derived using the present storm-tide statistics from the storm-tide model for the period 2010-2070 are shown in Figure 7 and Table 5. As noted in Section 5.1, the following discussion is confined to these results, rather than to those that were derived using the tide-gauge data.

Figure 7 and Table 5 suggest a suitable allowance of 0.3 metres, or possibly 0.4 metres (which would be more conservative), on the assumption that the allowances will be rounded to the nearest 0.1 metres.

5.4 2010-2100

The results derived using the present storm-tide statistics from tide-gauges for the period 2010-2100 are shown in Figure 8 and Table 6.

The results derived using the present storm-tide statistics from the storm-tide model for the period 2010-2100 are shown in Figure 9 and Table 7. As noted in Section 5.1, the following discussion is confined to these results, rather than to those that were derived using the tide-gauge data.

Figure 9 and Table 7 suggest a suitable allowance of 0.7 metres, or possibly 0.8 metres (which would be more conservative), on the assumption that the allowances will be rounded to the nearest 0.1 metres.

6 Recommendations for Future Work

The most important work required in the near future should be a reassessment of the allowances derived here, based on the new regional sea-level projections which will be provided by the IPCC Fifth Assessment Report (AR5; Working Group I), when it is released in September, 2013⁹.

The allowances depend also on the estimates of the present storm-tide statistics (specifically, the Gumbel scale parameter), derived either from tide-gauges or a storm-tide model. It was shown in Section 5.1 that the allowances derived using these two methods differed by only about 0.03 metres (for the period 2010-2100), and so the two source of data are complementary. The storm-tide model has the advantage of providing data along the whole Victorian coastline, while the tide-gauge data may be used as a validation of the storm-tide model. Longer, and additional, tide-gauge records could in the future provide further validation of the model, and there are other storm-tide models of the Victorian coastline which could be investigated (e.g. McInnes et al, 2009). However, it should be noted (from Equation 1, Figure 9 and Table 7) that the storm-tide statistics (combined with the uncertainty of the sea-level projections) contribute, at most, 0.27 metres (the difference between the allowance and the central value of the projection) to the allowance; there are therefore diminishing returns in improving the estimates of the storm-tide statistics.

Investigations should continue into issues of local subsidence and vertical survey control. For example, Freij-Ayoub et al (2007) predicted subsidence by as much as 0.5 metres during the

⁹See www.ipcc.ch/activities/key_dates_AR5_schedulepdf.pdf

first half of the 21st century along the Gippsland coast. Also, conventional levelling techniques can introduce a height uncertainty of typically 0.1 metres, a factor which should be taken into account, for example if the site of a proposed development is remote from the sea-level reference point (e.g. the nearest local tide gauge). The accurate vertical control of LIDAR surveys is also an important consideration.

The allowances developed here are based on the assumption that any change in the statistics of storm tides during the 21st century would have a negligible effect compared with the projected sea-level rise. Although this assumption is well founded (see Section 1), it should be verified over time using both tide-gauge observations and the results of storm-tide models forced by a future climate.

The allowances also depend on the assumption that the wave climate will not change significantly during the 21st century. So far, there have been only a few models of future wave climate (e.g. Wang and Swail, 2006), but the field is advancing rapidly (e.g. the Coordinated Ocean Wave Climate Project (COWCLIP)¹⁰) and the forthcoming IPCC AR5 is expected to provide much new information.

Finally, it is important that sea-level planning allowances are communicated clearly to the policy, planning and development community and to the public at large. There has been much misinformation disseminated within Australia about climate change, sea-level rise and the likely related impacts. In particular, sea-level allowances are often portrayed as being over-precautionary, in part because they have generally been based on an ‘upper limit’ (e.g. the 95-percentile) of the projections provided by the IPCC. The allowances presented here have the advantage of being based on a largely objective technique, which takes the best available projections and indicates how high infrastructure needs to be raised in order to keep the average frequency of inundation events the same as it is today. This message needs to be communicated clearly and widely.

¹⁰See www.jcomm.info/COWCLIP.

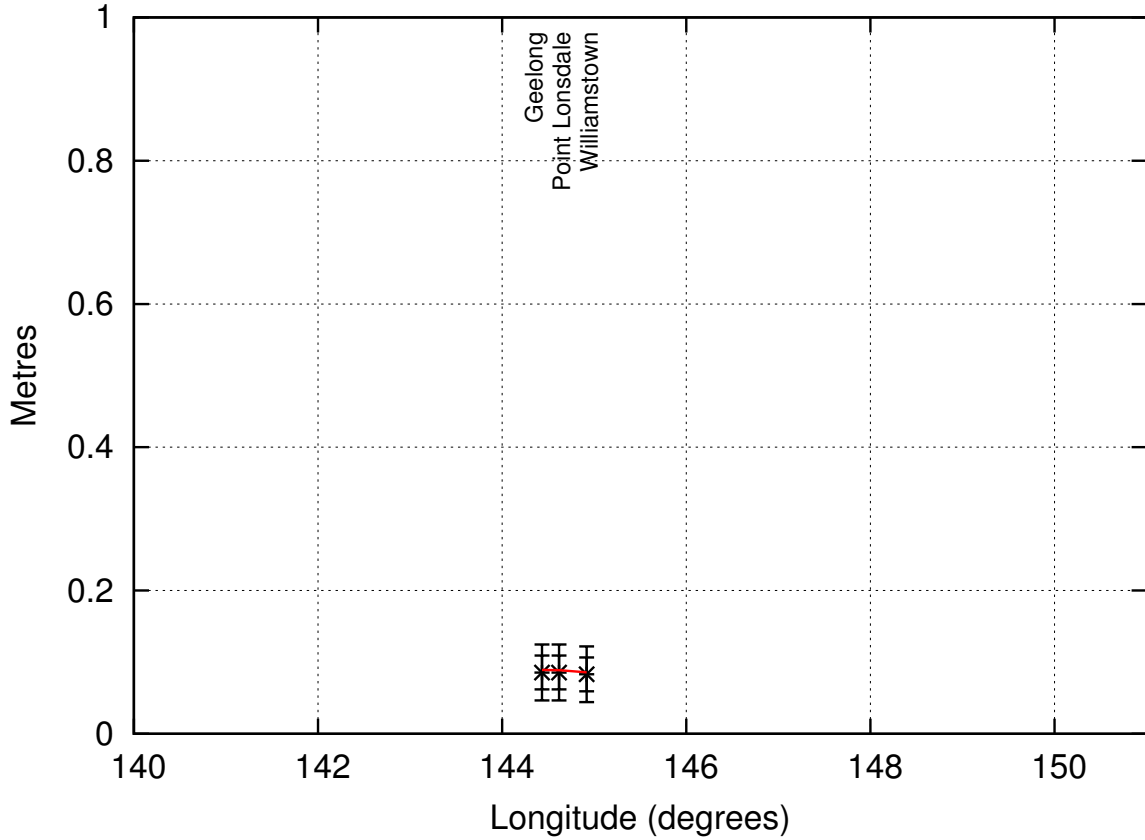


Figure 4: Sea-level projections (black bars; crosses indicating central value, inner range indicating \pm one standard deviation, and outer range indicating 5- to 95-percentile limits) and sea-level planning allowance (red curve), for SRES scenario A1FI and years 2010-2040, plotted against longitude for tide-gauge locations only. The allowances were derived using tide-gauge data.

Name	Longitude, Latitude ($^{\circ}$)	Gumbel scale parameter, λ (metres)	Projection $\Delta z, \sigma$ (metres)	Projection 5,95% (metres)	Allowance (metres)
Geelong	144.433, -38.167	0.077	0.09, 0.02	0.05, 0.12	0.09
Point Lonsdale	144.617, -38.300	0.085	0.09, 0.02	0.05, 0.12	0.09
Williamstown	144.917, -37.867	0.102	0.08, 0.02	0.04, 0.12	0.09

Table 2: Summary of locations, Gumbel scale parameter (from tide-gauge data), mean and standard deviation of sea-level projections, 5- 95-percentile range of sea-level projections, and sea-level planning allowances, for SRES scenario A1FI, years 2010-2040 and tide-gauge stations only.

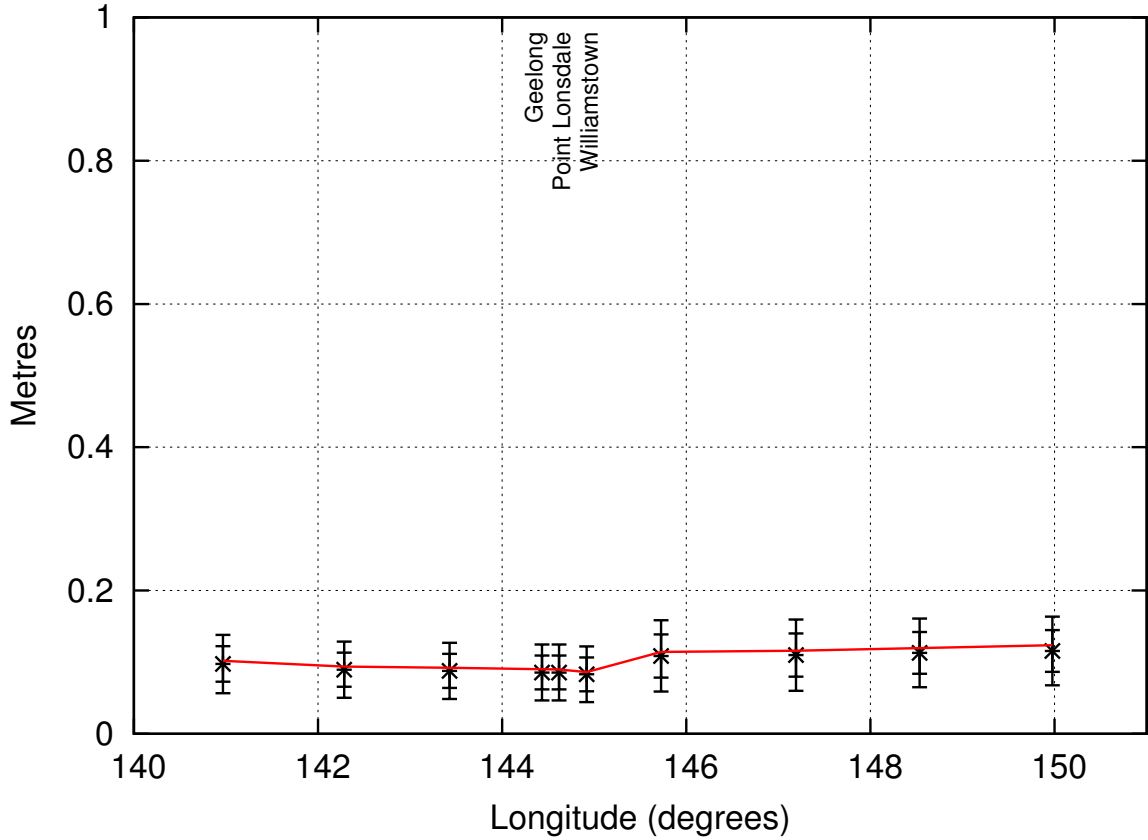


Figure 5: Sea-level projections (black bars; crosses indicating central value, inner range indicating \pm one standard deviation, and outer range indicating 5- to 95-percentile limits) and sea-level planning allowance (red curve), for SRES scenario A1FI and years 2010-2040, plotted against longitude for all locations. The allowances were derived using the storm-tide model.

Name	Longitude, Latitude ($^{\circ}$)	Gumbel scale parameter, λ (metres)	Projection $\Delta z, \sigma$ (metres)	Projection 5,95% (metres)	Allowance (metres)
Western coastal border	140.966, -38.056	0.067	0.10, 0.02	0.06, 0.14	0.10
East of Port Fairy	142.285, -38.364	0.066	0.09, 0.02	0.05, 0.13	0.09
West of Cape Otway	143.428, -38.783	0.067	0.09, 0.02	0.05, 0.13	0.09
Geelong	144.433, -38.167	0.060	0.09, 0.02	0.05, 0.12	0.09
Point Lonsdale	144.617, -38.300	0.069	0.09, 0.02	0.05, 0.12	0.09
Williamstown	144.917, -37.867	0.090	0.08, 0.02	0.04, 0.12	0.09
Inverloch	145.725, -38.639	0.082	0.11, 0.03	0.06, 0.16	0.11
Seaspray	147.190, -38.379	0.076	0.11, 0.03	0.06, 0.16	0.12
Marlo	148.534, -37.802	0.062	0.11, 0.03	0.07, 0.16	0.12
Eastern coastal border	149.975, -37.505	0.052	0.12, 0.03	0.07, 0.16	0.12

Table 3: Summary of locations, Gumbel scale parameter (from storm-tide model), mean and standard deviation of sea-level projections, 5- 95-percentile range of sea-level projections, and sea-level planning allowances, for SRES scenario A1FI, years 2010-2040, and all locations.

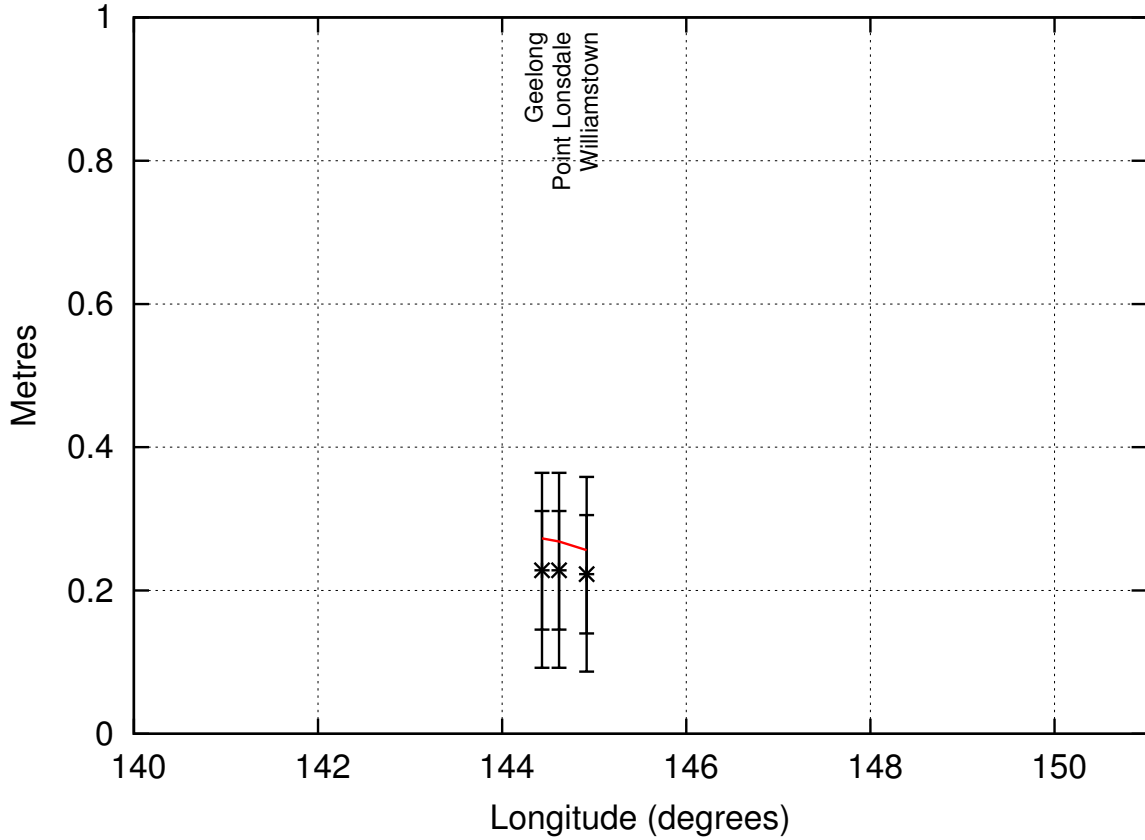


Figure 6: Sea-level projections (black bars; crosses indicating central value, inner range indicating \pm one standard deviation, and outer range indicating 5- to 95-percentile limits) and sea-level planning allowance (red curve), for SRES scenario A1FI and years 2010-2070, plotted against longitude for tide-gauge locations only. The allowances were derived using tide-gauge data.

Name	Longitude, Latitude ($^{\circ}$)	Gumbel scale parameter, λ (metres)	Projection $\Delta z, \sigma$ (metres)	Projection 5,95% (metres)	Allowance (metres)
Geelong	144.433, -38.167	0.077	0.23, 0.08	0.09, 0.36	0.27
Point Lonsdale	144.617, -38.300	0.085	0.23, 0.08	0.09, 0.36	0.27
Williamstown	144.917, -37.867	0.102	0.22, 0.08	0.09, 0.36	0.26

Table 4: Summary of locations, Gumbel scale parameter (from tide-gauge data), mean and standard deviation of sea-level projections, 5- 95-percentile range of sea-level projections, and sea-level planning allowances, for SRES scenario A1FI, years 2010-2070 and tide-gauge stations only.

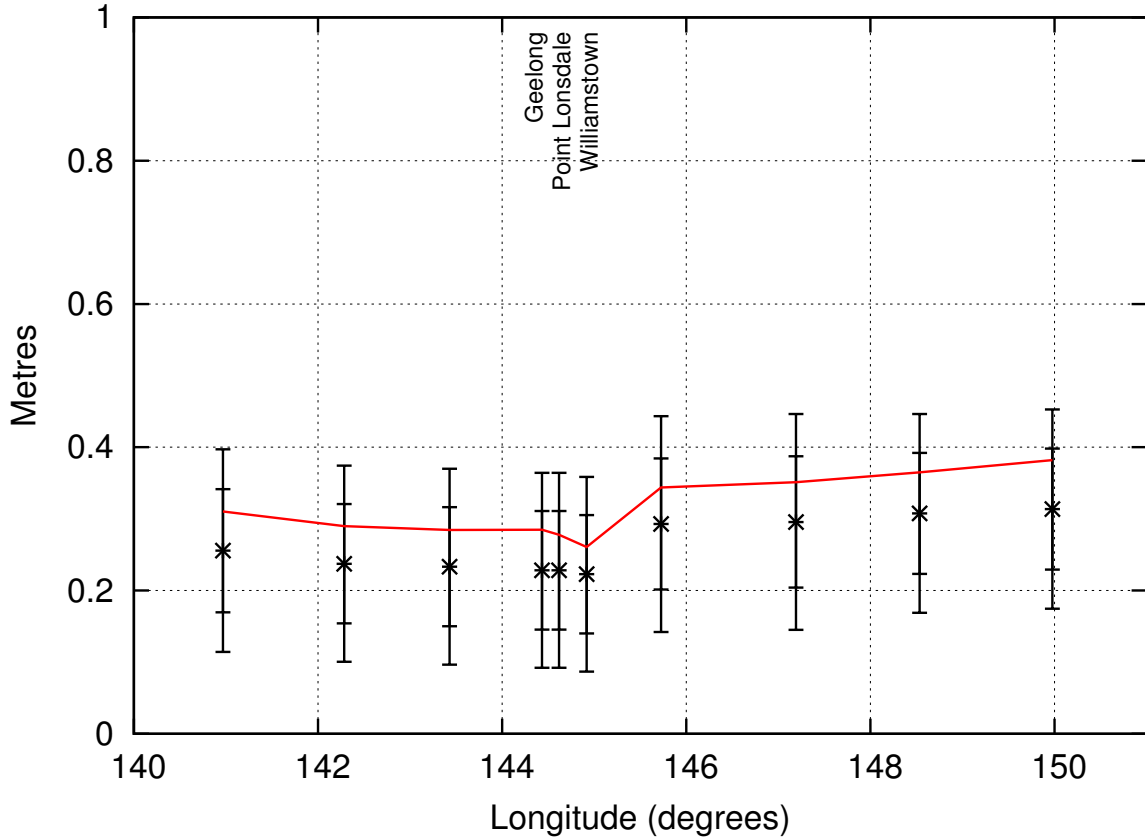


Figure 7: Sea-level projections (black bars; crosses indicating central value, inner range indicating \pm one standard deviation, and outer range indicating 5- to 95-percentile limits) and sea-level planning allowance (red curve), for SRES scenario A1FI and years 2010-2070, plotted against longitude for all locations. The allowances were derived using the storm-tide model.

Name	Longitude, Latitude (°)	Gumbel scale parameter, λ (metres)	Projection $\Delta z, \sigma$ (metres)	Projection 5,95% (metres)	Allowance (metres)
Western coastal border	140.966, -38.056	0.067	0.26, 0.09	0.11, 0.40	0.31
East of Port Fairy	142.285, -38.364	0.066	0.24, 0.08	0.10, 0.37	0.29
West of Cape Otway	143.428, -38.783	0.067	0.23, 0.08	0.10, 0.37	0.28
Geelong	144.433, -38.167	0.060	0.23, 0.08	0.09, 0.36	0.28
Point Lonsdale	144.617, -38.300	0.069	0.23, 0.08	0.09, 0.36	0.28
Williamstown	144.917, -37.867	0.090	0.22, 0.08	0.09, 0.36	0.26
Inverloch	145.725, -38.639	0.082	0.29, 0.09	0.14, 0.44	0.34
Seaspray	147.190, -38.379	0.076	0.30, 0.09	0.15, 0.45	0.35
Marlo	148.534, -37.802	0.062	0.31, 0.08	0.17, 0.45	0.36
Eastern coastal border	149.975, -37.505	0.052	0.31, 0.08	0.17, 0.45	0.38

Table 5: Summary of locations, Gumbel scale parameter (from storm-tide model), mean and standard deviation of sea-level projections, 5- 95-percentile range of sea-level projections, and sea-level planning allowances, for SRES scenario A1FI, years 2010-2070, and all locations.

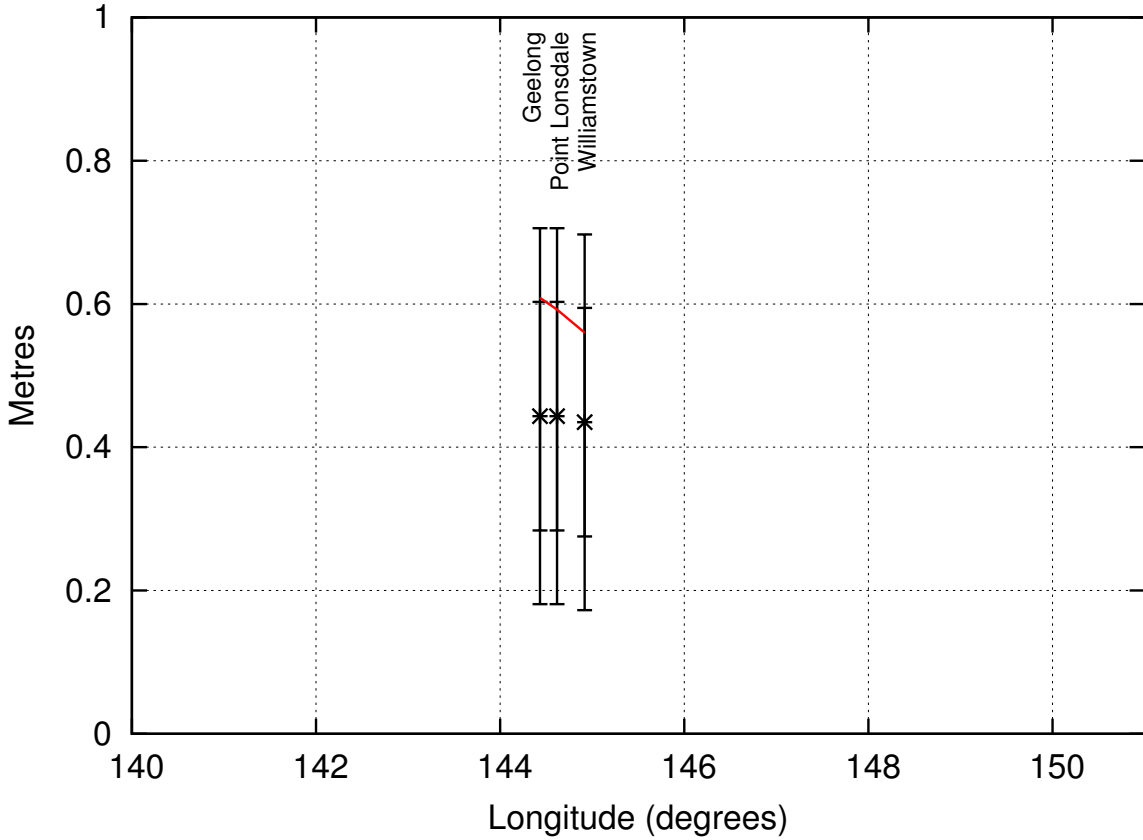


Figure 8: Sea-level projections (black bars; crosses indicating central value, inner range indicating \pm one standard deviation, and outer range indicating 5- to 95-percentile limits) and sea-level planning allowance (red curve), for SRES scenario A1FI and years 2010-2100, plotted against longitude for tide-gauge locations only. The allowances were derived using tide-gauge data.

Name	Longitude, Latitude ($^{\circ}$)	Gumbel scale parameter, λ (metres)	Projection $\Delta z, \sigma$ (metres)	Projection 5,95% (metres)	Allowance (metres)
Geelong	144.433, -38.167	0.077	0.44, 0.16	0.18, 0.71	0.61
Point Lonsdale	144.617, -38.300	0.085	0.44, 0.16	0.18, 0.71	0.59
Williamstown	144.917, -37.867	0.102	0.43, 0.16	0.17, 0.70	0.56

Table 6: Summary of locations, Gumbel scale parameter (from tide-gauge data), mean and standard deviation of sea-level projections, 5- 95-percentile range of sea-level projections, and sea-level planning allowances, for SRES scenario A1FI, years 2010-2100 and tide-gauge stations only.

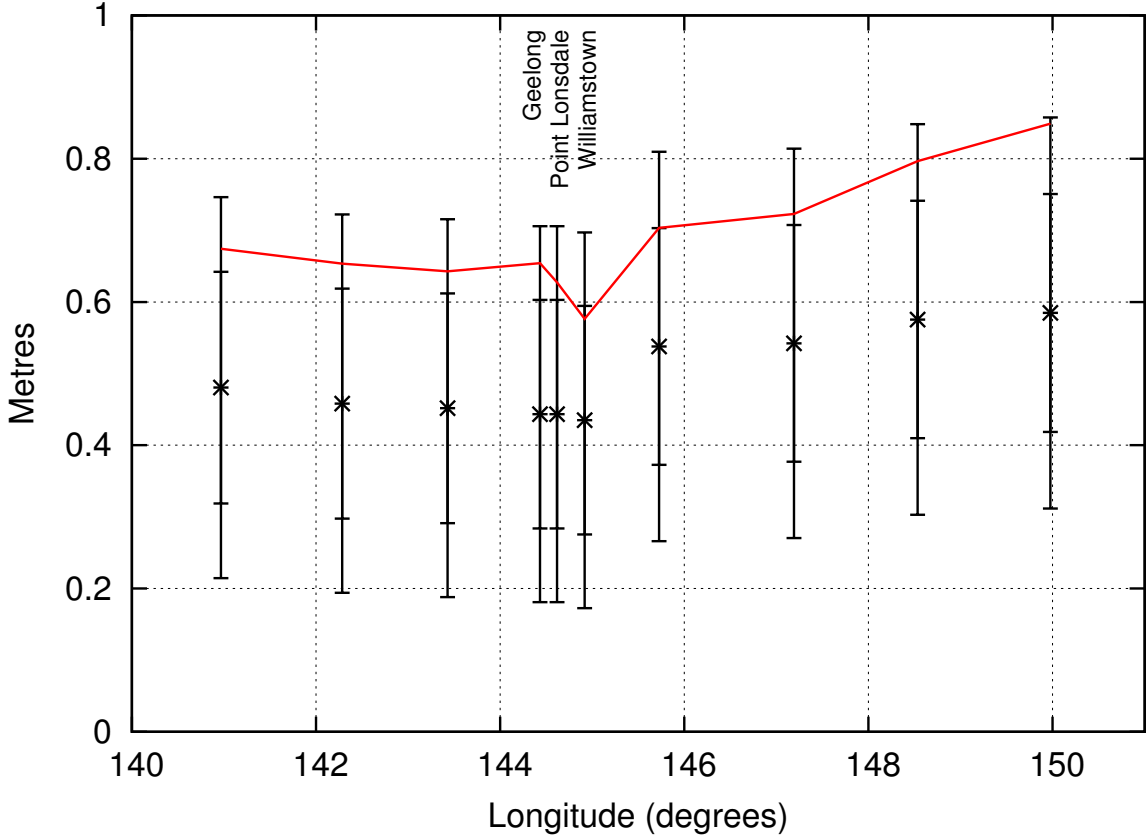


Figure 9: Sea-level projections (black bars; crosses indicating central value, inner range indicating \pm one standard deviation, and outer range indicating 5- to 95-percentile limits) and sea-level planning allowance (red curve), for SRES scenario A1FI and years 2010-2100, plotted against longitude for all locations. The allowances were derived using the storm-tide model.

Name	Longitude, Latitude ($^{\circ}$)	Gumbel scale parameter, λ (metres)	Projection $\Delta z, \sigma$ (metres)	Projection 5,95% (metres)	Allowance (metres)
Western coastal border	140.966, -38.056	0.067	0.48, 0.16	0.21, 0.75	0.67
East of Port Fairy	142.285, -38.364	0.066	0.46, 0.16	0.19, 0.72	0.65
West of Cape Otway	143.428, -38.783	0.067	0.45, 0.16	0.19, 0.72	0.64
Geelong	144.433, -38.167	0.060	0.44, 0.16	0.18, 0.71	0.65
Point Lonsdale	144.617, -38.300	0.069	0.44, 0.16	0.18, 0.71	0.63
Williamstown	144.917, -37.867	0.090	0.43, 0.16	0.17, 0.70	0.58
Inverloch	145.725, -38.639	0.082	0.54, 0.17	0.27, 0.81	0.70
Seaspray	147.190, -38.379	0.076	0.54, 0.17	0.27, 0.81	0.72
Marlo	148.534, -37.802	0.062	0.58, 0.17	0.30, 0.85	0.80
Eastern coastal border	149.975, -37.505	0.052	0.58, 0.17	0.31, 0.86	0.85

Table 7: Summary of locations, Gumbel scale parameter (from storm-tide model), mean and standard deviation of sea-level projections, 5- 95-percentile range of sea-level projections, and sea-level planning allowances, for SRES scenario A1FI, years 2010-2100, and all locations.

7 Glossary of Terms

AR4 Fourth Assessment Report of the Intergovernmental Panel on Climate Change.

AR5 Fifth Assessment Report of the Intergovernmental Panel on Climate Change.

COWCLIP Coordinated Ocean Wave Climate Project.

GESLA Global Extremes Sea-Level Analysis database.

IPCC Intergovernmental Panel on Climate Change.

LIDAR Light Detection and Ranging (a technique for remotely measuring land topography and sea bathymetry (in the present case, from the air)).

Sea-level planning allowance The vertical distance that a coastal entity needs to be raised in order to cope with the projected sea-level rise.

SRES Special Report on Emission Scenarios (Nakicenovic et al, 2000).

Storm tide The combination of tide and storm surge.

TAR Third Assessment Report of the Intergovernmental Panel on Climate Change.

8 Acknowledgements

An extended set of the regional projections of sea-level rise used by Hunter et al (2013) was provided by Neil White of the Commonwealth Scientific and Industrial Research Organisation. The tide-gauge data extracted from the GESLA database was provided by the National Tidal Centre. The data from the storm-tide model of the Australian region was provided by Steve George of the Antarctic Climate & Ecosystems Cooperative Research Centre.

References

- Bindoff N, Willebrand J, Artale V, Cazenave A, Gregory J, Gulev S, Hanawa K, Quéré CL, Levitus S, Nojiri Y, Shum C, Talley L, Unnikrishnan A (2007) Observations: Oceanic climate change and sea level. In: Solomon S, Qin D, Manning M, Chen Z, Marquis M, Averyt K, Tignor M, Miller H (eds) *Climate Change 2007: The Physical Science Basis. Contribution of Working Group I to the Fourth Assessment Report of the Intergovernmental Panel on Climate Change*, Cambridge University Press, Cambridge, United Kingdom and New York, NY, USA, chap 5, pp 385–432
- Church J, White N (2011) Sea-level rise from the late 19th to the early 21st century. *Surveys in Geophysics* 32(4-5):585–602, DOI 10.1007/s10712-011-9119-1
- Church J, Gregory J, Huybrechts P, Kuhn M, Lambeck K, Nhuan M, Qin D, Woodworth P (2001) Changes in sea level. In: Houghton J, Ding Y, Griggs D, Noguer M, van der Linden P, Dai X, Maskell K, Johnson C (eds) *Climate Change 2001: The Scientific Basis*,

Contribution of Working Group 1 to the Third Assessment Report of the Intergovernmental Panel on Climate Change, Cambridge University Press, Cambridge, United Kingdom and New York, NY, USA, chap 11, pp 639–693

- Church J, White N, Aarup T, Wilson W, Woodworth P, Domingues C, Hunter J, Lambeck K (2008) Understanding global sea levels: past, present and future. *Sustainability Science* 3(1):9–22
- Church J, Gregory J, White N, Platten S, Mitrovica J (2011) Understanding and projecting sea level change. *Oceanography* 24(2):130–143, DOI 10.5670/oceanog.2011.33
- Church J, Monselesan D, Gregory J, Marzeion B (2013) Evaluating the ability of process based models to project sea-level change. *Environmental Research Letters* 8(1):014,051, DOI 10.1088/1748-9326/8/1/014051
- Freij-Ayoub R, Underschultz J, Li F, Trefry C, Hennig A, Otto C, McInnes K (2007) Simulation of coastal subsidence and storm wave inundation risk in the Gippsland Basin. Tech. Rep. ‘CSIRO Petroleum Report 07-003’, Commonwealth Scientific and Industrial Research Organisation
- Grinsted A, Moore J, Jevrejeva S (2010) Reconstructing sea level from paleo and projected temperatures 200 to 2100 AD. *Climate Dynamics* 34:461–472, DOI 10.1007/s00382-008-0507-2
- Haigh I, Wijeratne E, MacPherson L, Mason M, Pattiaratchi C, Crompton R, S G (2012) Estimating present day extreme total water level exceedance probabilities around the Australian coastline. Tech. Rep. TR_STM05_120620, Antarctic Climate & Ecosystems Cooperative Research Centre
- Holgate S, Woodworth P (2004) Evidence for enhanced coastal sea level rise during the 1990s. *Geophysical Research Letters* 31(L07305), DOI 10.1029/2004GL019626
- Holgate S, Jevrejeva S, Woodworth P, Brewer S (2007) Comment on ‘a semi-empirical approach to projecting future sea-level rise’. *Science* 317(5846):1866b–1866c, DOI 10.1126/science.1140942
- Horton R, Herweijer C, Rosenzweig C, Liu J, Gornitz V, Ruane A (2008) Sea level rise projections for current generation cgcms based on the semi-empirical method. *Geophysical Research Letters* 35(L02715), DOI 10.1029/2007GL032486
- Hunter J (2012) A simple technique for estimating an allowance for uncertain sea-level rise. *Climatic Change* 113:239–252, DOI 10.1007/s10584-011-0332-1
- Hunter J, Church J, White N, Zhang X (2013) Towards a global regionally varying allowance for sea-level rise. *Ocean Engineering* (published online), DOI 10.1016/j.oceaneng.2012.12.041
- IPCC (2007a) *Climate Change 2007: The Physical Science Basis*. Contribution of Working Group I to the Fourth Assessment Report of the Intergovernmental Panel on Climate Change. Cambridge University Press, Cambridge, United Kingdom and New York, NY, USA

- IPCC (2007b) Summary for policymakers. In: Solomon S, Qin D, Manning M, Chen Z, Marquis M, Averyt K, Tignor M, Miller H (eds) *Climate Change 2007: The Physical Science Basis. Contribution of Working Group I to the Fourth Assessment Report of the Intergovernmental Panel on Climate Change*, Cambridge University Press, Cambridge, United Kingdom and New York, NY, USA, pp 1–18
- ISO (2009) 31000:2009 Risk Management – Principles and Guidelines. International Organisation for Standardization, www.iso.org
- Jevrejeva S, Grinsted A, Moore J, Holgate S (2006) Nonlinear trends and multiyear cycles in sea level records. *Journal of Geophysical Research* 111(C09012), DOI 10.1029/2005JC003229
- Le Quéré C, Raupach M, Canadell J, Marland G, et al (2009) Trends in the sources and sinks of carbon dioxide. *Nature Geoscience* 2:831–836, DOI 10.1038/ngeo689
- Lemke P, Ren J, Alley R, Allison I, Carrasco J, Flato G, Fujii Y, Kaser G, Mote P, Thomas R, Zhang T (2007) Observations: Changes in snow, ice and frozen ground. In: Solomon S, Qin D, Manning M, Chen Z, Marquis M, Averyt K, Tignor M, Miller H (eds) *Climate Change 2007: The Physical Science Basis. Contribution of Working Group I to the Fourth Assessment Report of the Intergovernmental Panel on Climate Change*, Cambridge University Press, Cambridge, United Kingdom and New York, NY, USA, chap 4, pp 337–383
- Lowe J, Woodworth P, Knutson T, McDonald R, McInnes K, Woth K, Von Storch H, Wolf J, Swail V, Bernier N, Gulev S, Horsburgh K, Unnikrishnan A, Hunter J, Weisse R (2012) Past and future changes in extreme sea levels and waves. In: Church J, Woodworth P, Aarup T, Wilson S (eds) *Understanding Sea-Level Rise and Variability*, Wiley-Blackwell, Oxford, United Kingdom, chap 11, pp 326–375
- McInnes K, Macadam I, Hubbert G, O’Grady J (2009) A modelling approach for estimating the frequency of sea level extremes and the impact of climate change in southeast Australia. *Natural Hazards* 51:115–137, DOI 10.1007/s11069-009-9383-2
- Meehl G, Stocker T, Collins W, Friedlingstein P, Gaye A, Gregory J, Kitoh A, Knutti R, Murphy J, Noda A, Raper S, Watterson I, Weaver A, Zhao ZC (2007) Global climate projections. In: Solomon S, Qin D, Manning M, Chen Z, Marquis M, Averyt K, Tignor M, Miller H (eds) *Climate Change 2007: The Physical Science Basis. Contribution of Working Group I to the Fourth Assessment Report of the Intergovernmental Panel on Climate Change*, Cambridge University Press, Cambridge, United Kingdom and New York, NY, USA, chap 10, pp 747–845
- Menéndez M, Woodworth P (2010) Changes in extreme high water levels based on a quasi-global tide-gauge data set. *Journal of Geophysical Research* 115(C10011), DOI 10.1029/2009JC005997
- Nakicenovic N, Alcamo J, Davis G, de Vries B, Fenhann J, Gaffin S, Gregory K, Grubler A, Jung T, Kram T, La Rovere E, Michaelis L, Mori S, Morita T, Pepper W, Pitcher H, Price L, Riahi K, Roehrl A, Rogner H, Sankovski A, Schlesinger M, Shukla P, Smith S, Swart R, van Rooijen S, Victor N, Dadi Z (2000) *Special Report on Emissions Scenarios. A Special Report of Working Group III of the Intergovernmental Panel on Climate Change*. Cambridge University Press, Cambridge, UK

- Nicholls R, Marinova N, Lowe J, Brown S, Vellinga P, de Gusmão D, Hinkel J, Tol R (2011) Sea-level rise and its possible impacts given a ‘beyond 4°C world’ in the twenty-first century. *Philosophical Transactions of the Royal Society A: Mathematical, Physical and Engineering Sciences* 369:161–181, DOI 10.1098/rsta.2010.0291
- Tasmanian Climate Change Office (2012) Derivation of the Tasmanian Sea Level Rise Planning Allowances. Tech. Rep. CA439492/4, Tasmanian Climate Change Office, Tasmanian Government
- Peel J (2005) *The Precautionary Principle in Practice*. Federation Press
- Pfeffer W, Harper J, O’Neel S (2008) Kinematic constraints on glacier contributions to 21st-century sea-level rise. *Science* 321(5894):1340–1343, DOI 10.1126/science.1159099
- Rahmstorf S (2007) A semi-empirical approach to projecting future sea-level rise. *Science* 315(5810):368–370, DOI 10.1126/science.1135456
- Rahmstorf S, Cazenave A, Church J, Hansen J, Keeling R, Parker D, Somerville R (2007) Recent climate observations compared to projections. *Science* 316(5825):709, DOI 10.1126/science.1136843
- Rahmstorf S, Foster G, Cazenave A (2012) Comparing climate projections to observations up to 2011. *Environmental Research Letters* 7(4):044,035, DOI 10.1088/1748-9326/7/4/044035
- Schmith T, Johansen S, Thejll P (2007) Comment on ‘a semi-empirical approach to projecting future sea-level rise’. *Science* 317(5846):1866c, DOI 10.1126/science.1143286
- Slangen A, Katsman C, van de Wal R, Vermeersen L, Riva R (2012) Towards regional projections of twenty-first century sea-level change based on IPCC SRES scenarios. *Climate Dynamics* 38:1191–1209, DOI 10.1007/s00382-011-1057-6
- Stein P (1999) Are decision-makers too cautious with the precautionary principle? In: *Land and Environment Court of New South Wales Annual conference*, Blue Mountains
- Vermeer M, Rahmstorf S (2009) Global sea level linked to global temperature. *Proceedings of the National Academy of Sciences* 106(51):21,527–21,532, DOI 10.1073/pnas.0907765106
- Wang X, Swail V (2006) Climate change signal and uncertainty in projections of ocean wave heights. *Climate Dynamics* 26:109–126, DOI 10.1007/s00382-005-0080-x
- Woodworth P, Blackman D (2004) Evidence for systematic changes in extreme high waters since the mid-1970s. *Journal of Climate* 17(6):1190–1197, DOI 10.1175/1520-0442(2004)017<1190:EFSCIE>2.0.CO;2
- Woodworth P, White N, Jevrejeva S, Holgate S, Church J, Gehrels W (2008) Evidence for the accelerations of sea level on multi-decade and century timescales. *International Journal of Climatology* 29:777–789, DOI 10.1002/joc.1771

A Copy of Hunter(2012) and Electronic Supplementary Material

A simple technique for estimating an allowance for uncertain sea-level rise

John Hunter

Received: 23 June 2011 / Accepted: 20 October 2011 / Published online: 23 November 2011
© Springer Science+Business Media B.V. 2011

Abstract Projections of climate change are inherently uncertain, leading to considerable debate over suitable allowances for future changes such as sea-level rise (an ‘allowance’ is, in this context, the amount by which something, such as the height of coastal infrastructure, needs to be altered to cope with climate change). Words such as ‘plausible’ and ‘high-end’ abound, with little objective or statistically valid support. It is firstly shown that, in cases in which extreme events are modified by an uncertain change in the average (e.g. flooding caused by a rise in mean sea level), it is preferable to base future allowances on estimates of the expected frequency of exceedances rather than on the probability of at least one exceedance. A simple method of determining a future sea-level rise allowance is then derived, based on the projected rise in mean sea level and its uncertainty, and on the variability of present tides and storm surges (‘storm tides’). The method preserves the expected frequency of flooding events under a given projection of sea-level rise. It is assumed that the statistics of storm tides relative to mean sea level are unchanged. The method is demonstrated using the *GESLA* (Global Extreme Sea-Level Analysis) data set of roughly hourly sea levels, covering 198 sites over much of the globe. Two possible projections of sea-level rise are assumed for the 21st century: one based on the Third and Fourth Assessment Reports of the Intergovernmental Panel on Climate Change and a larger one based on research since the Fourth Assessment Report.

Electronic supplementary material The online version of this article (doi:10.1007/s10584-011-0332-1) contains supplementary material, which is available to authorized users.

J. Hunter (✉)
Antarctic Climate & Ecosystems Cooperative Research Centre,
Private Bag 80, Hobart, TAS 7001, Australia
e-mail: john.hunter@utas.edu.au

1 Introduction

A major effect of climate change is a present and continuing increase in sea level, caused mainly by thermal expansion of seawater and the addition of water to the oceans from melted land ice (e.g. Meehl et al. (2007), as reported in the Fourth Assessment Report (AR4) of the Intergovernmental Panel on Climate Change (IPCC)). The present rate of global-average sea-level rise is about 3.2 mm yr^{-1} (Church and White 2011). At the time of AR4 in 2007, sea level was projected to rise at a maximum rate of about 10 mm yr^{-1} and to a maximum level of about 0.8 m (relative to 1990) by the last decade of the 21st century, in the absence of significant mitigation of greenhouse-gas emissions (Meehl et al. (2007, Table 10.7), including ‘scale-up ice sheet discharge’). However, since the AR4, there has been considerable debate about whether these projections are underestimates (e.g. Nicholls et al. (2011, Fig. 1) and [Online Resource](#), Table (i)), as discussed in Section 5.2.

Sea-level rise, like the change of many other climate variables, will be expressed mainly as an increase in the frequency or likelihood (probability) of extreme events, rather than simply as a steady increase in an otherwise constant state. One of the most obvious adaptations to sea-level rise is to raise infrastructure by a sufficient amount so that flooding events occur no more often than they did prior to the sea-level rise. The selection of such an *allowance* has often, unfortunately, been quite subjective and qualitative, involving concepts such as ‘plausible’ or ‘high-end’ projections.

This paper develops a simple technique for estimating an allowance for sea-level rise using elementary extreme-value theory. This allowance ensures that the expected, or average, number of extreme events in a given period is conserved. In other words, any infrastructure raised by this allowance would experience the same frequency of extreme events under sea-level rise as it would without the allowance and without sea-level rise.

Present evidence (Bindoff et al. 2007; Woodworth and Blackman 2004) suggests that the rise in mean sea level is generally the dominant cause of the observed increase in the frequency of extreme events (i.e. that the statistics of the effect of storminess on sea level is approximately stationary). It is therefore assumed here that there is no change in the variability of the extremes (specifically, the *scale parameter* of the Gumbel distribution; see Section 4). In other words, the statistics of storm tides relative to mean sea level are assumed to be unchanged.

The allowance derived from this method depends strongly on the probability distribution of the rise in mean sea level at some future time. However, once this distribution has been chosen, the remaining derivation of the allowance is entirely *objective*.

Unless otherwise stated, uncertainties are here given as \pm one standard deviation (indicated by ‘sd’) or as \pm the half-range (indicated by ‘lim’). In the latter case, the half-range represents true limits, with zero probability outside the indicated range.

2 Statistics which describe the likelihood of extremes

Extremes are generally described by *exceedance events* which are events which occur when some variable exceeds a given level.

Two statistics are conventionally used to describe the likelihood of extreme events such as flooding from the ocean. These are the *average recurrence interval* or *ARI* (R), and the *exceedance probability* (E) for a given period (T). The ARI is the average period between extreme events (observed over a long period with many events), while the exceedance probability is the probability of at least one exceedance event happening during the period T . Exceedance distributions are often expressed (as in Section 4) in terms of the *cumulative distribution function*, F , where $F = 1 - E$. F is just the probability that there will be *no* exceedances during the prescribed period, T . These statistics are related by (e.g. Pugh 1996):

$$F = 1 - E = \exp\left(-\frac{T}{R}\right) = \exp(-N) \tag{1}$$

where N is the expected, or average, number of exceedances during the period T .

Equation 1 involves the assumption (made throughout this paper) that exceedance events are independent; their occurrence therefore follows a Poisson distribution. This requires a further assumption about the relevant time scale of an event. If multiple closely-spaced events have a single cause (e.g. flooding events caused by one particular storm), they are generally combined into a single event using a declustering algorithm.

The occurrence of sea-level extremes, and therefore the ARI and the exceedance probability, will be modified by sea-level rise, the future of which has considerable uncertainty. For example, the projected sea-level rise for 2090–2099 relative to 1980–1999, for the A1FI Emission Scenario (which the world is broadly following at present; Le Quéré et al. 2009), is 0.50 ± 0.26 m (5–95% range, including scaled-up ice sheet discharge; Meehl et al. 2007), the range being larger than the central value.

Let us first consider a simple case in which there are two possible futures, with probabilities P_1 and P_2 ($P_1 + P_2 = 1$). If the exceedance probabilities in these two cases are E_1 and E_2 , respectively, then the overall exceedance probability (taking into account both possible futures) is just $P_1E_1 + P_2E_2$. However a similar relationship does not hold for the ARI; if the respective ARIs are R_1 and R_2 , then the ‘overall’ ARI, $P_1R_1 + P_2R_2$, has little meaning and is not useful for assessing risk. There is, nevertheless, a related variable which *may* be usefully combined probabilistically in this way - the *expected number of exceedances in a given period*.

If the period is T and the respective ARIs are R_1 and R_2 , then the expected number of exceedances in each case are $N_1 = T/R_1$ and $N_2 = T/R_2$, and the overall expected number of exceedances is $P_1N_1 + P_2N_2 = T(P_1/R_1 + P_2/R_2)$.

The above can, of course be readily extended to more realistic cases in which there are more than two futures, so long as each has an estimated probability of occurrence and the sum of all the probabilities is one. There are therefore two statistical quantities which can be readily used to estimate an ‘overall’ result under conditions of uncertainty: the *exceedance probability*, E , and the *expected number of exceedances*, N .

If the probability distribution of the exceedance probability is given by P_E , then the overall exceedance probability, E_{ov} , is given by

$$E_{ov} = \int_{-\infty}^{\infty} P_E E dE \tag{2}$$

Similarly, if the probability distribution of the expected number of exceedances is given by P_N , then the overall expected number of exceedances, N_{ov} , is given by

$$N_{ov} = \int_{-\infty}^{\infty} P_N N dN \tag{3}$$

What are the relative merits of these two statistics? For low exceedance probabilities ($E \ll 1$), Eq. 1 indicates, using a Taylor series approximation, that $E \approx N$ (i.e. the statistics are approximately equivalent) and so the question does not arise. However, the exceedance probability is the probability of *at least* one exceedance event happening during the period T and, as E increases above about 0.6, it becomes increasingly likely that the number of events will exceed one. If the exceedance statistic is to be used to estimate *risk* (i.e. the combination of *likelihood* (E) and *consequence* (e.g. the damage cost of each event)), then knowing only the probability of *one or more events* occurring may not be sufficient—an estimate of the expected number of exceedances, N , is generally more useful.

Section 3 discusses the relationship between the exceedance probability (E) and the expected number of exceedances (N) and, in particular, the way in which this relationship is modified by additional uncertainty (yielding E_{ov} and N_{ov}).

3 The effect of uncertainty on a Poisson-distributed variable

For exceedance events that are Poisson-distributed, the relationship between E and N is given in Eq. 1 and plotted in Fig. 1 (solid curve). The solid square indicates the well-known result (e.g. Pugh 2004, p. 181), that, if the expected number of exceedances in a given period is one, then the exceedance probability is 0.63 (63%). The solid circles (1 and 2) indicate two possible situations (or ‘futures’), as considered in the simple example of Section 2; these have exceedance probabilities $E_1 = 0.1$ (10%) and $E_2 = 0.9$ (90%), respectively. As discussed in Section 2, the overall

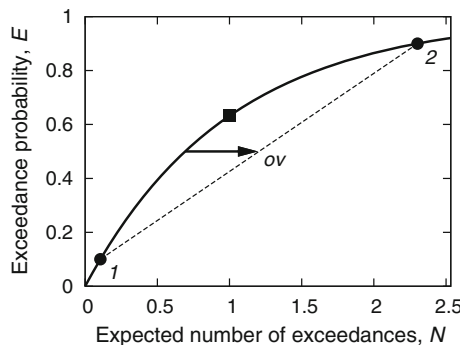


Fig. 1 Solid curve shows exceedance probability as a function of expected number of exceedances for a Poisson distribution. Solid square indicates exceedance probability of 0.63 (63%) for the case of one expected exceedance. Solid circles (1 and 2) indicate exceedance probabilities of 0.1 (10%) and 0.9 (90%), respectively. Dashed line represents range of possible exceedance probabilities and expected numbers of exceedances for a weighted average of values indicated by solid circles. Tail of arrow indicates exceedance probability of 0.5 (50%) for a Poisson distribution and head of arrow (‘ov’) indicates same exceedance probability but for simple average of values indicated by solid circles

exceedance probability and expected number of exceedances (taking into account both possible situations) are $P_1 E_1 + P_2 E_2$ and $P_1 N_1 + P_2 N_2$, respectively, where P_1 and P_2 are the respective probabilities of occurrence of situations 1 and 2. The dashed line therefore represents the range of possible exceedance probabilities and expected numbers of exceedances for the overall outcome, for all values of P_1 and P_2 (given that $P_1 + P_2 = 1$). For example, if $P_1 = P_2 = 0.5$, then the overall values, E_{ov} and N_{ov} , are as shown by the arrow head ('ov'). The tail of the arrow indicates the expected number of exceedances for an exceedance probability of 0.5 (50%), given a Poisson distribution.

The above illustrates the general rule that, if multiple situations are considered, and if each situation is governed by a different Poisson process, then the resultant overall values (E_{ov} and N_{ov}) do not accord with the Poisson relationship (the continuous curve in Fig. 1). In fact, due to the curvature of the $E(N)$ relationship, the expected number of exceedances is significantly higher than the value we would expect from a Poisson process with the same exceedance probability. In the present example, the overall expected number of exceedances is 1.20, compared with the 'Poisson' value of 0.69. For low exceedance probabilities, such as this, this difference is really only academic. However, if we take the case of $E_1 = 0.27$ (27%) and $E_2 = 0.99$ (99%), then (for $P_1 = P_2 = 0.5$) the overall expected number of exceedances is 2.5, compared with 1.0 for a Poisson process with the same overall exceedance probability (0.63 or 63%). It is clear from Fig. 1 that, as $E_2 \rightarrow 1$, the difference between the overall expected number of exceedances and those for a Poisson process $\rightarrow \infty$.

Planners and policymakers have had considerable experience in designing planning directives and building codes during a period of relatively unchanging climate. Let us suppose that, on the basis of previous experience, the situation for a particular item of infrastructure is presently regarded as 'safe' if the ARI (R), the exceedance probability (E) or the expected number of exceedances (N) satisfy one of the following constraints:

$$\begin{aligned}
 R &\geq R_{\text{safe}} \\
 E &\leq E_{\text{safe}} \quad \text{for a given period, } T \\
 N &\leq N_{\text{safe}} \quad \text{for a given period, } T
 \end{aligned}
 \tag{4}$$

where R_{safe} , E_{safe} and N_{safe} may be regarded as planning guidelines.

Until recently, the consideration of possible different situations (or 'futures') has not been necessary and so R_{safe} , E_{safe} , N_{safe} and T were related by Eq. 1. However, future climate change will bring not just *change* but also its accompanying *uncertainty*. Any new planning guidelines will therefore have to take Eqs. 2 and 3 into account, yielding estimates of E_{ov} and N_{ov} . Figure 2 indicates that, for any general future situation where the uncertainty of climate change has been taken into account, the critical constraint is $N_{ov} \leq N_{\text{safe}}$; if this is satisfied, so also is $E_{ov} \leq E_{\text{safe}}$ (e.g. point A). However, $E_{ov} \leq E_{\text{safe}}$ does not ensure that $N_{ov} \leq N_{\text{safe}}$ (e.g. point B).

It is therefore concluded that future allowances for climate change extremes (e.g. related to sea-level rise) should be based on estimates of the *expected number of exceedances* rather than on the *exceedance probability*. Section 4 now describes the derivation of an allowance for uncertain sea-level rise which conserves the expected number of exceedances in a given period.

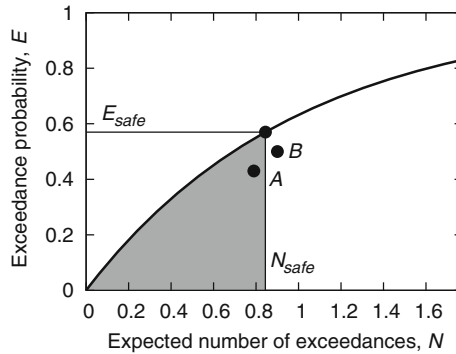


Fig. 2 Solid curve shows exceedance probability as a function of expected number of exceedances for a Poisson distribution. Solid circle (at N_{safe}, E_{safe}) represents a situation regarded as safe under conditions of relatively unchanging climate. Shaded area shows region for which $N_{ov} \leq N_{safe}$ and $E_{ov} \leq E_{safe}$ for situations (described by N_{ov}, E_{ov} in Eqs. 2 and 3) in which the uncertainty of climate change has been taken into account (requiring that they must lie to the right of or below the curve). The critical constraint is $N_{ov} \leq N_{safe}$; if this is satisfied, so also is $E_{ov} \leq E_{safe}$ (e.g. point A). However, $E_{ov} \leq E_{safe}$ does not ensure that $N_{ov} \leq N_{safe}$ (e.g. point B)

4 Theory

The probability of exceedances above a given level and over a given period is often well described by a generalised extreme-value distribution (GEV). The simplest of these, the Gumbel distribution, fits most sea-level extremes quite well (e.g. van den Brink and Können 2011). The Gumbel distribution may be expressed as (e.g. Coles 2001, p. 47)

$$F = \exp\left(-\exp\left(\frac{\mu - z}{\lambda}\right)\right) \tag{5}$$

where z is the height, μ is the ‘location parameter’ and λ is the ‘scale parameter’ (an e-folding distance in the vertical). F is the probability that there will be no exceedances $> z$ during the prescribed period, T .

From Eqs. 1 and 5

$$N = \exp\left(\frac{\mu - z}{\lambda}\right) \tag{6}$$

μ is therefore the value of z for which $N = 1$ during the period T .

As noted in Section 1, it is assumed that the scale parameter, λ , does not change with a rise in sea level.

Given that the scale parameter is a key player in the present work, it is worth considering the factors which determine its magnitude. Firstly, the scale parameter relates to extremes and therefore to the variability of the maxima in sea level (over some prescribed period such as a year), rather than to the total variability in sea level. Therefore a large tidal range, with only weak modulation (i.e. almost a pure sinusoid) would have a small scale parameter. Conversely, a small tidal range, with strong modulation (e.g. a strong neap/spring cycle) would have a large scale parameter. The situation is further complicated by the character of the storm surges, so that tidal

range is not a good indicator of the magnitude of the scale parameter. For example, in Australia, the tidal range at Sydney (1.3 m) is over twice the range at Fremantle (0.6 m). However, the scale parameter at Sydney (0.06 m) is only half of the scale parameter at Fremantle (0.12 m).

Mean sea level is now raised by an amount $\Delta z + z'$, where Δz is the central value of the estimated rise and z' is a random variable with zero mean and a distribution function, $P(z')$, to be chosen below. This effectively increases the location parameter, μ , by $\Delta z + z'$. From Eqs. 3 and 6, the expected number (N_{ov}) of exceedances ($> z$) during the period T , now becomes

$$\begin{aligned}
 N_{ov} &= \int_{-\infty}^{\infty} P(z') \exp\left(\frac{\mu - z + \Delta z + z'}{\lambda}\right) dz' \\
 &= N \exp\left(\left(\Delta z + \lambda \ln\left(\int_{-\infty}^{\infty} P(z') \exp\left(\frac{z'}{\lambda}\right) dz'\right)\right) / \lambda\right) \quad (7)
 \end{aligned}$$

(noting that we again use the subscript ‘ov’ to indicate integration over a range of possibilities).

The term $\lambda \ln(\dots)$ in the last part of Eq. 7 represents an *additional* allowance arising from the *uncertainty* in future sea-level rise. It is evaluated for three types of distribution: a normal distribution, a boxcar (uniform) distribution and a raised cosine distribution (see [Online Resource](#), Section A). The resulting allowances are all expressed as simple analytical expressions, involving the Gumbel scale parameter, λ , the central value of the estimated rise, Δz , and its standard deviation, σ . The boxcar and raised cosine distributions, which have upper and lower limits, are considered here because there are quite strong physical constraints on sea-level rise. For example, it is highly unlikely that sea level will fall under global warming and Pfeffer et al. (2008) deduced an upper limit of sea-level rise for the 21st century of 2.0 m. The raised cosine distribution (which is used later to describe a possible 21st-century sea-level rise projection) is given by:

$$P(z') = \frac{1}{W} \left(1 + \cos\left(\frac{2\pi z'}{W}\right)\right) \quad \text{for } -W/2 < z' < W/2 \quad \text{otherwise } 0 \quad (8)$$

where W is the full-width of the distribution.

5 Projections of sea-level rise

The sea-level rise allowance described in Section 4 requires an estimate of the mean sea-level rise, Δz , and its uncertainty, σ . These estimates may be provided by combining results from the IPCC Assessment Reports (specifically, the Third Assessment Report (TAR; Church et al. 2001) and the AR4 (Meehl et al. 2007)), and from research conducted since the AR4, as summarised for example by Nicholls et al. (2011). As will be seen, these two sources of information (i.e. TAR/AR4 and post-AR4) lead to two rather distinct ranges and are treated separately in the following discussion. At present, it is unclear which of the two is the more appropriate.

It should also be noted that there is considerable disagreement between models as to the regional variation of future sea-level rise (Meehl et al. 2007, Fig. 10.32). The present work uses only projections of *global-average* sea-level rise; regional variation therefore represents additional uncertainty.

The projections described here apply only to the component of sea-level rise that is related to anthropogenic climate change. They do not include any effects of vertical land movement, such as those associated with glacial isostatic adjustment, tectonic activity or local land sinkage (e.g. due to groundwater withdrawal). Any such movement, and its uncertainty, should be incorporated into the projections, to yield the sea-level rise relative to the land.

5.1 The TAR and AR4 projections

For each of the six ‘marker’ emission scenarios (A1B, A1T, A1FI, A2, B1 and B2), the TAR gave the ‘range of all AOGCMs (*Atmosphere-Ocean General Circulation Models*)... including uncertainty in land-ice changes, permafrost changes and sediment deposition’ at decadal increments through the 21st century, relative to 1990 (Church et al. 2001, Table II.5.1). The ‘range of all AOGCMs’ has been interpreted to be ± 2 standard deviations (Church et al. 2001, Box 11.1; Meehl et al. 2007, 10.A.6). On the other hand, the AR4 gave the ‘5 to 95% range (m) of the rise in sea level’ and included an additional contribution (‘scaled-up ice sheet discharge’) to account for ‘rapid dynamical changes’ in ice sheets that were not simulated by continental ice sheet models (Meehl et al. 2007). The AR4 results were only presented as the sea-level rise for 2090–2099 relative to 1980–1999. Both the TAR and AR4 results apparently relate to the *spread* of model projections (akin to the *standard deviation*) rather than to the uncertainty (akin to the *standard error*) of the best estimate of the projections. The uncertainty, σ , used in Section 4 and in [Online Resource](#), Section A, Eqs. (viii), (ix) and (x), strictly relates to the *standard error*. However, for reasons discussed in [Online Resource](#), Section B, the uncertainty, σ , is here associated with the *standard deviation* (rather than the *standard error*) of the projections.

In order to obtain time series of model projections through the 21st century that are compatible with the AR4, Hunter (2010) fitted the time series of TAR projections through the AR4 projections for 2090–2099. The resultant tables (Hunter 2010, Tables 1 and 2) are similar to Table II.5.1 of the TAR, except that they relate to the 5–95% range, rather than to the ‘range of all AOGCMs’. They are here referred to as the *AR4-adjusted TAR projections*. It should be noted that, for the last decade of the 21st century, these *are* the AR4 projections.

Therefore, the first set of sea-level rise allowances is based on the A1FI emission scenario (which the world is broadly following at present; Le Quéré et al. 2009) and the *AR4-adjusted TAR projections*, as follows:

1. the mean sea-level rise, Δz , was derived from the average of the 5 and 95% values, and
2. the uncertainty, σ , was approximated by the *standard deviation* of the projections, assuming a normal distribution fitted through the 5 and 95% values.

This is here denoted the *IPCC A1FI Projection*.

5.2 Post-AR4 projections

Prior to the publication of the AR4, Rahmstorf et al. (2007) compared the projections of the TAR with observations from 1990 to 2006 and concluded that the observations were following the ‘model maximum’ projections, which are about 70% greater than

the central value of the projections. Further, the present observed rate since 1993 (3.2 mm yr^{-1} , Church and White 2011) is about 60% greater than the central value of sea-level rise from 1990 to 2010 (about 2.0 mm yr^{-1}), derived from the *AR4-adjusted TAR projections* (see Section 5.1 and Hunter 2010). However, simple comparisons between the projected and observed sea-level rise over the past two decades should be treated with some caution for two main reasons:

1. The comparison may be confounded by interannual and decadal variability. For example, Church and White (2011) showed that the satellite altimeter observations started (in 1993) during a period of relatively low sea level following (and possibly forced by) the Mt. Pinatubo eruption in 1991; allowance for this relative low in observed sea level reduces the disagreement between observations and projections for 1990–2010 from 60% to about 45% (with the observations still being larger than the projections).
2. There is no obvious physical reason why any present proportional relationship between observations and projections should be maintained until the end of the century.

Nicholls et al. (2011) summarized projections of sea-level rise published since the AR4 (Online Resource, Table (i) and their Fig. 1). They suggested ‘a pragmatic range of 0.5–2 m for twenty-first century sea-level rise, assuming a 4°C or more rise in temperature’. This temperature rise (which is for 2090–2099 relative to 1980–1999), is achieved by the AR4 temperature projections for emission scenarios A1B, A2 and A1FI. They also concluded that ‘the upper part of this range is considered unlikely to be realized’ (the 2 m upper limit of this range being derived from Pfeffer et al. 2008). It is also highly unlikely that sea level will fall under global warming. These considerations are here translated into a 21st century sea-level rise of $1.0 \text{ m} \pm 1.0 \text{ (lim) m}$, using a raised-cosine probability distribution giving zero probability outside this range (Eq. 8). The second set of sea-level rise allowances is provided, based on this projection, which is here denoted the *1.0/1.0 m Projection*.

5.3 Summary of projections

Two sets of allowances are therefore provided for 2100:

1. The *IPCC A1FI Projection* for 2100 relative to 1990, which is based on the A1FI emission scenario and the *AR4-adjusted TAR projections* (Hunter 2010), giving $\Delta z = 0.542 \text{ m}$ and $\sigma = 0.168 \text{ m}$ (normal distribution), and
2. The *1.0/1.0 m Projection* for the 21st century, which is based on post-AR4 results (Nicholls et al. 2011), giving $\Delta z = 1.0 \text{ m}$ and $W/2 = 1.0 \text{ m}$ (raised cosine distribution, Eq. 8). The standard deviation of this projection is 0.362 m (see Online Resource, Section A), so that the *1.0/1.0 m Projection* is roughly twice as large in both mean and standard deviation as the *IPCC A1FI Projection*.

These probability distributions are shown in Fig. 3. Given the present uncertainties in the processes which determine sea-level rise, it is difficult to assign meaningful weights to these two projections. However, it should be noted from Section 5.2 that the present observations of sea-level rise lie roughly mid-way between the two projections.

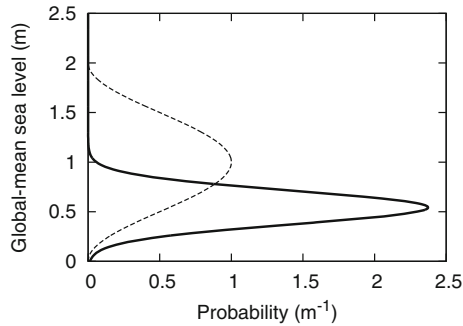


Fig. 3 Probability distributions for global-average rise in mean sea level. *Solid curve* shows *IPCC A1FI Projection* for 1990–2100, based on A1FI emission scenario and *AR4-adjusted TAR projections* (normal distribution with $\Delta z = 0.542$ m and $\sigma = 0.168$ m). *Dashed curve* shows *1.0/1.0 m Projection* for the 21st century, based on post-AR4 results (raised cosine with $\Delta z = 1.0$ m and $W/2 = 1.0$ m)

6 Application of the method

6.1 Introduction

The scale parameter (λ) was estimated from the *GESLA* (Global Extreme Sea-Level Analysis) sea-level database (see Menéndez and Woodworth 2010) which has been collected through a collaborative activity of the Antarctic Climate & Ecosystems Cooperative Research Centre, Australia, and the National Oceanography Centre Liverpool (NOCL), UK. The data covers a large portion of the world and is sampled at least hourly (except where there are data gaps). The database was downloaded from NOCL on 26 October 2010 and contains 675 files. However, many of these files are near-duplicates provided by different agencies. Many are also as short as one or two years and are therefore not suitable for the analysis of extremes. Initial data processing was therefore performed as described in [Online Resource](#), Section C.

Prior to extremes analysis, the data were ‘binned’, so as to produce files with a minimum sampling interval of one hour, and detrended. Annual maxima were estimated using a declustering algorithm such that any extreme events closer than 3 days were counted as a single event, and any gaps in time were removed from the record. These annual maxima were then fitted to a Gumbel distribution using the *ismev* package (Coles 2001, p. 48), implemented in the statistical language *R* (R Development Core Team 2008). This yielded the scale parameter (λ) for each of the 198 records. It is assumed that λ does not change in time.

The results are here presented in three different ways. Firstly, the scale parameter indicates the way in which the frequency of extreme events changes for a given rise in mean sea level. From Eq. 6, a rise of mean sea level, δz , (which effectively increases the location parameter, μ , by δz) increases the expected number of exceedances, N , by a factor $\exp(\delta z/\lambda)$. This factor is shown (using the *left-hand key* in the figures) for a rise in mean sea level of 0.5 metres in Fig. 4 (for the world) and in [Online Resource](#), Fig. (i) (for Australia).

The other, and closely related, way of presenting the results is in terms of the sea-level rise allowances for a normal uncertainty distribution ([Online Resource](#), Section

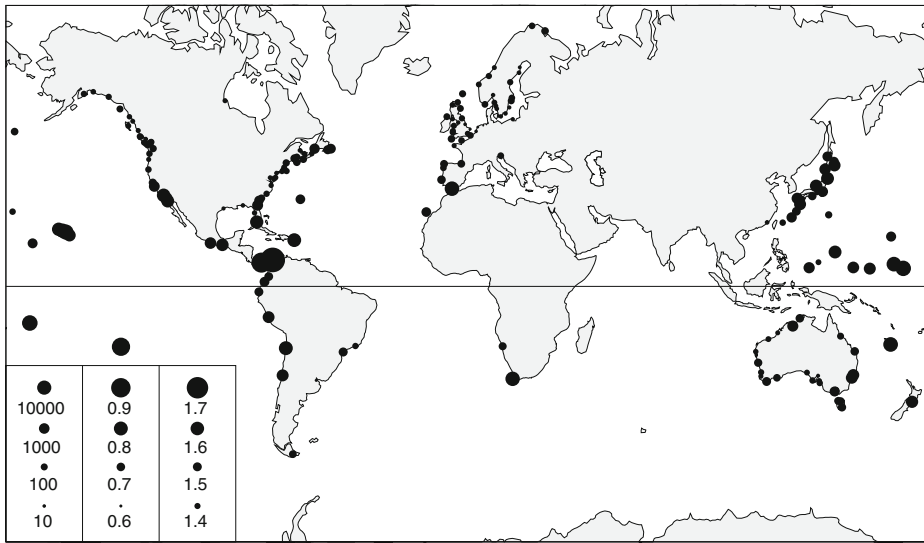


Fig. 4 Results of global analysis, indicated by dot diameter. **a** Factor by which frequency of flooding events will increase with a rise in sea level of 0.5 metres (key is left-hand column of dots in the bottom left-hand corner). **b** Sea-level rise allowance (metres) for 1990–2100 which conserves frequency of flooding events for the *IPCC A1FI Projection* based on A1FI emission scenario and *AR4-adjusted TAR projections* (normal distribution with $\Delta z = 0.542$ m and $\sigma = 0.168$ m); key is central column of dots in the bottom left-hand corner. **c** Sea-level rise allowance (metres) for 21st century which conserves frequency of flooding events for the *1.0/1.0 m Projection*, based on post-AR4 results (raised cosine distribution with $\Delta z = 1.0$ m and $W/2 = 1.0$ m); key is right-hand column of dots in the bottom left-hand corner

A, Eq. (viii)) and for a raised-cosine uncertainty distribution (Online Resource, Section A, Eq. (x)). Since all three ways of presenting the results depend spatially only on the scale parameter, λ , they are here plotted in the same figures, but with different keys (the allowances being shown by the *middle* and *right-hand* keys).

The results are also summarized for a number of specific locations in Online Resource, Table (ii).

6.2 Multiplying factor for 0.5 m sea-level rise

Figure 4 shows significant global variability of the Gumbel scale parameter, and hence in the increase in frequency of flooding events for a given sea-level rise (*left-hand* key). The largest values of this multiplying factor are in the southern Caribbean Sea (Cristóbal and Cartagena) while the smallest lie along the Pacific coast of Alaska, Canada and the northwest USA; in the mid-east coast of the USA; and around the northwest European shelf and the Baltic. The *large* values of multiplying factor coincide with *small* values of the scale parameter and *vice versa*.

For the world, the reciprocal of the scale parameter and its spatial variation are 10.2 ± 4.6 (sd) m^{-1} . The \pm one standard deviation range yields a range of multiplying factor for 0.5 m sea-level rise of 16 to 1600.

[Online Resource](#), Fig. (i), shows the same data, but restricted to the Australian continent. For Australia, the reciprocal of the scale parameter and its spatial variation are 9.8 ± 2.8 (sd) m^{-1} . The \pm one standard deviation range yields a range of multiplying factors for 0.5 m sea-level rise of 33 to 540.

6.3 IPCC A1FI projection

These results cover the period 1990–2100, and are based on the A1FI emission scenario and the *AR4-adjusted TAR projections* (normal probability distribution, with $\Delta z = 0.542$ m and $\sigma = 0.168$ m). The sea-level rise allowance is shown (using the *central key* in the figures) in Fig. 4 (for the world) and in [Online Resource](#), Fig. (i) (for Australia).

For the world, the sea-level rise allowance and its spatial variation are 0.686 ± 0.064 (sd) m. The average allowance represents a 26% increase over the mean sea-level rise, 0.542 m.

For Australia, the sea-level rise allowance and its spatial variation are 0.681 ± 0.040 (sd) m. The average allowance again represents a 26% increase over the mean sea-level rise, 0.542 m.

6.4 1.0/1.0 m projection

These results cover the 21st century and are based on post-AR4 results (raised-cosine probability distribution, with $\Delta z = 1.0$ m and $W/2 = 1.0$ m). The sea-level rise allowance is shown (using the *right-hand key* in the figures) in Fig. 4 (for the world) and in [Online Resource](#), Fig. (i) (for Australia).

For the world, the sea-level rise allowance and its spatial variation are 1.440 ± 0.105 (sd) m. The average allowance represents a 44% increase over the mean sea-level rise of 1.0 m.

For Australia, the sea-level rise allowance and its spatial variation are 1.444 ± 0.073 (sd) m. The average allowance again represents a 44% increase over the mean sea-level rise of 1.0 m.

7 Summary

Climate change requires that designers, planners and policymakers make suitable allowances for future conditions. On the coast, new infrastructure needs to be built higher, and planning schemes and policies need to be adapted to account for the raised sea level. It was shown in Section 3 that, in cases in which extreme flooding events are modified by an *uncertain* change in mean sea level, it is preferable to base future allowances upon estimates of the *expected number of exceedances in a given period* rather than on the *exceedance probability*. An allowance based on exceedance probability would tend, in cases where the exceedance probability is relatively high (say, > 0.5), to significantly underestimate the number of exceedances.

In Section 4, a simple relationship was developed which defines a sea-level rise allowance which conserves the *expected number of exceedances* under conditions of uncertain sea-level rise. This allowance depends only on the projected rise in mean sea level and its uncertainty, and on the scale parameter of a Gumbel distribution

fitted to the cumulative distribution function (it is assumed that the scale parameter does not change with a rise in sea level). An attractive feature of this allowance is that it does not require that the expected number of exceedances be prescribed; it is independent of the chosen level of precaution.

This allowance is always *greater* than the mean projection of sea-level rise, Δz , because the Gumbel distribution ($N = \exp((\mu - z)/\lambda)$) has a *positive* second derivative ($N/(\lambda^2)$) with respect to z (as is also the case with the more general GEV distribution when fitted to observed storm tides). If, instead, the distribution had a zero second derivative (i.e. with N varying linearly with z) then the allowance would be exactly Δz for any uncertainty distribution, P .

The technique has been demonstrated using a near-global database of sea-level records, and two possible projections of sea-level rise for the 21st century: one based on the TAR and AR4 of the IPCC (the *IPCC AIFI Projection*), and the other based on research since the AR4 (the *1.0/1.0 m Projection*). The *1.0/1.0 m Projection* is about twice as large, both in mean and standard deviation, as the *IPCC AIFI Projection*.

The global variation of the Gumbel scale parameter is illustrated by showing the expected increase in the number of flooding events for a 0.5 m sea-level rise (the world: Fig. 4 and [Online Resource](#), Table (ii); and Australia: [Online Resource](#), Fig. (i)). This multiplying factor covers a typical range of 16–1600.

The sea-level rise allowance (Fig. 4; [Online Resource](#), Fig. (i) and Table (ii)) also shows a significant spatial variation (due to changes in the Gumbel scale parameter), even though the projections of sea-level rise and its uncertainty are assumed constant. The *IPCC AIFI Projection* yields allowances for 1990–2100 of 0.686 ± 0.064 (sd) m, while the *1.0/1.0 m Projection* yields allowances for the 21st century of 1.440 ± 0.105 (sd) m (covering the near-global data set).

In conclusion, allowances for future sea-level rise need to account for both the *statistics of the storm tide* and the *statistics of the sea-level rise projections*.

Acknowledgements This paper was supported by the Australian Government's Cooperative Research Centres Programme through the Antarctic Climate & Ecosystems Cooperative Research Centre. Sea-level data were supplied by European Sea-Level Service, Global Sea Level Observing System (GLOSS) Delayed Mode Centre, Helpdesk Water (Netherlands), Instituto Español de Oceanografía (Spain), Istituto Talassografico di Trieste (Italy), Marine Environmental Data Service (Canada), National Oceanography Centre Liverpool (UK), National Tidal Centre (Bureau of Meteorology, Australia), Norwegian Mapping Authority, Service Hydrographique et Océanographique de la Marine (France), Swedish Meteorological and Hydrological Institute and University of Hawaii Sea Level Centre (USA).

References

- Bindoff N, Willebrand J, Artale V, Cazenave A, Gregory J, Gulev S, Hanawa K, Quéré CL, Levitus S, Nojiri Y, Shum C, Talley L, Unnikrishnan A (2007) Climate change 2007: the physical science basis. Contribution of working group I to the fourth assessment report of the Intergovernmental Panel on Climate Change, chap 5. Cambridge University Press, Cambridge, pp 385–432
- Church J, White N (2011) Sea-level rise from the late 19th to the early 21st century. *Surv Geophys*. doi:10.1007/s10712-011-9119-1, published online: 30 March 2011
- Church J, Gregory J, Huybrechts P, Kuhn M, Lambeck K, Nhuan M, Qin D, Woodworth P (2001) Climate change 2001: the scientific basis. Contribution of working group 1 to the third assessment report of the Intergovernmental Panel on Climate Change, chap 11. Cambridge University Press, Cambridge, pp 639–693

- Coles S (2001) An introduction to statistical modeling of extreme values. Springer, London
- Hunter J (2010) Estimating sea-level extremes under conditions of uncertain sea-level rise. *Clim Change* 99(3):331–350. doi:[10.1007/s10584-009-9671-6](https://doi.org/10.1007/s10584-009-9671-6)
- Le Quéré C, Raupach M, Canadell J, Marland G et al (2009) Trends in the sources and sinks of carbon dioxide. *Nature Geoscience* 2:831–836. doi:[10.1038/ngeo689](https://doi.org/10.1038/ngeo689)
- Meehl G, Stocker T, Collins W, Friedlingstein P, Gaye A, Gregory J, Kitoh A, Knutti R, Murphy J, Noda A, Raper S, Watterson I, Weaver A, Zhao ZC (2007) Climate change 2007: the physical science basis. Contribution of working group I to the fourth assessment report of the Intergovernmental Panel on Climate Change, chap 10. Cambridge University Press, Cambridge, pp 747–845
- Menéndez M, Woodworth P (2010) Changes in extreme high water levels based on a quasi-global tide-gauge data set. *J Geophys Res* 115(C10011). doi:[10.1029/2009JC005997](https://doi.org/10.1029/2009JC005997)
- Nicholls R, Marinova N, Lowe J, Brown S, Vellinga P, de Gusmão D, Hinkel J, Tol R (2011) Sea-level rise and its possible impacts given a ‘beyond 4°C world’ in the twenty-first century. *Phil Trans R Soc A* 369:161–181. doi:[10.1098/rsta.2010.0291](https://doi.org/10.1098/rsta.2010.0291)
- Pfeffer W, Harper J, O’Neel S (2008) Kinematic constraints on glacier contributions to 21st-century sea-level rise. *Science* 321(5894):1340–1343. doi:[10.1126/science.1159099](https://doi.org/10.1126/science.1159099)
- Pugh D (1996) Tides, surges and mean sea-level. Wiley, Chichester. Reprinted with corrections, <http://eprints.soton.ac.uk/19157/01/sea-level.pdf>
- Pugh D (2004) Changing sea levels: effects of tides, weather, and climate. Cambridge University Press, Cambridge
- R Development Core Team (2008) R: a language and environment for statistical computing. R Foundation for Statistical Computing, Vienna, Austria. <http://www.R-project.org>, ISBN 3-900051-07-0
- Rahmstorf S, Cazenave A, Church J, Hansen J, Keeling R, Parker D, Somerville R (2007) Recent climate observations compared to projections. *Science* 316(5825):709. doi:[10.1126/science.1136843](https://doi.org/10.1126/science.1136843)
- van den Brink H, Können G (2011) Estimating 10000-year return values from short time series. *Int J Climatol* 31:115–126. doi:[10.1002/joc.2047](https://doi.org/10.1002/joc.2047)
- Woodworth P, Blackman D (2004) Evidence for systematic changes in extreme high waters since the mid-1970s. *J Climate* 17(6):1190–1197. doi:[10.1175/1520-0442\(2004\)017<1190:EFSCIE>2.0.CO;2](https://doi.org/10.1175/1520-0442(2004)017<1190:EFSCIE>2.0.CO;2)

Electronic Supplementary Material

A simple technique for estimating an allowance for uncertain sea-level rise

Climatic Change

John Hunter, Antarctic Climate & Ecosystems Cooperative Research Centre, Hobart, Tasmania, Australia

john.hunter@utas.edu.au

A Derivation of Allowances

Eq. 7 of main paper is:

$$\begin{aligned} N_{ov} &= \int_{-\infty}^{\infty} P(z') \exp\left(\frac{\mu - z + \Delta z + z'}{\lambda}\right) dz' \\ &= N \exp\left(\left(\Delta z + \lambda \ln\left(\int_{-\infty}^{\infty} P(z') \exp\left(\frac{z'}{\lambda}\right) dz'\right)\right) / \lambda\right) \end{aligned} \quad (i)$$

which is here evaluated for three different probability distributions, $P(z')$:

Normal Distribution:

If $P(z')$ is a normal distribution of zero mean and standard deviation, σ , then

$$P(z') = \frac{1}{\sigma\sqrt{2\pi}} \exp\left(-\frac{(z')^2}{2\sigma^2}\right) \quad (ii)$$

and Eq. (i) becomes

$$N_{ov} = N \exp\left(\left(\Delta z + \frac{\sigma^2}{2\lambda}\right) / \lambda\right) \quad (iii)$$

in which z in the original Gumbel distribution (N in Eq. 6 in main paper) has been replaced by $z - \Delta z - \sigma^2/(2\lambda)$; the distribution has been shifted vertically by $\Delta z + \sigma^2/(2\lambda)$.

Boxcar Distribution:

If, $P(z')$ is a boxcar (uniform) distribution of zero mean and full-width, W (and therefore standard deviation, $\sigma = W/(2\sqrt{3})$), then

$$P(z') = \frac{1}{W} \quad \text{for} \quad -W/2 < z' < W/2 \quad \text{otherwise} \quad 0 \quad (\text{iv})$$

and Eq. (i) becomes

$$\begin{aligned} N_{ov} &= N \exp \left(\left(\Delta z + \lambda \ln \left(\frac{2\lambda}{W} \sinh \left(\frac{W}{2\lambda} \right) \right) \right) / \lambda \right) \\ &= N \exp \left(\left(\Delta z + \lambda \ln \left(\frac{\lambda}{\sigma\sqrt{3}} \sinh \left(\frac{\sigma\sqrt{3}}{\lambda} \right) \right) \right) / \lambda \right) \end{aligned} \quad (\text{v})$$

in which z in the original Gumbel distribution (N in Eq. 6 in main paper) has been replaced by $z - \Delta z - \lambda \ln(\dots)$; the distribution has been shifted vertically by $\Delta z + \lambda \ln(\dots)$.

Raised Cosine Distribution:

Finally, if $P(z')$ is a raised cosine distribution of zero mean and full-width, W (and therefore standard deviation, $\sigma = (W/2)\sqrt{1/3 - 2/(\pi^2)} = W/(2K)$ where $K = 1/\sqrt{1/3 - 2/(\pi^2)}$), then

$$P(z') = \frac{1}{W} \left(1 + \cos \left(\frac{2\pi z'}{W} \right) \right) \quad \text{for} \quad -W/2 < z' < W/2 \quad \text{otherwise} \quad 0 \quad (\text{vi})$$

and Eq. (i) becomes

$$\begin{aligned} N_{ov} &= N \exp \left(\left(\Delta z + \lambda \ln \left(\frac{2\lambda}{W} \sinh \left(\frac{W}{2\lambda} \right) \left(\frac{(2\pi\lambda/W)^2}{1 + (2\pi\lambda/W)^2} \right) \right) \right) / \lambda \right) \\ &= N \exp \left(\left(\Delta z + \lambda \ln \left(\frac{\lambda}{K\sigma} \sinh \left(\frac{K\sigma}{\lambda} \right) \left(\frac{(\pi\lambda/\sigma)^2}{K^2 + (\pi\lambda/\sigma)^2} \right) \right) \right) / \lambda \right) \end{aligned} \quad (\text{vii})$$

in which z in the original Gumbel distribution (N in Eq. 6 in main paper) has been replaced by $z - \Delta z - \lambda \ln(\dots)$; the distribution has been shifted vertically by $\Delta z + \lambda \ln(\dots)$.

Summary:

Therefore, the appropriate allowances (Z_n , Z_b and Z_r , for normal, boxcar and raised cosine distributions, respectively) for uncertain sea-level rise, which maintain the same expected number of flooding events in a given period, are

$$Z_n = \Delta z + \frac{\sigma^2}{2\lambda}$$

for a normal distribution,

(viii)

$$Z_b = \Delta z + \lambda \ln \left(\frac{2\lambda}{W} \sinh \left(\frac{W}{2\lambda} \right) \right)$$

$$= \Delta z + \lambda \ln \left(\frac{\lambda}{\sigma\sqrt{3}} \sinh \left(\frac{\sigma\sqrt{3}}{\lambda} \right) \right)$$

for a boxcar distribution, and

(ix)

$$Z_r = \Delta z + \lambda \ln \left(\frac{2\lambda}{W} \sinh \left(\frac{W}{2\lambda} \right) \left(\frac{(2\pi\lambda/W)^2}{1 + (2\pi\lambda/W)^2} \right) \right)$$

$$= \Delta z + \lambda \ln \left(\frac{\lambda}{K\sigma} \sinh \left(\frac{K\sigma}{\lambda} \right) \left(\frac{(\pi\lambda/\sigma)^2}{K^2 + (\pi\lambda/\sigma)^2} \right) \right)$$

for a raised cosine distribution

(x)

It may be shown that $Z_n \geq Z_b$ and $Z_n \geq Z_r$ for all σ/λ . A conservative allowance for sea-level rise is therefore Z_n (Eq. (viii)). However, the raised cosine distribution (which yields the allowance given by Eq. (x)) is probably the more appropriate, given that there are physical constraints (and hence probable limits) on the rate of future sea-level rise (see Section 5.2 of main paper).

B The Uncertainty of the Projections

The derivation of the standard error of the best estimate of the projections from the results of the TAR (Third Assessment Report of the Intergovernmental Panel on Climate Change or IPCC) and AR4 (Fourth Assessment Report of the IPCC) is not straightforward. If the projections from individual models were independent, then it would only be necessary to estimate the number of degrees of freedom, n , and to calculate the standard error, σ , from the standard deviation, s , from

$$\sigma^2 = \frac{s^2}{n}$$
(xi)

The AR4 projections were based on 19 AOGCMs (Atmosphere-Ocean General Circulation Models), which were run on emission scenarios B1, A1B and A2. The remaining scenarios were modelled using the MAGICC (Model for the Assessment of Greenhouse-gas Induced

Climate Change) simple climate model (e.g. Meinshausen et al 2011), using empirical time-dependent ratios between pairs of scenarios (one of which was modelled using AOGCMs). It is tempting to assume that the models are independent and to associate the number of degrees of freedom, n , with the number of models used in the preparation of the AR4 projections (of order 20). However, Masson and Knutti (2011) performed a hierarchical clustering of the CMIP3 (phase 3 of the Coupled Model Intercomparison Project; the models reported in AR4) climate models and concluded that, due to widespread sharing of history, algorithms and components between models, ‘the number of structurally different models is small’, indicating that the actual number of degrees of freedom is significantly smaller than 20. Pennell and Reichler (2011) statistically analysed the results of 24 CMIP3 models and concluded that the effective number of models was only about 8. Furthermore, due to the strong interdependence of the models, it is likely that important aspects of the physics is either missing or wrong in *all models*, giving a bias which cannot be deduced from the scatter of model results, and which represents an *additional* uncertainty. Clear examples of this are the treatment of glaciers, ice caps and ice sheets (for which there is only *one* series of models contributing to the AR4 results) and the modelling of sulfate aerosols (a number of models sharing common observational data). Due to these considerations, the uncertainty, σ , is here associated with the *standard deviation* (rather than the *standard error*) of the projections.

C Initial Processing of the GESLA Sea-Level Database

The GESLA (Global Extreme Sea-Level Analysis) dataset was initially processed as follows:

1. only files which are at least 30 years in length (defined by the number of months containing at least some data, divided by 12) were selected,
2. non-physical outliers (identified as outliers which did not have any obvious cause, such as a tsunami or a tropical cyclone) and datum shifts (identified by a clear vertical offset, often bracketing a significant data gap) were addressed, either by removal or adjustment of data,
3. known tsunamis were removed,
4. where records were duplicated in separate files, the one which appeared most free of errors was selected, and
5. co-located data covering different time periods was joined, with appropriate adjustment for any datum shift.

This resulted in 198 records, of which 166 were unchanged from the original *GESLA* files, 28 were subject to some modification and 4 were the result of joining records. These records contain both tides and storm surges.

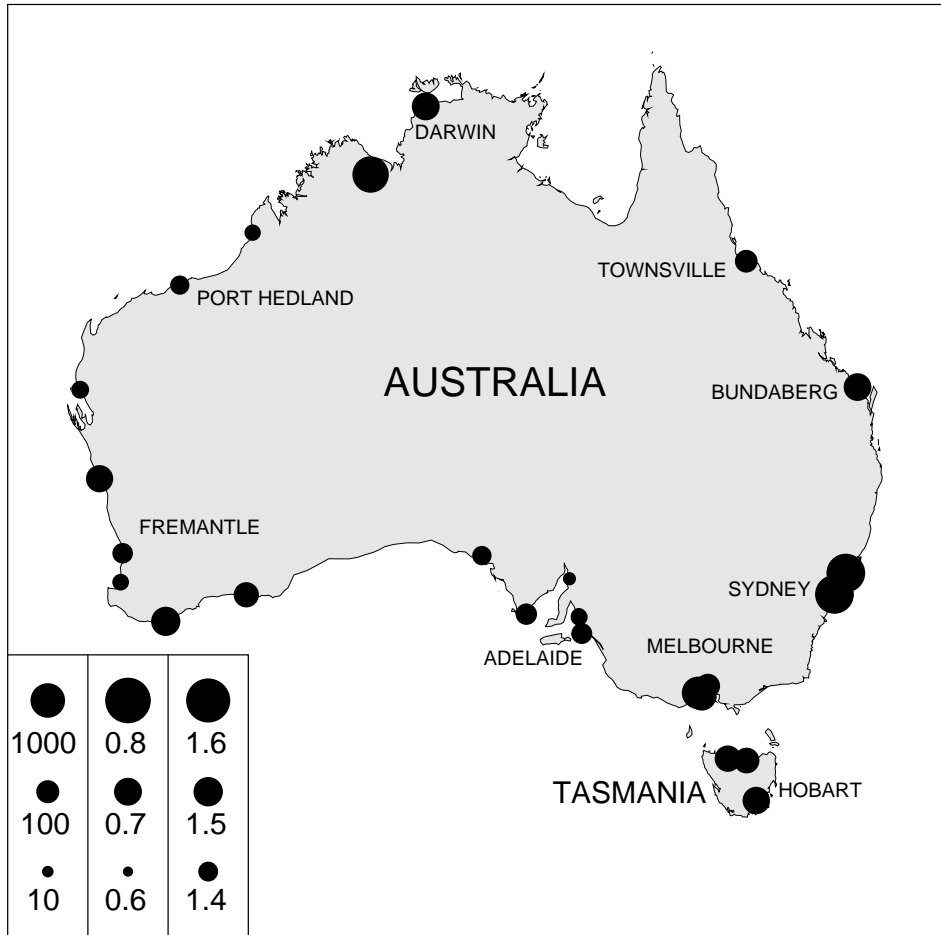


Figure (i): Results of Australian analysis, indicated by dot diameter. (a) Factor by which frequency of flooding events will increase with a rise in sea level of 0.5 metres (key is left-hand column of dots in the bottom left-hand corner). (b) Sea-level rise allowance (metres) for 1990-2100 which conserves frequency of flooding events for the *IPCC A1FI Projection* based on A1FI emission scenario and *AR4-adjusted TAR projections* (normal distribution with $\Delta z = 0.542$ m and $\sigma = 0.168$ m); key is central column of dots in the bottom left-hand corner. (c) Sea-level rise allowance (metres) for 21st century which conserves frequency of flooding events for the *1.0/1.0 m Projection*, based on post-AR4 results (raised cosine distribution with $\Delta z = 1.0$ m and $W/2 = 1.0$ m); key is right-hand column of dots in the bottom left-hand corner.

Table (i): Range of global sea-level rise from post-AR4 research (after Nicholls et al 2011). ^aHigher rates are possible for shorter periods. ^bFor the twenty-first century. ^cFor the best palaeo-temperature record.

Sea-level Rise (m century ⁻¹)	Methodological approach	Source
0.5-1.4	semi-empirical projection ^b	Rahmstorf 2007
0.8-2.4 ^a	palaeo-climate analogue	Rohling et al 2008
0.55-1.10	synthesis ^b	Vellinga et al 2009
0.8-2.0	physical-constraint analysis ^b	Pfeffer et al 2008
0.56-0.92 ^a	palaeo-climate analogue	Kopp et al 2009
0.75-1.90	semi-empirical projection ^b	Vermeer and Rahmstorf 2009
0.72-1.60 ^c	semi-empirical projection ^b	Grinsted et al 2010

Table (ii): Summary of analyses for specific locations. ^aLarge values such as this indicate that any locations which have been flooded in the past will be flooded on a daily basis with 0.5 m of sea-level rise (the ranges of sea-level variation at Cristóbal and Rikitea are only 0.6-0.9 m).

Location	Increase in frequency of flooding events for sea-level rise of 0.5 m	Sea-level rise allowance, 1990- 2100, <i>IPCC A1FI</i> <i>Projection</i> (m)	Sea-level rise allowance, twenty- first century, <i>1.0/</i> <i>1.0 m Projection</i> (m)
Antofagasta (Chile)	9,000	0.800	1.608
Canary Islands (Spain)	571	0.722	1.521
Cape Town (South Africa)	12,600	0.809	1.616
Cristóbal (Panama)	465,000 ^a	0.911	1.686
Fremantle (Australia)	61.2	0.659	1.409
Furuögrund (Sweden)	13.6	0.616	1.297
Honningsvåg (Norway)	74.6	0.664	1.421
Honolulu (USA)	6,010	0.788	1.597
Key West (USA)	5,970	0.788	1.597
Kwajalein (Marshall Islands)	15,100	0.814	1.621
La Coruña (Spain)	181	0.689	1.470
Nagasaki (Japan)	1,700	0.753	1.560
New York (USA)	22.3	0.630	1.338
Oslo (Norway)	18.0	0.624	1.321
Rikitea (French Polynesia)	147,000 ^a	0.879	1.667
Rio de Janeiro (Brazil)	65.1	0.661	1.413
San Diego (USA)	3,160	0.770	1.579
Seattle (USA)	117	0.677	1.447
Sheerness (UK)	35.2	0.643	1.372
Sydney (Australia)	2,250	0.761	1.569
Trieste (Italy)	84.2	0.668	1.428
Wellington (New Zealand)	2,910	0.768	1.577

References

- Grinsted A, Moore J, Jevrejeva S (2010) Reconstructing sea level from paleo and projected temperatures 200 to 2100 AD. *Climate Dynamics* 34:461–472, DOI 10.1007/s00382-008-0507-2
- Kopp R, Simons F, Mitrovica J, Maloof A, Oppenheimer M (2009) Probabilistic assessment of sea level during the last interglacial stage. *Nature* 462:863–867, DOI 10.1038/nature08686
- Masson D, Knutti R (2011) Climate model genealogy. *Geophysical Research Letters* 38(L08703), DOI 10.1029/2011GL046864
- Meinshausen M, Raper S, Wigley T (2011) Emulating coupled atmosphere-ocean and carbon cycle models with a simpler model, MAGICC6 – Part 1: Model description and calibration. *Atmospheric Chemistry and Physics* 11:1417–1456, DOI 10.5194/acp-11-1417-2011
- Nicholls R, Marinova N, Lowe J, Brown S, Vellinga P, de Gusmão D, Hinkel J, Tol R (2011) Sea-level rise and its possible impacts given a ‘beyond 4°C world’ in the twenty-first century. *Philosophical Transactions of the Royal Society A: Mathematical, Physical and Engineering Sciences* 369:161–181, DOI 10.1098/rsta.2010.0291
- Pennell C, Reichler T (2011) On the effective number of climate models. *Journal of Climate* 24:2358–2367, DOI 10.1175/2010JCLI3814.1
- Pfeffer W, Harper J, O’Neel S (2008) Kinematic constraints on glacier contributions to 21st-century sea-level rise. *Science* 321(5894):1340–1343, DOI 10.1126/science.1159099
- Rahmstorf S (2007) A semi-empirical approach to projecting future sea-level rise. *Science* 315(5810):368–370, DOI 10.1126/science.1135456
- Rohling E, Grant K, Hemleben C, Siddall M, Hoogakker B, Bolshaw M, Kucera M (2008) High rates of sea-level rise during the last interglacial period. *Nature Geoscience* 1:38–42, DOI 10.1038/ngeo.2007.28
- Vellinga P, Katsman C, Sterl A, Beersma J, Hazeleger W, Church J, Kopp R, Kroon D, Oppenheimer M, Plag H, Rahmstorf S, Lowe J, Ridley J, von Storch H, Vaughan D, van de Wal R, Weisse R, Kwadijk J, Lammersen R, Marinova N (2009) Exploring high-end climate change scenarios for flood protection of the Netherlands. Tech. Rep. WR 2009-05, Wageningen University and Research Centre / Alterra and Royal Netherlands Meteorological Institute (KNMI)
- Vermeer M, Rahmstorf S (2009) Global sea level linked to global temperature. *Proceedings of the National Academy of Sciences* 106(51):21,527–21,532, DOI 10.1073/pnas.0907765106

B Copy of Hunter et al. (2013)



Towards a global regionally varying allowance for sea-level rise

J.R. Hunter^{a,*}, J.A. Church^b, N.J. White^b, X. Zhang^b

^a Antarctic Climate & Ecosystems Cooperative Research Centre, Private Bag 80, Hobart, Tasmania 7001, Australia

^b Centre for Australian Weather and Climate Research and Wealth from Oceans Flagship, CSIRO Marine and Atmospheric Research, GPO Box 1538, Hobart, Tasmania 7000, Australia

ARTICLE INFO

Keywords:

Sea-level rise
Storm tide
Climate change
Climate projection

ABSTRACT

Allowances have been developed for future rise of relative sea-level (i.e. sea level relative to the land) based on the projections of regional sea-level rise, its uncertainty, and the statistics of tides and storm surges (storm tides). An 'allowance' is, in this case, the vertical distance that an asset needs to be raised under a rising sea level, so that the present likelihood of flooding does not increase. This continues the work of Hunter (2012), which presented allowances based on global-average sea level and local storm tides. The inclusion of regional variations of sea-level rise (and its uncertainty) significantly increases the global spread of allowances. For the period 1990–2100 and the A1FI emission scenario (which the world is broadly following at present), these range from negative allowances caused by land uplift (in the northern regions of North America and Europe) to the upper 5-percentile which is greater than about 1 m (e.g. on the eastern coastline of North America).

© 2013 Elsevier Ltd. All rights reserved.

1. Introduction

A major effect of climate change is a present and continuing increase in sea level, caused mainly by thermal expansion of seawater and the addition of water to the oceans from melted land ice (e.g. Meehl et al., 2007, as reported in the Fourth Assessment Report (AR4) of the Intergovernmental Panel on Climate Change (IPCC)). Over the last two decades, the rate of global-average sea-level rise was about 3.2 mm yr^{-1} (Church and White, 2011). At the time of AR4 in 2007, sea level was projected to rise at a maximum rate of about 10 mm yr^{-1} and to a maximum level of about 0.8 m (relative to 1990) by the last decade of the 21st century, in the absence of significant mitigation of greenhouse-gas emissions (Meehl et al., 2007, Table 10.7, including 'scaled-up ice sheet discharge').

Sea-level rise, like the change of many other climate variables, will be experienced mainly as an increase in the frequency or likelihood (probability) of extreme events, rather than simply as a steady increase in an otherwise constant state. One of the most obvious adaptations to sea-level rise is to raise an asset (or its protection) by an amount that is sufficient to achieve a required level of precaution. The selection of such an allowance has often, unfortunately, been quite subjective and qualitative, involving concepts such as 'plausible' or 'high-end' projections. Hunter (2012) described a simple technique for estimating an allowance for sea-level rise using extreme-value theory. This allowance ensures that

the expected, or average, number of extreme (flooding) events in a given period is preserved. In other words, any asset raised by this allowance would experience the same frequency of flooding events under sea-level rise as it would without the allowance and without sea-level rise. It is important to note that this allowance only relates to the effect of sea-level rise on *inundation* and *not* on the recession of soft (e.g. sandy) shorelines or on other impacts.

Under conditions of uncertain sea-level rise, the 'expected number of flooding events in a given period' is here defined in the following way. It is supposed that there are n possible futures, each with a probability, P_i , of being realised. For each of these futures, the expected number of flooding events in a given period is given by N_i . The effective, or overall, expected number of flooding events (considering all possible futures) is then considered to be $\sum_{i=1}^n P_i N_i$, where $\sum_{i=1}^n P_i = 1$.

In the terminology of risk assessment (e.g. ISO, 2009), the expected number of flooding events in a given period is known as the *likelihood*. If a specific cost may be attributed to one flooding event, then this cost is termed the *consequence*, and the combined effect (generally the product) of the likelihood and the consequence is the *risk* (i.e. the total effective cost of damage from flooding over the given period). The allowance is the height that an asset needs to be raised under sea-level rise in order to keep the flooding likelihood the same. If the cost, or consequence, of a single flooding event is constant than this also preserves the flooding risk.

An important property of the allowance is that it is *independent of the required level of precaution* (when measured in terms of *likelihood of flooding*). In the case of coastal infrastructure, an appropriate height should first be selected, based on *present* conditions and an acceptable degree of precaution (e.g. an average of one flooding event

* Corresponding author. Tel.: +61 4 2709 8831; fax: +61 3 6226 2440.

E-mail addresses: jrh@johnroberthunter.org (J.R. Hunter), John.Church@csiro.au (J.A. Church), Neil.White@csiro.au (N.J. White), Xuebin.Zhang@csiro.au (X. Zhang).

in 100 years). If this height is then raised by the allowance calculated for a specific period, the required level of precaution will be sustained until the end of this period.

The method assumes that there is no change in the variability of the extremes (specifically, the scale parameter of the Gumbel distribution; see Section 2). In other words, the statistics of tides and storm surges (storm tides) relative to mean sea level are assumed to be unchanged. It is also assumed that there is no change in wave climate (and therefore in wave setup and runup). The allowance derived from this method depends also on the distribution function of the uncertainty in the rise in mean sea level at some future time. However, once this distribution and the Gumbel scale parameter has been chosen, the remaining derivation of the allowance is entirely objective.

If the future sea-level rise were known exactly (i.e. the uncertainty was zero), then the allowance would be equal to the central value of the estimated rise. However, because of the exponential nature of the Gumbel distribution (which means that overestimates of sea-level rise more than compensate for underestimates of the same magnitude), uncertainties in the projected rise *increase* the allowance above the central value.

Hunter (2012) combined the Gumbel scale parameters derived from 198 tide-gauge records in the *GESLA* (Global Extremes Sea-Level Analysis) database (see Menéndez and Woodworth, 2010) with projections of global-average sea-level rise, in order to derive estimates of the allowance around much of the world's coastlines. The spatial variation of this allowance therefore depended only on variations of the Gumbel scale parameter. We here derive improved estimates of the allowance using the same *GESLA* tide-gauge records, but spatially varying projections of sea level from the IPCC AR4 (Meehl et al., 2007) with enhancements to account for glacial isostatic adjustment (GIA), and ongoing changes in the Earth's loading and gravitational field (Church et al., 2011). We use projections for the A1FI emission scenario (which the world is broadly following at present; Le Quéré et al., 2009).

The results presented here relate to an approximation of *relative sea level* (i.e. sea level relative to the land). They include the effects of vertical land motion due to changes in the Earth's loading and gravitational field caused by past and ongoing changes in land ice. They do not include effects due to local land subsidence produced, for example, by deltaic processes or groundwater withdrawal; *separate allowances should be applied to account for these latter effects*.

A fundamental problem with existing sea-level rise projections is a lack of information on the upper bound for sea-level rise during the 21st century, in part because of our poor knowledge of the contribution from ice sheets (IPCC, 2007). This effectively means that the likelihood of an extreme high sea-level rise (the upper tail of the distribution function of the sea-level rise uncertainty) is poorly known. The results described here are based on relatively thin-tailed distributions (normal and raised cosine) and may therefore not be appropriate if the distribution is fat-tailed (Section 6). For cases where consequence of flooding would be 'dire' (in the sense that the consequence of flooding would be unbearable, no matter how low the likelihood), a more appropriate allowance would be based on the best estimate of the maximum possible rise.

2. Theory

Extremes are generally described by *exceedance events* which are events which occur when some variable exceeds a given level. Two statistics are conventionally used to describe the likelihood of extreme events such as flooding from the ocean. These are the *average recurrence interval* (or *ARI*), R , and the *exceedance probability*, E , for a given period, T . The *ARI* is the average period between extreme events (observed over a long period with many

events), while the exceedance probability is the probability of at least one exceedance event happening during the period T . Exceedance distributions are often expressed in terms of the *cumulative distribution function*, F , where $F = 1 - E$. F is just the probability that there will be *no* exceedances during the prescribed period, T . These statistics are related by (e.g. Pugh, 1996)

$$F = 1 - E = \exp\left(-\frac{T}{R}\right) = \exp(-N) \quad (1)$$

where N is the expected, or average, number of exceedances during the period T .

Eq. (1) involves the assumption (made throughout this paper) that exceedance events are independent; their occurrence therefore follows a Poisson distribution. This requires a further assumption about the relevant time scale of an event. If multiple closely spaced events have a single cause (e.g. flooding events caused by one particular storm), they are generally combined into a single event using a declustering algorithm.

The occurrence of sea-level extremes, and therefore, the *ARI* and the exceedance probability, will be modified by sea-level rise, the future of which has considerable uncertainty. For example, the projected sea-level rise for 2090–2099 relative to 1980–1999, for the A1FI emission scenario (which the world is broadly following at present; Le Quéré et al., 2009), is 0.50 ± 0.26 m (5–95% range, including scaled-up ice sheet discharge; Meehl et al., 2007), the range being larger than the central value.

The expected number of exceedances above a given level and over a given period may, in general, be described by

$$N = \mathcal{N}\left(\frac{\mu - z_p}{\lambda}\right) \quad (2)$$

where \mathcal{N} is some general dimensionless function, z_p is the physical height (e.g. the height of a critical part of the asset), μ is a 'location parameter' and λ is a 'scale parameter'. As noted in Section 1, it is assumed that there is no change in the variability of the extremes, which implies that the scale parameter, λ , does not change with a rise in sea level.

Mean sea level is now raised by an amount $\Delta z + z'$, where Δz is the central value of the estimated rise and z' is a random variable with zero mean and a distribution function, $P(z')$, to be chosen below. This effectively increases the location parameter, μ , by $\Delta z + z'$. At the same time, the asset is raised by an allowance, a , so that it is now located at a height $z_p + a$. Under these conditions of (uncertain) sea-level rise and raising of the asset, the overall (or effective) expected number, N_{ov} , of exceedances ($> z_p + a$) during the period T , becomes

$$N_{ov} = \int_{-\infty}^{\infty} P(z') \mathcal{N}\left(\frac{\mu - z_p + \Delta z + z' - a}{\lambda}\right) dz' \quad (3)$$

The function, \mathcal{N} , is often well-fitted by a *generalised extreme-value distribution* (*GEV*). The simplest of these, the *Gumbel* distribution, fits most sea-level extremes quite well (e.g. van den Brink and Können, 2011). The Gumbel distribution may be expressed as (e.g. Coles, 2001, p. 47)

$$F = \exp\left(-\exp\left(\frac{\mu - z_p}{\lambda}\right)\right) \quad (4)$$

where F is the probability that there will be no exceedances $> z_p$ during the prescribed period, T .

From Eqs. (1), (2) and (4)

$$N = \mathcal{N}\left(\frac{\mu - z_p}{\lambda}\right) = \exp\left(\frac{\mu - z_p}{\lambda}\right) \quad (5)$$

μ is therefore the value of z_p for which $N=1$ during the period T , and λ , the 'scale parameter', is an e-folding distance in the vertical. Globally, the scale parameter has a quite narrow range; for the sea-level records described in Section 4, the 5-percentile,

median and 95-percentile values of the scale parameter are 0.05 m, 0.12 m and 0.19 m, respectively.

Again, as noted in Section 1, it is assumed that the scale parameter, λ , does not change with a rise in sea level. It will also be noted later (Section 6) that Eq. (5) is only valid over the restricted range of z_p that encompasses the high extreme values.

Eq. (3) therefore becomes (Hunter, 2012):

$$N_{ov} = \int_{-\infty}^{\infty} P(z') \exp\left(\frac{\mu - z_p + \Delta z + z' - a}{\lambda}\right) dz'$$

$$= N \exp\left(\left(\Delta z + \lambda \ln\left(\int_{-\infty}^{\infty} P(z') \exp\left(\frac{z'}{\lambda}\right) dz'\right) - a\right) / \lambda\right) \quad (6)$$

In order to preserve the expected number of exceedances (or flooding events), we require that $N_{ov} = N$. Therefore, the allowance, a , is equal to the term $\Delta z + \lambda \ln(\dots)$ in the last part of Eq. (6). This allowance is composed of two parts: the mean sea-level rise, Δz , and the term $\lambda \ln(\dots)$, which arises from the uncertainty in future sea-level rise. Hunter (2012) evaluated the allowance for three types of uncertainty distribution for future sea-level rise: a normal distribution, a boxcar (uniform) distribution and a raised cosine distribution. The resulting allowances may all be expressed as simple analytical expressions, involving the Gumbel scale parameter, λ , the central value of the estimated rise, Δz , and its standard deviation, σ . We here estimate the allowances using normal and raised cosine distributions, the former having fatter tails and therefore yielding higher allowances (the raised-cosine distribution falls to zero at a finite distance from the central value, the total range of the distribution being about 1.7 times the 5- to 95-percentile range). Both distributions were fitted to the 5- and 95-percentile range of the IPCC AR4 projections of sea-level rise, with the central value, Δz , being the mean of the 5- and 95-percentile values.

For a normal uncertainty distribution of future sea-level rise, the allowance is given by $\Delta z + \sigma^2 / (2\lambda)$ (Hunter, 2012). A typical sea-level rise projection for 2100 relative to 1990 for the A1FI emission scenario is 0.5 ± 0.2 (standard deviation) m, and a typical Gumbel scale parameter is 0.1 m. In this case, the allowance is equal to 0.5 m (the mean sea-level rise) + 0.2 m (associated with the uncertainty) = 0.7 m, which is significant larger than the mean sea-level rise. However, in general, the allowance is less than the 95-percentile upper limit (which is 0.83 m in this typical case).

3. Projections of regional sea-level rise

Projections of the future climate are based on models driven by plausible scenarios for the emissions of greenhouse gases. In the case of the IPCC AR4 and the projections to be described in this section, emissions were based on the Special Report on Emission Scenarios (SRES; Nakicenovic et al., 2000).

The derivation of the projections of regional sea-level rise followed Church et al. (2011) and Slangen et al. (2012), and is described in detail in Appendix A. The resultant projections are composed of terms due to

1. the global-average sea-level rise (including 'scaled-up ice sheet discharge' (Meehl et al., 2007; see Fig. 1)),
2. spatially varying 'fingerprints' to account for changes in the loading of the Earth and in the gravitational field, in response to ongoing changes in land ice (Mitrovica et al., 2001, 2011),
3. glacial isostatic adjustment (GIA; Kendall et al., 2005) (GIA is the result of changes in the Earth's loading and gravitational field caused by past changes in land ice (predominantly, the most recent deglaciation from about 20,000 years ago). The northern regions of North America and Europe show

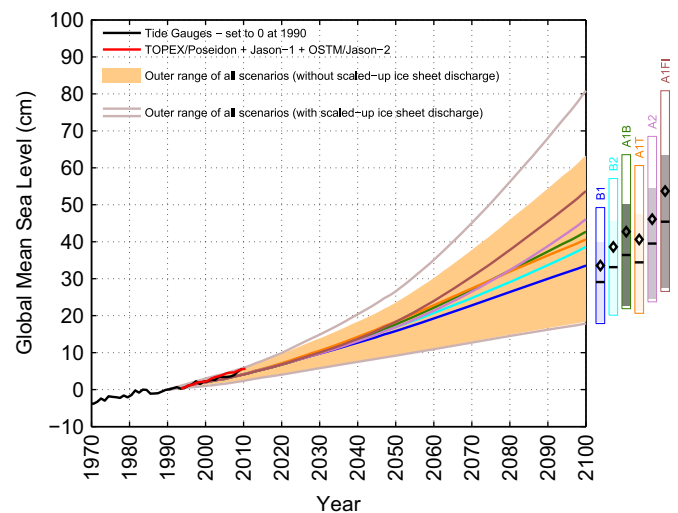


Fig. 1. Global-average projections of sea-level rise relative to 1990, based on the IPCC AR4 (Meehl et al., 2007) and reproduced in Church et al. (2011). The outer light lines and the shaded region show the 5- to 95-percentile range of projections with and without 'scaled-up ice sheet discharge' (SUISD), respectively. The continuous coloured lines from 1990 to 2100 indicate the central value of the projections, with SUISD. The open and shaded bars at the right show the 5- to 95-percentile range of projections for 2100 for the various SRES scenarios, with and without SUISD. The diamonds and horizontal lines in the bars are the central values with and without SUISD. The observational estimates of global-average sea level based on tide-gauge measurements and satellite altimeter data are shown in black and red, respectively. The tide-gauge data are set to zero at the start of the projections in 1990, and the altimeter data are set equal to the tide-gauge data at the start of the record in 1993. (For interpretation of the references to color in this figure legend, the reader is referred to the web version of this article.)

significant uplift, which may lower relative sea level (i.e. sea level relative to the land) by as much as 20 mm yr^{-1} . In contrast, the eastern coastline of North America is sinking and shows positive GIA contributions as large as 2 mm yr^{-1} , and

4. spatially varying sea-level change due to change in ocean density and dynamics (e.g. Meehl et al., 2007, Section 10.6.2 and Fig. 10.32).

While terms (2) and (3) are generated by effectively the same models of crustal loading and gravitational field, they are forced by quite different time-series of land-ice change. It should also be noted that the terms (1)–(4) have been generated by separate models and are added linearly; nonlinear interactions between the terms are ignored.

The spatially varying sea-level rise related to change in ocean density and dynamics (term (4), above) is provided by atmosphere-ocean general circulation models (AOGCMs). While global-average sea-level rise has been reported for six emission scenarios (B1, B2, A1B, A1T, A2, A1FI; Meehl et al., 2007), results from AOGCMs are only available for scenarios B1, A1B and A2. For estimating spatially varying projections for A1FI (the highest of the SRES scenarios), the central values and uncertainties derived from combining terms (1)–(4), above, were scaled using ratios of the global-average projections for A1FI and A2.

4. Statistics of storm tides

The scale parameter, λ , was estimated from the GESLA (Global Extreme Sea-Level Analysis) sea-level database (see Menéndez and Woodworth, 2010) which has been collected through a collaborative activity of the Antarctic Climate & Ecosystems Cooperative Research Centre, Australia, and the National Oceanography Centre Liverpool

(NOCL), UK. The data covers a large portion of the world and is sampled at least hourly (except where there are data gaps). The database was downloaded from NOCL on 26 October 2010 and contains 675 files. However, many of these files are near-duplicates provided by different agencies. Many are also as short as one or two years and are therefore not suitable for the analysis of extremes (it is generally considered that ARIs of up to about four times the record length may be derived from tide-gauge records (e.g. Pugh, 1996) so that, for example, the estimation of 100-year ARIs requires records of at least 25 years duration). Hunter (2012) performed initial data processing, resulting in 198 tidal records, each of which was at least 30 years long. However, one of these is from Trieste in the Mediterranean, which is poorly resolved by the ocean components of the AOGCMs (the Mediterranean is omitted altogether from Meehl et al., 2007, Fig. 10.32, which shows the projected spatially varying sea-level change due to change in ocean density and dynamics). The data from Trieste was not therefore used in the present analysis, which is therefore based on 197 global sea-level records.

Prior to extreme analysis, the data was 'binned', so as to produce files with a minimum sampling interval of one hour, and detrended. Annual maxima were estimated using a declustering algorithm such that any extreme events closer than 3 days were counted as a single event, and any gaps in time were removed from the record. These annual maxima were then fitted to a Gumbel distribution using the *ismev* package (Coles, 2001, p. 48) implemented in the statistical language *R* (R Development Core Team, 2008). This yielded the scale parameter, λ , for each of the 197 records. It is assumed that λ does not change in time.

5. Regional allowances

Allowances for future sea-level rise have generally been based on global-average projections, without adjustment for regional variations (which are related to the land-ice fingerprint, GIA, and change in ocean density and dynamics). Fig. 2 shows the vertical allowance for sea-level rise from 1990 to 2100 for the A1FI emission scenario, at each of the 197 tide-gauge locations. The allowance is based on the global-average rise in mean sea level and on the statistics of storm tides observed at each location (Section 4). The uncertainty in the projections of sea-level rise was fitted to a normal distribution. The use of a raised-cosine distribution, which has thinner tails, yields a smaller allowance. Fig. 2 shows effectively the same information as Fig. 4 of Hunter (2012), except for being based on a slightly different projection of mean sea-level rise. Fig. 3 shows the

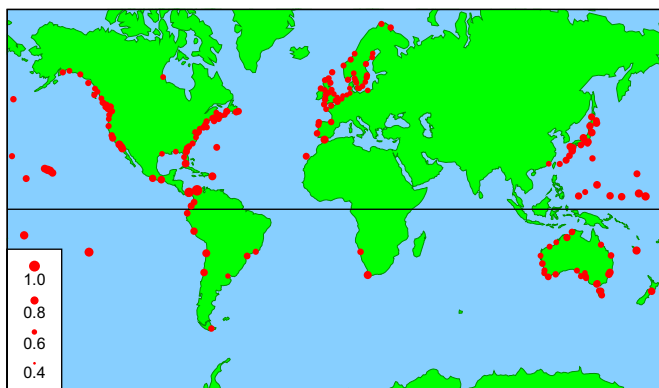


Fig. 2. Allowances using global-average sea-level rise. Vertical allowances (m) for sea-level rise from 1990 to 2100 for the A1FI emission scenario, indicated by the dot diameter. The allowances are based on a global-average rise in mean sea level, derived from the IPCC AR4, and on the statistics of storm tides observed at each location. The uncertainty in the projections of sea-level rise was fitted to a normal distribution.

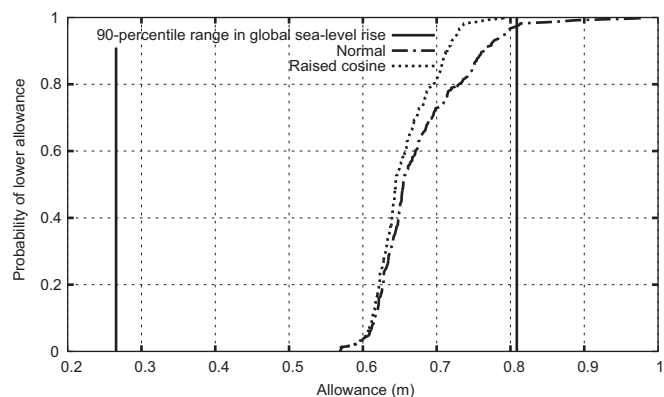


Fig. 3. Allowances using global-average sea-level rise. Cumulative distribution function for vertical allowances for sea-level rise from 1990 to 2100 for the A1FI emission scenario, estimated from 197 tide-gauge locations, for normal and raised-cosine uncertainty distributions. The allowances are based on a global-average rise in mean sea level, derived from the IPCC AR4, and on the statistics of storm tides observed at each location. Also shown is the 90-percentile (5- to 95-percentile) range of the global-average rise in mean sea level, from the IPCC AR4.

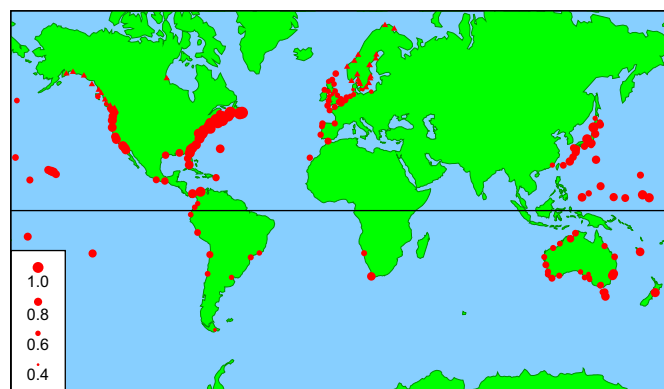


Fig. 4. Allowances using spatially varying sea-level rise. Vertical allowances (m) for sea-level rise from 1990 to 2100 for the A1FI emission scenario, indicated by the dot diameter. The allowances are based on a spatially varying rise in mean sea level, and on the statistics of storm tides observed at each location. The uncertainty in the projections of sea-level rise was fitted to a normal distribution. Filled triangles indicate allowances less than 0.4 m.

cumulative distribution function for these allowances, for normal and raised-cosine uncertainty distributions, constructed from the 197 tide-gauge allowances. Figs. 2 and 3 show that the allowances have only a small variation, 90% falling within the ranges 0.61–0.79 m and 0.61–0.73 m, for normal and raised-cosine uncertainty distributions, respectively. The difference between allowances based on normal and raised-cosine uncertainty distributions increases monotonically with the allowance, reaching a maximum of about 0.18 m (in accordance with the results of Eq. (6), with constant Δz , variable λ , and $P(z')$ chosen as normal or raised-cosine distributions).

Figs. 4 and 5 show the same information as Figs. 2 and 3 but with the global-average rise in mean sea level replaced by a spatially varying rise. The allowance is therefore based on a spatially varying rise in mean sea level (Section 3) and on the statistics of storm tides observed at each location (Section 4). Fig. 5 shows that, for a given probability, the difference between using normal and raised-cosine uncertainty distributions is at most about 0.08 m, but it should be noted that, due to the spatial variation in the sea-level rise projections, the difference at any one location may be larger than this. A striking feature of Fig. 5 is the relatively large number of sites (about 4.5%) with negative allowances (these are all indicated by filled triangles in Fig. 4, which denote allowances less than 0.4 m).

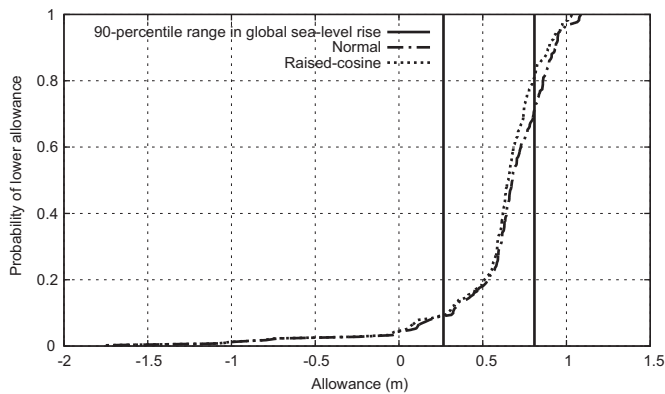


Fig. 5. Allowances using spatially varying sea-level rise. Cumulative distribution function for vertical allowances for sea-level rise from 1990 to 2100 for the A1FI emission scenario, estimated from 197 tide-gauge locations, for normal and raised-cosine uncertainty distributions. The allowances are based on a spatially varying rise in mean sea level, and on the statistics of storm tides observed at each location. Also shown is the 90-percentile (5- to 95-percentile) range of the global-average rise in mean sea level, from the IPCC AR4. It should be noted that the horizontal scale is quite different from the scale used in Fig. 3.

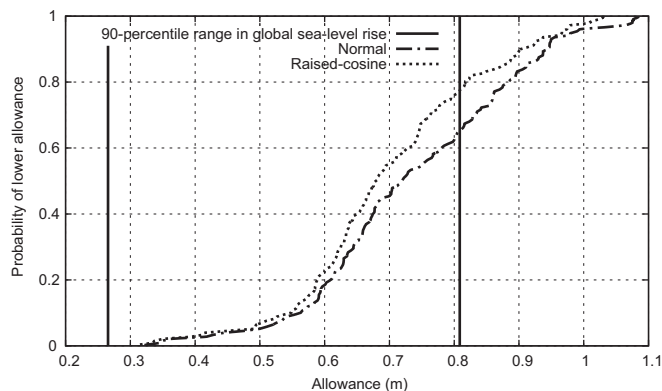


Fig. 6. As Fig. 5 but excluding all locations north of latitude 55° North.

Some of these (in the northern regions of North America and Europe) are caused by strongly negative GIA (land uplift), while the remainder (in the northwest region of North America) are caused by present changes in glaciers and icecaps. The top 5% of the locations have allowances greater than 0.97 m and 0.95 m for normal and raised-cosine uncertainty distributions, respectively.

Sites with negative or small positive allowances may be removed by excluding all locations north of latitude 55° North, as shown in Fig. 6, which is otherwise similar to Fig. 5. Rejecting these locations makes little difference to the top 5% of the remaining locations, which have allowances greater than 0.98 m and 0.97 m for normal and raised-cosine uncertainty distributions, respectively.

The results for each location and for a spatially varying sea-level rise are summarised in Appendix B, which shows allowances for the A1FI emission scenario, and for periods 1990–2100 and 2010–2100 (the latter being the more appropriate for present-day planning and policy decisions). The projections of sea-level rise used to derive these allowances were fitted to a normal distribution.

6. Applicability of the allowance and the problem of a fat upper tail

As noted in Section 1, a fundamental problem with existing sea-level rise projections is a lack of information on the upper bound for sea-level rise during the 21st century, in part because of our poor

knowledge of the contribution from ice sheets (IPCC, 2007). This effectively means that the likelihood of an extreme high sea-level rise (the upper tail of the distribution function of the sea-level rise uncertainty) is poorly known.

The allowance depends on the Gumbel distribution, which only describes extreme events. Eq. (5) therefore only applies to the range of z_p that encompasses the high sea-level extremes. The allowance is therefore valid in cases where the uncertainty distribution of sea-level rise, $P(z')$, spans only the portion of $\mathcal{N}((\mu - z_p + \Delta z + z' - a)/\lambda)$ (Eq. (3)) that fits a Gumbel distribution. This is generally satisfied if $P(z')$ has thin tails (e.g. it is normal or raised-cosine). For the A1FI emission scenario and the period 1990–2100, the 5- to 95-percentile range spans 0.54 m, which is typically five times the scale parameter, λ , a range which the Gumbel distribution will generally cover satisfactorily.

However, if $P(z')$ had a fat upper tail, the distributions used here (normal and raised-cosine) would underestimate the allowance by not including the contribution from the tail in the integral in Eq. (3). This problem may be examined in terms of both likelihood, \mathcal{N} , and risk. In general, risk may be treated in the same way as likelihood, so that the analogue of Eq. (2) is

$$R = \mathcal{R} \left(\frac{\mu - z_p}{\lambda} \right) \quad (7)$$

and the analogue of Eq. (3) is

$$R_{ov} = \int_{-\infty}^{\infty} P(z') \mathcal{R} \left(\frac{\mu - z_p + \Delta z + z' - a}{\lambda} \right) dz' \quad (8)$$

where R is the risk and \mathcal{R} is some general dimensionless function.

If the consequence of each flooding event is a constant, c , then $\mathcal{R} = c\mathcal{N}$ and $R_{ov} = cN_{ov}$. In this case, any allowance that preserves the overall likelihood, N_{ov} , also preserves the overall risk, R_{ov} .

There is one situation where fat-tailed $P(z')$ may not significantly influence the overall likelihood, and another where it may not significantly influence the overall risk.

Firstly, $\mathcal{N}((\mu - z_p + \Delta z + z' - a)/\lambda)$ may be less than the value given by a Gumbel distribution at large values of $(\mu - z_p + \Delta z + z' - a)/\lambda$, thereby reducing the effect of a fat upper tail in $P(z')$ on the overall likelihood, \mathcal{N}_{ov} (Eq. (3)). A trivial (and extreme) example of this is where the fat upper tail spans the range in which the asset lies between mean sea level and the minimum high water level (e.g. mean high water neaps). Within this range, \mathcal{N} is approximately constant at about one or two flooding events per day (for diurnal and semidiurnal tides, respectively); i.e. in this range the flooding likelihood, \mathcal{N} does not increase with z' , and the contribution of the fat upper tail to the overall likelihood N_{ov} may be small or negligible.

Secondly, even if the overall likelihood, N_{ov} , increases significantly due to a fat upper tail in $P(z')$, it is quite possible that the consequence of each flooding event decreases under these conditions, so that the overall risk, R_{ov} , is not dominated by the fat tail. A simple example of this is where the consequence is just the cost of rebuilding after each flooding event. When the likelihood (or frequency) of flooding events gets so large that rebuilding becomes impracticable, the risk becomes constant and roughly equivalent to the cost of abandoning the location altogether. In this case, \mathcal{R} does not increase with z' , and the contribution of the fat upper tail to the overall risk R_{ov} may be small or negligible.

The determination of the total risk resulting from a probability distribution with a poorly known upper tail (in this case, $P(z')$), combined with a function which may increase exponentially in the direction of the tail (in this case, \mathcal{N} or \mathcal{R}) is non-trivial, and is the subject of some debate. In a related problem (the economic implications of projections of global temperature), Weitzman (2009) introduced a 'dismal theorem' which suggested that the

effective risk associated with fat tails could become infinite, although subsequent papers (e.g. Nordhaus, 2011; Pindyck, 2011) have argued that the conditions for the validity of the 'dismal theorem' are quite restrictive.

Luckily, there is good reason to believe that the probability distribution of future sea-level rise is bounded. On a millennial scale, if all the ice and snow on land were transferred to the ocean, the rise would be limited to about 64 m (Lemke et al., 2007), and Pfeffer et al. (2008) has estimated an upper bound for sea-level rise for the 21st century of 2.0 m. Given that the detailed shape of the uncertainty distribution is largely unknown, a precautionary approach in cases where the consequence of flooding would be 'dire' (in the sense that the consequence of flooding would be unbearable, no matter how low the likelihood) is to choose an allowance based on the best estimate of the maximum possible rise (an example being the Netherlands, where coastal flood planning is based on an ARI of 10,000 years Maaskant et al., 2009). However, in other cases, where the consequences of unforeseen flooding events (i.e. 'getting the allowance wrong') are manageable, the allowance presented here represents a practical solution to planning for sea-level rise while preserving an acceptable level of likelihood or risk.

7. Discussion and conclusions

A vertical allowance for sea-level rise has been defined such that any asset raised by this allowance would experience the same frequency of flooding events under sea-level rise as it would without the allowance and without sea-level rise (Hunter, 2012). Allowances have been evaluated by combining spatially varying projections of sea-level rise with the statistics of observed storm tides at 197 tide-gauge sites. These allowances relate to the A1FI emission scenario, and the periods 1990–2100 and 2010–2100 (the latter being the more appropriate for present-day planning and policy decisions). We use the A1FI emission scenario because this is the one that the world is broadly following at present (Le Quéré et al., 2009). It must, however, be emphasised that the choice of emission scenario represents a major additional source of uncertainty, the central value of the 1990–2100 projection for the highest SRES scenario (A1FI) being about 60% larger than the projection for the lowest SRES scenario (B1).

Two uncertainty distributions were used (normal and raised-cosine); Figs. 2 and 4, and Appendix B, show the results for a normal distribution which has fatter tails and which yields a slightly higher allowance.

Planning allowances have typically been selected by choosing a specific percentile of a projection of future global-average sea-level rise. Often the 95-percentile upper limit, which is the one provided by the IPCC AR4 (Meehl et al., 2007), has been chosen. However, as shown in Fig. 3 (for the period 1990–2100), if sea-level rise were globally uniform, an allowance equal to the 95-percentile limit is generally significantly larger than would be required to preserve the frequency of flooding events under sea-level rise; for the period 1990–2100, only 2.6% of the locations considered have allowances greater than the 95-percentile upper limit. The spread of allowances in Fig. 3 is entirely due to spatial variations in the statistics of storm tides (specifically, the Gumbel scale parameter).

When the spatial variation of projected sea-level rise (due to ongoing changes in the Earth's loading and gravitational field, thermal expansion, ocean dynamics and GIA) is included, the distribution of the allowances widens significantly (Fig. 5, for the period 1990–2100). This widening is related to locations (in northern regions of North America and Europe) which experience strongly negative GIA, and others (in the northwest region of

North America) which are influenced by present changes in glaciers and icecaps. These processes contribute a significant fall in sea level, leading to negative 'allowances', some of which are less than -1 m. The spread of allowances covers the entire 90-percentile range of the A1FI projections of global-average sea-level rise, with 9% of the locations having allowances less than the 5-percentile lower limit and 29% of the locations having allowances greater than the 95-percentile upper limit.

Fig. 4 shows the global distribution of the allowances for the period 1990–2100. Obvious features are the low and negative allowances in the northern regions of North America and Europe (where the land is rising due to GIA and to present changes in glaciers and icecaps), and higher allowances along the eastern coastline of North America (where the land is sinking, again due to GIA).

Appendix B provides a table of allowances for the periods 1990–2100 and 2010–2100. These may be used as a starting point for the determination of allowances for planning and policy decisions. However, the following caveats should be recognised:

1. The determination of allowances given in this paper is based on the assumption that the Gumbel scale parameter (and hence the variability of the storm tides) will not change in time. This is supported by the fact that present evidence (Bindoff et al., 2007; Lowe et al., 2012; Menéndez and Woodworth, 2010; Woodworth and Blackman, 2004) suggests that the rise in mean sea level is generally the dominant cause of any observed increase in the frequency of extreme events. In addition, using model projections of storm tides in southeast Australia to 2070, McInnes et al. (2009) showed that the increase in the frequency of flooding events was dominated by sea-level rise.
2. The allowance includes no contribution due to possible changes in wave setup or runup.
3. The allowance includes no contribution due to the change in tides caused by sea-level rise, which are generally small and confined to quite specific locations in shelf seas (e.g. Pickering et al., 2012).
4. The allowance depends on the shape of the distribution of the uncertainty of the projections of mean sea-level rise. Two distributions have been considered here: a normal and a raised-cosine distribution. The raised-cosine distribution, which is limited to about 1.7 times the 5- to 95-percentile range (it is zero outside these limits), was included because of the arguments for an upper bound to the rate of sea-level rise (Pfeffer et al., 2008). For spatially varying sea-level rise, the allowances based on normal and raised-cosine distributions differ by about 0.08 m at most, the normal distribution giving the larger allowance. However, the possibility of the uncertainty distribution having fatter tails than a normal distribution has been considered (Section 6). Unfortunately the IPCC AR4 gives no guidance as to the choice of an appropriate uncertainty distribution, nor any indication of an 'upper bound for sea-level rise' (IPCC, 2007), and we have here based our allowances in Figs. 2 and 4, and in Appendix A, on the normal distribution. These allowances represent a practical solution to planning for sea-level rise while preserving an acceptable level of flooding likelihood, in cases where 'getting the allowance wrong' is manageable. However, in cases where the consequence of flooding would be 'dire' (in the sense that the consequence of flooding would be unbearable, no matter how low the likelihood, as in the case of the Netherlands), a precautionary approach is to choose an allowance based on the best estimate of the maximum possible rise.
5. The projections of the IPCC AR4 apparently relate to the spread of model projections (akin to the *standard deviation*) rather than to the uncertainty (akin to the *standard error*) of the best estimate of

the projections. The metric of uncertainty, σ (see Section 2), strictly relates to the *standard error*. However, for reasons discussed by Hunter (2012), σ is here associated with the *standard deviation* (rather than the *standard error*) of the projections.

There are therefore significant unknowns associated with the shape and extent of the uncertainty distribution of the projections of sea-level rise. Improved allowances for sea-level rise require better estimates of future sea level and, just as importantly, of its uncertainty distribution and the behaviour of its upper tail.

Appendix A. The derivation of regionally varying sea-level rise projections

Projections of regional relative sea-level rise were derived as in Church et al. (2011) and consist of

$$\Delta P(x,y,t) = \Delta S(t) + \Delta R(t) + \Delta F(x,y,t) + \Delta A(x,y,t) + \Delta D(x,y,t) \quad (\text{A.1})$$

where $\Delta P(x,y,t)$ is the spatially and temporally varying projection of regional relative sea-level rise, x and y are the horizontal spatial coordinates, t is the time, and

1. $\Delta S(t)$ is the global-average sea-level rise, based on the best-available modelling at the time of the IPCC AR4. This term is consistent with the sixth row (labelled 'Sea level rise') of Table 10.7 of Meehl et al. (2007). It is composed of

$$\Delta S(t) = \Delta S_T(t) + \Delta S_I(t) + \Delta S_C(t) + \Delta S_A(t) \quad (\text{A.2})$$

where $\Delta S_T(t)$ is the contribution from thermal expansion (consistent with the first row of Meehl et al. (2007, Table 10.7)). $\Delta S_I(t)$, $\Delta S_C(t)$ and $\Delta S_A(t)$ are contributions due to melting ice from 'glaciers and ice caps', Greenland and Antarctica, respectively, estimated from surface mass balance; they are consistent with the second, third and fourth rows of Table 10.7 of Meehl et al. (2007).

Annual time series of $\Delta S(t)$, and the 5- and 95-percentile uncertainty range, were obtained for emission scenarios B1, B2, A1B, A1T, A2 and A1FI (Gregory, pers. comm.). $\Delta S(t)$ is just the mean of the 5- and 95-percentile range, and we derived the uncertainty half-range, $\delta S(t)$, from half the difference between the 5- and 95-percentile values.

2. $\Delta R(t)$ is a component accounting for poorly quantified 'rapid dynamical changes' to land ice. This term is consistent with the seventh row (labelled 'Scaled-up ice sheet discharge') of Table 10.7 of Meehl et al. (2007). It was assumed that one-third of this comes from Greenland and two-thirds from West Antarctica. $\Delta R(t)$ was provided (Gregory, pers. comm.) and we derived the uncertainty, $\delta R(t)$ (the 5- to 95-percentile half-range), by assuming a coefficient of variation (the ratio of the standard deviation to the central value) of 0.677 (Gregory, pers. comm.) and converting from the standard deviation to the half-range by multiplying by 1.6448537 (assuming a normal distribution), so

$$\delta R(t) = \Delta R(t) \times 0.677 \times 1.6448537 \quad (\text{A.3})$$

3. $\Delta F(x,y,t)$ is a spatially and temporally varying 'fingerprint' term accounting for changes in the loading of the Earth and in the gravitational field, in response to ongoing changes in land ice (Mitrovica et al., 2001, 2011). It is composed of

$$\begin{aligned} \Delta F(x,y,t) = & (F_I(x,y) - 1)\Delta S_I(t) + (F_C(x,y) - 1)\Delta S_C(t) \\ & + (F_A(x,y) - 1)\Delta S_A(t) + 0.333(F_G(x,y) - 1)\Delta R(t) \\ & + 0.667(F_W(x,y) - 1)\Delta R(t) \end{aligned} \quad (\text{A.4})$$

where $F_I(x,y)$, $F_C(x,y)$, $F_A(x,y)$ and $F_W(x,y)$ are 'fingerprints' for ice loss from 'glaciers and ice caps', Greenland, Antarctica as a whole, and West Antarctica, respectively, and:

$$\overline{F_I(x,y)} = 1, \quad \overline{F_C(x,y)} = 1, \quad \overline{F_A(x,y)} = 1, \quad \overline{F_W(x,y)} = 1 \quad (\text{A.5})$$

where the overbar indicates a global average, so that the global-average of each term in Eq. (A.4) is zero. The uncertainty, $\delta F(x,y,t)$, of this 'fingerprint' term was estimated from:

$$\delta F(x,y,t) = \frac{|\Delta F(x,y,t)|\delta S(t)}{\Delta S(t)} \quad (\text{A.6})$$

4. $\Delta A(x,y,t)$ is glacial isostatic adjustment or GIA from Kendall et al. (2005). This is spatially varying with a zero global-average:

$$\overline{\Delta A(x,y,t)} = 0 \quad (\text{A.7})$$

$\Delta A(x,y,t)$ increases linearly with time. No uncertainty was estimated for this term.

5. $\Delta D(x,y,t)$ is a spatially and temporally varying term related to change in ocean density and dynamics (Meehl et al., 2007). This is expressed as the deviation of regional sea-level rise from the global average, so:

$$\overline{\Delta D(x,y,t)} = 0 \quad (\text{A.8})$$

The uncertainty of this term, $\delta D(x,y,t)$, was estimated from the spread of simulations from different models.

The uncertainties in terms (1)–(3) were added linearly, and the result was added in quadrature to the error in term (5), in order to obtain the uncertainty, $\delta P(x,y,t)$, in $\Delta P(x,y,t)$:

$$\delta P(x,y,t) = \sqrt{(\delta S(t) + \delta R(t) + \delta F(x,y,t))^2 + (\delta D(x,y,t))^2} \quad (\text{A.9})$$

The spatially and temporally varying sea-level rise related to change in ocean density and dynamics, $\Delta D(x,y,t)$, was provided by atmosphere–ocean general circulation models (AOGCMs). While global-average sea-level rise ($\Delta S(t) + \Delta R(t)$) has been estimated for six emission scenarios (B1, B2, A1B, A1T, A2, A1FI; Meehl et al., 2007), results from AOGCMs are only available for scenarios B1, A1B and A2. Spatially and temporally varying projections ($\Delta P(x,y,t)$, $\delta P(x,y,t)$) for B2, A1T and A1FI were here obtained by using the results for ($\Delta P(x,y,t)$, $\delta P(x,y,t)$) for the nearest adjacent projections for B1, A1B or A2, and scaling using ratios derived from the respective global-average projections ($\Delta S(t) + \Delta R(t)$, $\delta S(t) + \delta R(t)$). The present paper discusses A1FI projections derived from spatially varying A2 projections and global-average projections for A1FI and A2. Therefore (omitting the variables x , y and t , for clarity):

$$\Delta P(\text{A1FI}) = \frac{\Delta P(\text{A2})(\Delta S(\text{A1FI}) + \Delta R(\text{A1FI}))}{(\Delta S(\text{A2}) + \Delta R(\text{A2}))} \quad (\text{A.10})$$

and

$$\delta P(\text{A1FI}) = \frac{\delta P(\text{A2})(\delta S(\text{A1FI}) + \delta R(\text{A1FI}))}{(\delta S(\text{A2}) + \delta R(\text{A2}))} \quad (\text{A.11})$$

Appendix B. Summary of values for each location with a spatially varying sea-level rise and a normal distribution of uncertainty

The summary of locations, 5- to 95-percentile ranges of projections of mean sea-level rise, and allowances, for the periods 1990–2100 and 2010–2100 is given in Table B1.

Table B1

Summary of locations, 5- to 95-percentile ranges of projections of mean sea-level rise, and allowances, for the periods 1990–2100 and 2010–2100.

Site name	Longitude, latitude (deg.)	Projection 1990–2100 5,95% (m)	Projection 2010–2100 5,95% (m)	Allowance 1990–2100 (m)	Allowance 2010–2100 (m)
Abashiri	144.28, 44.02	0.09, 0.68	0.12, 0.64	0.59	0.53
Aberdeen	357.93, 57.14	0.04, 0.76	0.08, 0.70	0.62	0.55
Aburatsu	131.42, 31.57	0.24, 0.84	0.25, 0.76	0.68	0.60
Acapulco-A	260.09, 16.84	0.18, 0.77	0.22, 0.70	0.72	0.62
Adak	183.37, 51.86	0.15, 0.76	0.18, 0.67	0.63	0.54
Albany	117.88, –35.03	0.25, 0.82	0.25, 0.76	0.71	0.64
Alert Bay	233.07, 50.59	–0.08, 0.62	–0.03, 0.57	0.43	0.38
Antofagasta	289.60, –23.65	0.10, 0.71	0.12, 0.66	0.72	0.63
Argentina	306.02, 47.30	0.39, 1.14	0.32, 1.01	1.08	0.92
Astoria	236.23, 46.21	0.34, 0.99	0.32, 0.87	0.83	0.72
Atlantic City	285.58, 39.35	0.48, 1.16	0.46, 0.98	0.98	0.81
Balboa	280.43, 8.96	0.18, 0.75	0.20, 0.68	0.58	0.53
Baltimore	283.42, 39.27	0.43, 1.11	0.42, 0.95	0.91	0.77
Bamfield	234.86, 48.84	0.09, 0.81	0.11, 0.73	0.66	0.57
Bella Bella	231.86, 52.16	–0.15, 0.55	–0.09, 0.51	0.35	0.32
Bermuda	295.30, 32.40	0.28, 0.92	0.28, 0.81	0.84	0.71
Boston	288.95, 42.35	0.36, 1.12	0.32, 0.98	0.95	0.81
Brest	355.50, 48.38	0.19, 0.84	0.20, 0.76	0.64	0.58
Broome	122.22, –18.00	0.18, 0.83	0.19, 0.74	0.63	0.56
Buenaventura	282.90, 3.90	0.15, 0.71	0.17, 0.65	0.60	0.53
Buenos Aires	301.50, –34.67	0.12, 0.86	0.17, 0.69	0.59	0.48
Bunbury	115.63, –33.32	0.20, 0.83	0.21, 0.74	0.63	0.57
Bundaberg	152.38, –24.77	0.26, 0.82	0.25, 0.75	0.70	0.63
Burnie	145.92, –41.05	0.22, 0.81	0.22, 0.75	0.68	0.62
Calais	1.87, 50.97	0.17, 0.87	0.19, 0.79	0.72	0.64
Callao-B	282.85, –12.05	0.10, 0.73	0.14, 0.66	0.70	0.59
Campbell River	234.75, 50.04	–0.13, 0.57	–0.08, 0.53	0.36	0.33
Cananea	312.07, –25.02	0.18, 0.75	0.16, 0.68	0.65	0.57
Cape May	285.04, 38.97	0.50, 1.18	0.48, 1.00	0.99	0.83
Carnarvon	113.62, –24.88	0.15, 0.83	0.18, 0.74	0.64	0.57
Cartagena	284.47, 10.38	0.22, 0.77	0.25, 0.67	0.95	0.72
Cascais	350.58, 38.69	0.18, 0.79	0.22, 0.71	0.67	0.58
Ceuta	354.68, 35.90	0.14, 0.72	0.17, 0.66	0.73	0.62
Charleston	280.07, 32.78	0.38, 1.04	0.36, 0.91	0.91	0.78
Charlottetown	296.88, 46.23	0.33, 1.13	0.29, 0.99	0.94	0.80
Cherbourg	358.38, 49.65	0.14, 0.80	0.16, 0.72	0.64	0.57
Chesapeake	283.89, 36.97	0.45, 1.13	0.43, 0.97	0.94	0.80
Chichijima	142.18, 27.10	0.11, 0.93	0.19, 0.78	0.82	0.64
Churchill	265.80, 58.78	–2.30, –1.54	–1.67, –1.58	–1.74	–1.63
Cordova-B	214.25, 60.56	–0.74, 0.33	–0.60, 0.33	0.18	0.15
Crescent City	235.82, 41.74	0.41, 1.02	0.36, 0.91	0.86	0.75
Cristobal	280.08, 9.36	0.23, 0.78	0.26, 0.69	0.88	0.70
Cuxhaven	8.72, 53.87	0.15, 0.89	0.19, 0.80	0.58	0.53
Darwin	130.85, –12.47	0.21, 0.82	0.19, 0.75	0.70	0.63
Delfzijl	6.93, 53.33	0.17, 0.91	0.20, 0.81	0.60	0.55
Den Helder	4.75, 52.97	0.19, 0.91	0.21, 0.82	0.64	0.58
Dover	1.32, 51.11	0.18, 0.88	0.20, 0.80	0.68	0.61
Draghallan	17.47, 62.33	–1.33, –0.56	–1.04, –0.41	–0.72	–0.58
Eastport	293.01, 44.90	0.35, 1.12	0.31, 0.98	1.03	0.87
Ensenada	243.37, 31.85	0.31, 0.89	0.30, 0.79	0.86	0.73
Esbjerg	8.43, 55.47	0.04, 0.79	0.09, 0.71	0.47	0.44
Esperance	121.90, –33.87	0.22, 0.79	0.22, 0.73	0.66	0.60
Fishguard	355.02, 52.01	0.10, 0.76	0.13, 0.70	0.59	0.53
Fort Denison	151.23, –33.85	0.33, 0.93	0.31, 0.85	0.88	0.79
Fort Pulaski	279.10, 32.03	0.36, 1.03	0.34, 0.90	0.95	0.80
Fremantle	115.73, –32.05	0.17, 0.83	0.19, 0.74	0.66	0.58
Fulford Harbour	236.55, 48.77	–0.05, 0.71	–0.01, 0.65	0.55	0.48
Furuogrund	21.23, 64.92	–1.60, –0.83	–1.28, –0.63	–1.07	–0.86
Galveston	265.21, 29.31	0.33, 0.97	0.33, 0.84	0.75	0.65
Geelong	144.43, –38.17	0.18, 0.76	0.18, 0.71	0.67	0.61
Georgetown	146.85, –41.13	0.33, 0.91	0.29, 0.84	0.78	0.71
Geraldton	114.58, –28.78	0.14, 0.82	0.16, 0.74	0.71	0.62
Goteborg	11.80, 57.68	–0.31, 0.45	–0.20, 0.43	0.24	0.23
Guam	144.65, 13.43	0.25, 0.83	0.28, 0.72	0.80	0.65
Hakodate	140.73, 41.78	0.15, 0.92	0.23, 0.75	0.94	0.67
Halifax	296.42, 44.67	0.49, 1.19	0.42, 1.04	1.06	0.91
Heimsjoe	9.12, 63.43	–0.57, 0.26	–0.42, 0.30	0.10	0.13
Heysham	357.09, 54.03	0.05, 0.71	0.08, 0.66	0.50	0.46
Hilo	204.93, 19.73	0.21, 0.81	0.24, 0.72	0.78	0.65
Hobart	147.33, –42.88	0.35, 0.95	0.31, 0.87	0.83	0.75
Hook of Holland	4.12, 51.98	0.19, 0.91	0.22, 0.82	0.66	0.59
Holyhead	355.37, 53.31	0.07, 0.74	0.10, 0.67	0.57	0.51
Honningsvaag	25.98, 70.98	–0.58, 0.21	–0.42, 0.21	0.07	0.05

Table B1 (continued)

Site name	Longitude, latitude (deg.)	Projection 1990–2100 5,95% (m)	Projection 2010–2100 5,95% (m)	Allowance 1990–2100 (m)	Allowance 2010–2100 (m)
Honolulu-B	202.13, 21.31	0.18, 0.81	0.21, 0.73	0.81	0.68
Hosojima	131.68, 32.42	0.23, 0.83	0.24, 0.75	0.68	0.60
Ilha Fiscal	316.83, -22.90	0.16, 0.76	0.17, 0.68	0.60	0.52
Immingham	359.81, 53.63	0.13, 0.84	0.15, 0.76	0.59	0.54
Ishigaki	124.15, 24.33	0.28, 0.86	0.27, 0.77	0.70	0.62
Johnston	190.47, 16.74	0.24, 0.82	0.27, 0.71	0.73	0.61
Kahului	203.53, 20.90	0.19, 0.81	0.21, 0.73	0.86	0.71
Ketchikan	228.38, 55.33	-0.22, 0.52	-0.16, 0.49	0.33	0.30
Key West	278.19, 24.55	0.28, 0.87	0.27, 0.77	0.86	0.72
Klagshamn	12.90, 55.52	-0.04, 0.70	0.03, 0.64	0.45	0.41
Kungsholmsfort	15.58, 56.10	-0.22, 0.53	-0.12, 0.50	0.31	0.30
Kushimoto	135.78, 33.47	0.26, 0.85	0.26, 0.76	0.73	0.64
Kushiro	144.38, 42.97	0.14, 0.80	0.18, 0.75	0.80	0.70
Kwajalein	167.73, 8.73	0.19, 0.84	0.21, 0.74	0.90	0.73
La Coruna	351.60, 43.37	0.19, 0.81	0.20, 0.73	0.68	0.60
La Libertad	279.08, -2.20	0.12, 0.72	0.15, 0.66	0.62	0.54
Landsort	17.87, 58.75	-0.63, 0.13	-0.46, 0.16	-0.01	0.02
Lerwick	358.86, 60.16	0.07, 0.82	0.11, 0.75	0.69	0.61
Lewes	284.88, 38.78	0.47, 1.16	0.45, 0.98	0.95	0.80
Los Angeles	241.73, 33.72	0.32, 0.91	0.31, 0.80	0.89	0.75
Lower Escuminac	295.12, 47.08	0.18, 0.98	0.16, 0.86	0.77	0.66
Lowestoft	1.75, 52.48	0.17, 0.87	0.19, 0.79	0.62	0.56
Maaloey	5.12, 61.93	-0.29, 0.50	-0.18, 0.47	0.32	0.29
Magueyes Island	292.95, 17.97	0.22, 0.77	0.25, 0.69	0.74	0.63
Maisaka	137.62, 34.68	0.26, 0.86	0.27, 0.78	0.69	0.61
Majuro	171.37, 7.11	0.19, 0.83	0.22, 0.73	0.89	0.71
Malakal-A	134.48, 7.33	0.19, 0.87	0.22, 0.76	0.84	0.68
Malin Head	352.67, 55.37	0.05, 0.79	0.08, 0.72	0.64	0.57
Mayport	278.57, 30.39	0.32, 0.98	0.31, 0.86	0.94	0.78
Mera	139.83, 34.92	0.29, 0.86	0.28, 0.78	0.78	0.70
Midway	182.63, 28.22	0.21, 0.86	0.24, 0.75	0.70	0.60
Milford Haven	354.99, 51.70	0.13, 0.79	0.15, 0.72	0.63	0.56
Miyakejima	139.48, 34.06	0.29, 0.86	0.28, 0.79	0.67	0.61
Mokuoloe	202.20, 21.43	0.18, 0.81	0.21, 0.73	0.84	0.70
Montauk	288.04, 41.05	0.42, 1.11	0.40, 0.94	0.90	0.75
Monterey	238.11, 36.60	0.33, 0.93	0.31, 0.82	0.86	0.73
Nagasaki	129.87, 32.73	0.26, 0.83	0.26, 0.75	0.77	0.67
Naha	127.67, 26.22	0.28, 0.90	0.27, 0.80	0.83	0.70
Nantucket	289.90, 41.28	0.45, 1.12	0.43, 0.95	0.95	0.79
Nawiliwili	200.65, 21.97	0.18, 0.80	0.19, 0.73	0.81	0.69
Naze	129.50, 28.38	0.30, 0.88	0.29, 0.78	0.77	0.66
Neah Bay	235.38, 48.37	0.12, 0.81	0.14, 0.73	0.63	0.55
Newcastle	151.80, -32.92	0.32, 0.92	0.30, 0.84	0.87	0.78
New London	287.91, 41.35	0.40, 1.08	0.38, 0.92	0.86	0.72
Newlyn	354.46, 50.10	0.17, 0.82	0.18, 0.74	0.69	0.61
Newport	288.67, 41.51	0.42, 1.11	0.40, 0.94	0.95	0.79
New Westminster	237.09, 49.20	-0.18, 0.57	-0.12, 0.53	0.35	0.32
New York	285.99, 40.70	0.44, 1.12	0.41, 0.95	0.91	0.77
Nishinomote	130.99, 30.73	0.29, 0.86	0.29, 0.78	0.80	0.71
Northshields	358.56, 55.01	0.07, 0.78	0.10, 0.72	0.62	0.56
North Sydney	299.75, 46.22	0.39, 1.18	0.34, 1.03	0.99	0.84
Noumea	166.44, -22.29	0.29, 0.85	0.31, 0.75	0.85	0.71
Ofunato	141.72, 39.07	0.25, 0.84	0.28, 0.76	0.81	0.70
Olands Norra Udde	17.10, 57.37	-0.41, 0.34	-0.28, 0.34	0.11	0.13
Oslo	10.75, 59.90	-0.55, 0.21	-0.40, 0.23	-0.01	0.02
Pago Pago	189.32, -14.28	0.20, 0.78	0.19, 0.70	0.80	0.70
Patricia Bay	236.55, 48.65	-0.05, 0.71	-0.01, 0.65	0.53	0.47
Pensacola	272.79, 30.40	0.35, 0.99	0.34, 0.87	0.78	0.68
Pohnpei-B	158.24, 6.99	0.21, 0.82	0.23, 0.73	0.79	0.66
Point Atkinson	236.75, 49.34	-0.16, 0.60	-0.10, 0.55	0.42	0.37
Point Lonsdale	144.62, -38.30	0.18, 0.76	0.18, 0.71	0.65	0.59
Port Adelaide (inner)	138.50, -34.85	0.18, 0.76	0.19, 0.70	0.57	0.53
Port Adelaide (outer)	138.48, -34.78	0.18, 0.76	0.19, 0.70	0.56	0.52
Port-aux-Basques	300.87, 47.57	0.30, 1.09	0.27, 0.96	1.08	0.91
Port Hardy	232.51, 50.72	-0.03, 0.67	0.01, 0.61	0.52	0.45
Port Hedland	118.58, -20.30	0.16, 0.83	0.18, 0.74	0.65	0.57
Portland	289.75, 43.66	0.29, 1.05	0.26, 0.93	0.93	0.79
Port Lincoln	135.87, -34.72	0.21, 0.78	0.21, 0.72	0.63	0.57
Portpatrick	354.88, 54.84	0.05, 0.77	0.08, 0.71	0.57	0.52
Port Pirie	138.02, -33.17	0.17, 0.75	0.18, 0.70	0.54	0.50
Prince Rupert	229.68, 54.32	-0.18, 0.53	-0.12, 0.49	0.32	0.30
Puerto de la Luz	344.58, 28.13	0.19, 0.76	0.22, 0.69	0.67	0.58
Puerto Williams	292.38, -54.93	-0.02, 0.61	0.01, 0.56	0.48	0.43
Queen Charlotte City	227.93, 53.25	0.11, 0.78	0.12, 0.71	0.61	0.54

Table B1 (continued)

Site name	Longitude, latitude (deg.)	Projection 1990–2100 5.95% (m)	Projection 2010–2100 5.95% (m)	Allowance 1990–2100 (m)	Allowance 2010–2100 (m)
Ratan	20.92, 64.00	−1.54, −0.77	−1.22, −0.59	−0.99	−0.79
Rikitea	225.05, −23.12	0.13, 0.72	0.17, 0.64	0.80	0.66
Roervik	11.25, 64.87	−0.70, 0.17	−0.53, 0.23	−0.04	0.02
Saint John	293.94, 45.25	0.29, 1.06	0.26, 0.93	0.93	0.79
Salina Cruz	264.80, 16.16	0.15, 0.77	0.21, 0.68	0.75	0.62
San Diego	242.83, 32.71	0.32, 0.90	0.31, 0.80	0.86	0.73
San Francisco	237.53, 37.81	0.35, 0.95	0.32, 0.83	0.82	0.71
Seattle	237.66, 47.60	0.03, 0.79	0.05, 0.71	0.66	0.57
Seward-C	210.57, 60.12	−0.46, 0.47	−0.37, 0.44	0.33	0.29
Sheerness	0.75, 51.44	0.17, 0.87	0.19, 0.79	0.68	0.61
Simon's Bay	18.43, −34.18	0.24, 0.82	0.28, 0.73	0.83	0.68
Sitka	224.66, 57.05	−0.26, 0.53	−0.19, 0.49	0.40	0.35
Smogen	11.22, 58.37	−0.46, 0.29	−0.33, 0.30	0.12	0.12
Socoa	358.32, 43.40	0.15, 0.79	0.17, 0.72	0.66	0.59
South Beach	235.96, 44.62	0.43, 1.06	0.39, 0.94	0.87	0.76
Spikarna	17.53, 62.37	−1.33, −0.56	−1.04, −0.41	−0.80	−0.63
St. Johns	307.28, 47.57	0.41, 1.13	0.34, 1.00	1.08	0.93
Stockholm	18.08, 59.32	−0.84, −0.09	−0.64, −0.02	−0.24	−0.18
St. Petersburg	277.37, 27.76	0.32, 0.94	0.31, 0.83	0.76	0.66
Thevenard	133.65, −32.15	0.19, 0.76	0.20, 0.70	0.59	0.54
Tofino	234.09, 49.15	−0.03, 0.70	0.01, 0.63	0.53	0.46
Townsville	146.83, −19.25	0.24, 0.81	0.24, 0.74	0.66	0.59
Toyama	137.22, 36.77	0.20, 0.90	0.26, 0.76	0.93	0.70
Tregde	7.57, 58.00	−0.26, 0.49	−0.16, 0.47	0.35	0.31
Truk	151.85, 7.45	0.20, 0.84	0.23, 0.74	0.82	0.67
Tumaco	281.27, 1.83	0.15, 0.71	0.17, 0.65	0.62	0.54
Ullapool	354.84, 57.90	0.04, 0.76	0.09, 0.69	0.58	0.52
Valparaiso	288.37, −33.03	0.04, 0.66	0.08, 0.60	0.63	0.54
Vancouver	236.89, 49.29	−0.16, 0.60	−0.10, 0.55	0.44	0.39
Varberg	12.22, 57.10	−0.33, 0.42	−0.21, 0.41	0.21	0.21
Vardo	31.10, 70.33	−0.57, 0.24	−0.42, 0.24	0.14	0.11
Victor Harbor	138.63, −35.57	0.19, 0.77	0.20, 0.72	0.61	0.56
Victoria	236.63, 48.42	−0.05, 0.71	−0.01, 0.65	0.51	0.45
Vigo	351.27, 42.23	0.18, 0.79	0.19, 0.72	0.63	0.57
Wake	166.62, 19.28	0.19, 0.81	0.24, 0.70	0.73	0.60
Wakkanai	141.68, 45.42	0.07, 0.67	0.11, 0.63	0.59	0.53
Walvis Bay	14.50, −22.95	0.20, 0.77	0.25, 0.68	0.65	0.55
Wellington	174.78, −41.28	0.31, 0.91	0.30, 0.80	0.88	0.74
Wick	356.91, 58.44	0.06, 0.80	0.09, 0.74	0.64	0.58
Williamstown	144.92, −37.87	0.17, 0.75	0.17, 0.70	0.61	0.56
Wilmington	282.05, 34.23	0.39, 1.06	0.37, 0.91	0.89	0.75
Wladyslawowo	18.42, 54.80	0.02, 0.76	0.08, 0.69	0.54	0.48
Wood Islands	297.30, 45.68	0.42, 1.22	0.36, 1.06	0.98	0.84
Woods Hole	289.33, 41.52	0.45, 1.12	0.43, 0.95	0.91	0.76
Wyndham	128.10, −15.45	0.18, 0.81	0.16, 0.74	0.76	0.68
Xiamen	118.07, 24.45	0.21, 0.78	0.20, 0.72	0.59	0.54
Yakutat	220.26, 59.55	−0.86, 0.25	−0.69, 0.26	0.16	0.12
Yap-B	138.13, 9.51	0.23, 0.84	0.24, 0.75	0.67	0.59
Yarmouth	293.88, 43.83	0.42, 1.19	0.37, 1.04	1.07	0.91
Ystad	13.82, 55.42	−0.06, 0.69	0.01, 0.63	0.47	0.42

References

- Bindoff, N., Willebrand, J., Artale, V., Cazenave, A., Gregory, J., Gulev, S., Hanawa, K., Quéré, C.L., Levitus, S., Nojiri, Y., Shum, C., Talley, L., Unnikrishnan, A., 2007. Observations: oceanic climate change and sea level. In: Solomon, S., Qin, D., Manning, M., Chen, Z., Marquis, M., Averyt, K., Tignor, M., Miller, H. (Eds.), *Climate Change 2007: The Physical Science Basis. Contribution of Working Group I to the Fourth Assessment Report of the Intergovernmental Panel on Climate Change*. Cambridge University Press, Cambridge, United Kingdom and New York, NY, USA, pp. 385–432 (Chapter 5).
- van den Brink, H., Können, G., 2011. Estimating 10,000-year return values from short time series. *Int. J. Climatol.* 31, 115–126, <http://dx.doi.org/10.1002/joc.2047>.
- Church, J., White, N., 2011. Sea-level rise from the late 19th to the early 21st century. *Surv. Geophys.* 32 (4–5), 585–602, <http://dx.doi.org/10.1007/s10712-011-9119-1>.
- Church, J., Gregory, J., White, N., Platten, S., Mitrovica, J., 2011. Understanding and projecting sea level change. *Oceanography* 24 (2), 130–143, <http://dx.doi.org/10.5670/oceanog.2011.33>.
- Coles, S., 2001. *An Introduction to Statistical Modeling of Extreme Values*. Springer-Verlag, London, Berlin, Heidelberg.

- Hunter, J., 2012. A simple technique for estimating an allowance for uncertain sea-level rise. *Climatic Change* 113, 239–252, <http://dx.doi.org/10.1007/s10584-011-0332-1>.
- IPCC, 2007. Summary for policymakers. In: Solomon, S., Qin, D., Manning, M., Chen, Z., Marquis, M., Averyt, K., Tignor, M., Miller, H. (Eds.), *Climate Change 2007: The Physical Science Basis. Contribution of Working Group I to the Fourth Assessment Report of the Intergovernmental Panel on Climate Change*. Cambridge University Press, Cambridge, United Kingdom and New York, NY, USA, pp. 1–18.
- ISO, 2009. 31000:2009 Risk Management—Principles and Guidelines. International Organisation for Standardization. <www.iso.org>.
- Kendall, R., Mitrovica, J., Milne, G., 2005. On post-glacial sea level: II. Numerical formulation and comparative results on spherically symmetric models. *Geophys. J. Int.* 161 (3), 679–706, <http://dx.doi.org/10.1111/j.1365-246X.2005.02553.x>.
- Le Quéré, C., Raupach, M., Canadell, J., Marland, G., et al., 2009. Trends in the sources and sinks of carbon dioxide. *Nat. Geosci.* 2, 831–836, <http://dx.doi.org/10.1038/ngeo689>.
- Lemke, P., Ren, J., Alley, R., Allison, I., Carrasco, J., Flato, G., Fujii, Y., Kaser, G., Mote, P., Thomas, R., Zhang, T., 2007. Observations: changes in snow, ice and frozen ground. In: Solomon, S., Qin, D., Manning, M., Chen, Z., Marquis, M., Averyt, K., Tignor, M., Miller, H. (Eds.), *Climate Change 2007: The Physical Science Basis. Contribution of Working Group I to the Fourth Assessment Report of the*

- Intergovernmental Panel on Climate Change. Cambridge University Press, Cambridge, United Kingdom and New York, NY, USA, pp. 337–383 (Chapter 4).
- Lowe, J., Woodworth, P., Knutson, T., McDonald, R., McInnes, K., Woth, K., Von Storch, H., Wolf, J., Swail, V., Bernier, N., Gulev, S., Horsburgh, K., Unnikrishnan, A., Hunter, J., Weisse, R., 2012. Past and future changes in extreme sea levels and waves. In: Church, J., Woodworth, P., Aarup, T., Wilson, S. (Eds.), *Understanding Sea-Level Rise and Variability*. Wiley-Blackwell, Oxford, United Kingdom, pp. 326–375 (Chapter 11).
- Maaskant, B., Jonkman, S., Bouwer, L., 2009. Future risk of flooding: an analysis of changes in potential loss of life in South Holland (The Netherlands). *Environ. Sci. Policy* 12, 157–169, <http://dx.doi.org/10.1016/j.envsci.2008.11.004>.
- McInnes, K., Macadam, I., Hubbert, G., O'Grady, J., 2009. A modelling approach for estimating the frequency of sea level extremes and the impact of climate change in southeast Australia. *Nat. Hazards* 51, 115–137, <http://dx.doi.org/10.1007/s11069-009-9383-2>.
- Meehl, G., Stocker, T., Collins, W., Friedlingstein, P., Gaye, A., Gregory, J., Kitoh, A., Knutti, R., Murphy, J., Noda, A., Raper, S., Watterson, I., Weaver, A., Zhao, Z.C., 2007. Global climate projections. In: Solomon, S., Qin, D., Manning, M., Chen, Z., Marquis, M., Averyt, K., Tignor, M., Miller, H. (Eds.), *Climate Change 2007: The Physical Science Basis. Contribution of Working Group I to the Fourth Assessment Report of the Intergovernmental Panel on Climate Change*. Cambridge University Press, Cambridge, United Kingdom and New York, NY, USA, pp. 747–845 (Chapter 10).
- Menéndez, M., Woodworth, P., 2010. Changes in extreme high water levels based on a quasi-global tide-gauge data set. *J. Geophys. Res.* 115 (C10011), <http://dx.doi.org/10.1029/2009JC005997>.
- Mitrovica, J., Tamisiea, M., Davis, J., Milne, G., 2001. Recent mass balance of polar ice sheets inferred from patterns of global sea-level change. *Nature* 409 (6823), 1026–1029, <http://dx.doi.org/10.1038/35059054>.
- Mitrovica, J., Gomez, N., Morrow, E., Hay, C., Latychev, K., Tamisiea, M., 2011. On the robustness of predictions of sea level fingerprints. *Geophys. J. Int.* 187, 729–742, <http://dx.doi.org/10.1111/j.1365-246X.2011.05090.x>.
- Nakicenovic, N., Alcamo, J., Davis, G., de Vries, B., Fenhann, J., Gaffin, S., Gregory, K., Grubler, A., Jung, T., Kram, T., La Rovere, E., Michaelis, L., Mori, S., Morita, T., Pepper, W., Pitcher, H., Price, L., Riahi, K., Roehrl, A., Rogner, H., Sankovski, A., Schlesinger, M., Shukla, P., Smith, S., Swart, R., van Rooijen, S., Victor, N., Dadi, Z., 2000. *Special Report on Emissions Scenarios. A Special Report of Working Group III of the Intergovernmental Panel on Climate Change*. Cambridge University Press, Cambridge, UK.
- Nordhaus, W., 2011. The economics of tail events with an application to climate change. *Rev. Environ. Econ. Policy* 5 (2), 240–257.
- Pfeffer, W., Harper, J., O'Neil, S., 2008. Kinematic constraints on glacier contributions to 21st-century sea-level rise. *Science* 321 (5894), 1340–1343, <http://dx.doi.org/10.1126/science.1159099>.
- Pickering, M., Wells, N., Horsburgh, K., Green, J., 2012. The impact of future sea-level rise on the European Shelf tides. *Cont. Shelf Res.* 35, 1–15, <http://dx.doi.org/10.1016/j.csr.2011.11.011>.
- Pindyck, R., 2011. Fat tails, thin tails, and climate change policy. *Rev. Environ. Econ. Policy* 5 (2), 258–274.
- Pugh, D., 1996. *Tides, Surges and Mean Sea-Level*. John Wiley & Sons, reprinted with corrections, <http://eprints.soton.ac.uk/19157/01/sea-level.pdf>, Chichester, New York, Brisbane, Toronto and Singapore.
- R Development Core Team, 2008. *R: A Language and Environment for Statistical Computing*. R Foundation for Statistical Computing, Vienna, Austria, URL <http://www.R-project.org>, ISBN 3-900051-07-0.
- Slangen, A., Katsman, C., van de Wal, R., Vermeersen, L., Riva, R., 2012. Towards regional projections of twenty-first century sea-level change based on IPCC SRES scenarios. *Climate Dyn.* 38, 1191–1209, <http://dx.doi.org/10.1007/s00382-011-1057-6>.
- Weitzman, M., 2009. On modeling and interpreting the economics of catastrophic climate change. *Rev. Econ. Stat.* 91 (1), 1–19.
- Woodworth, P., Blackman, D., 2004. Evidence for systematic changes in extreme high waters since the mid-1970s. *J. Climate* 17 (6), 1190–1197, [http://dx.doi.org/10.1175/1520-0442\(2004\)017<1190:EFSCIE>2.0.CO;2](http://dx.doi.org/10.1175/1520-0442(2004)017<1190:EFSCIE>2.0.CO;2).